Determination of Thermo-Mechanical Variables During Plane Strain Compression Testing

A thesis submitted to the Faculty of Engineering and Built Environment of the University of Cape Town in partial fulfilment of the requirements for the degree of Master of Science in Engineering

By
James M^{c}Callum Buchanan
Centre for Materials Engineering
January 2002

Abstract

Plane strain compression (PSC) testing is a method used to simulate the deformation condition of industrial rolling, namely that of plane strain, and is used extensively to describe the influence of deformation variables, being strain, strain rate and temperature, on microstructural evolution. However, the strain and strain rate within deformed PSC specimens is not homogeneous and for high strain rate deformation (>1sec^{-1}) localized adiabatic heating may occur. Nominal values of strain and strain rate do not describe the mechanical deformation variables in a particular volume of the PSC specimen. Therefore, for analytical microstructural models to have better predictive value, the determination of the thermo-mechanical variables during PSC testing is required.

The strain and strain rate distribution during PSC testing of aluminium is investigated using visioplastic experiments and the Finite Element Method (FEM). Visioplastic analysis allows the real state of deformation to be investigated, which is then used to verify and validate the FEM prediction. The study showed that graphite lubrication breakdown occurs progressively above 300 °C, leading to a change in strain and strain rate distribution because of an increased coefficient of friction as the test temperature is increased. Lubrication breakdown has been characterised using a Coulomb friction model for PSC testing temperatures between 25 and 440 °C, which when incorporated into a FEM model for a specific deformation temperature more accurately predicts the real state of deformation within the PSC specimen.

The temperature distribution during PSC testing has been investigated using the FEM, microstructural investigation and microhardness analysis. With the strain and strain rate having being characterised, the temperature distribution has been investigated by considering the stored energy variation attributed to partially recrystallized microstructures and microhardness distributions for a particular combination of strain, strain rate and temperature. The study showed that the temperature distribution before and during PSC testing is not homogeneous. The inhomogeneous temperature distribution is attributed to the electrical resistance heating method employed to heat the PSC specimen. The inhomogeneity of temperature distribution was not characterised as it was beyond the scope of the study.

Acknowledgements

I would like to thank the following people who each in their own was made it possible for this dissertation to be completed.

My supervisor, Associate Professor R. Knutsen, for his supervision and guidance.

Dr. J. Basson for her enthusiasm, encouragement and guidance.

Mr. G. Newins and Mr. P. Jacobs for their time in the workshop in producing an endless number of specimens.

The Medical Imaging Unit's Dr. E. Meintjies for her assistance in using the reflex microscope.

Hulett Aluminium (Pitermaritzburg, South Africa) and Foundation for Research and Development (FRD) for funding of this thesis as well as their interest in the project.

Students and Staff in the Centre of Materials Engineering and the Centre for Research in Computational and Applied Mechanics (CERECAM) who made my university career that much more enjoyable.

Finally, to my parents for their unconditional support over the years. I wouldn't be where I am if it wasn't for you.

Table of Contents

CHAPTER ONE - INTRODCUTION

1.1 Project Background

Plane Strain Compression (PSC) testing is a test method used to simulate the deformation condition experienced during industrial rolling, namely that of plane strain, and is regarded as a suitable test method to simulate the thermo-mechanical variables experienced during industrial hot rolling on a laboratory scale. Consequently, the microstructural evolution that develops during industrial hot rolling can be investigated by analysing the microstructural development using the PSC test.

PSC testing allows control of the thermo-mechanical variables, being strain, strain rate and temperature. The mechanical variables, being strain and strain rate, are not homogeneous through the thickness of the deformed PSC specimen and for high strain rate deformation ($> 1\ sec^{-1}$) localized adiabatic heating occurs. For the PSC test to be successful in characterising microstructural evolution, the strain, strain rate and temperature distribution in the PSC specimen must be well characterised.

Since the friction condition and temperature distribution may be unique to the particular testing apparatus, these conditions need to be characterised in order to analyse the strain, strain rate and temperature distribution during a particular PSC test. A better understanding of the strain, strain rate and temperature distribution during PSC testing of aluminium would allow the microstructural development during hot rolling to be more accurately characterised.

The strain, strain rate and temperature distribution during PSC testing is therefore investigated for PSC testing of aluminium. The aluminium alloy used in the investigation is commercial purity aluminium alloy, AA1200, produced by Hullett Aluminium, Pietermaritzburg, South Africa.

1.2 Research Objectives

The objectives of this thesis are:

To predict the strain and strain rate distribution during PSC testing for any thermo-mechanical operating parameters.

To predict the temperature distribution during PSC testing for any thermo-mechanical operating parameters.

1.3 Experimental Approach

The experimental approach followed in pursuit of the research objectives is as follows:

- The Finite Element Method (FEM) is used to create a numerical model that approximates the thermo-mechanical variables experienced during a PSC testing event under specified nominal strain, strain rate and deformation temperature conditions.

- Visioplasticity experiments are used to investigate the friction condition between the specimen and the anvils when using graphite lubrication. The visioplastic results are used to verify and validate the friction condition by comparison with FEM strain and strain rate distribution results for different simulated coefficients of friction.

- Microscopy is used to investigate the microstructural evolution for different thermo-mechanical processing variables.

- Micro-hardness measurements are used to obtain a pattern that reflects a stored energy distribution within PSC specimens.

- The FEM is used to investigate adiabatic heating effects within PSC specimens deformed at high strain rate deformation.

CHAPTER TWO - LITERATURE REVIEW

The material under investigation is a commercial purity aluminium alloy, AA1200, containing 99-wt% Al with minor additions of Fe and Si. In order to assess the microstructural evolution for a predetermined thermo-mechanical process it is necessary to review the relevant literature on aluminium alloys and thermo-mechanical testing techniques.

2.1 Material

2.1.1 General Overview of Aluminium

Aluminium is an extremely useful engineering material due to a number of physical, chemical and mechanical properties. Aluminium is used extensively in applications of transport, packaging and building primarily due to its low density and good corrosion resistance. Pure aluminium has an ultimate tensile strength of approximately 90 MPa, with the main method for strengthening purity aluminium by strain hardening, which occurs during working operations[1].

2.1.2 Commercial Purity Aluminium

AA1200 is a non-heat-treatable aluminium alloy whose mechanical properties are determined by the process conditions associated with manufacture. AA1200 has a low tensile strength and good elongation in the annealed condition. Commercial purity aluminium is used extensively for extrusions, sheet and foil products due to its good workability and ductility[1].

2.1.3 Rolling of Aluminium

The control of grain size and texture development is at the core of quality control procedures in sheet metal production. A large grain size may be undesirable for reasons relating to strength and ductility or texture effects, which is important in controlling anisotropy[2].

Hot working is defined as the deformation process carried out above the recrystallization temperature of the metal, whilst cold working is performed below that temperature[1]. With the increase in the size of aluminium sheet ingots combined with more powerful mills, the tendency has been for higher temperatures to be retained during hot rolling and for larger reductions to be taken. Despite the strong recovery effect in aluminium, there

is a greater chance that recrystallization will occur during rolling[3]. Because of the effects of structural changes during fabrication on the properties of the final sheet, it is important to identify under what circumstances recrystallization takes place, to what extent and at what stage in the fabrication process.

2.2 Microstructural Evolution of Deformed Aluminium

Microstructural modelling of thermo-mechanical processing is a valuable process for optimising processing conditions. In order to control the microstructural evolution, texture development and mechanical properties of an alloy during an industrial thermo-mechanical treatment, it is necessary to predict the effect of the processing parameter on the material being produced. The deformed microstructure is thermodynamically unstable and on annealing, diffusive processes allow atomic-scale rearrangement, which results in a lowering of the stored energy of the deformed microstructure. The microstructural changes are complex and are strongly dependent on the metal, solute content and thermo-mechanical parameters of deformation[4].

The microstructural changes that take place during the deformation process are referred to as "dynamic" changes, and changes taking place during the interpass time as "static" microstructural changes. In order to understand the microstructural evolution during industrial working operations it is necessary to consider the characteristics of the two types of structural changes individually.

The principle factors governing microstructural evolution in association with hot rolling are[5]:

Dynamic Recovery

Static Recovery

Recrystallization Kinetics

Recrystallized grain size

Grain growth after recrystallization

2.2.1 Recovery and Recrystallization

The dislocation multiplication that occurs during plastic deformation leads to an increase in stored energy of the microstructure. Consequently, there is a driving force to reduce the stored energy. The processes whereby atomic-scale rearrangement lowers the stored energy of the deformed microstructure are known as recovery and recrystallization. Both recovery and recrystallization are related to the preceding deformation and are thermally activated processes driven by the stored energy arising from a particular combination of strain, strain rate and temperature.

Recovery and recrystallization can occur during deformation (dynamic recovery/recrystallization) and during subsequent deformation annealing treatments (static recovery/recrystallization); however, it is generally accepted that in most cases aluminium does not dynamically recrystallise, as there is no direct microstructural evidence after hot deformation[6].

2.2.1.1 Recovery

Recovery is the process of the reduction of the dislocation line energy stored during the deformation of the material. Recovery is the rearrangement of dislocations into lower energy configurations, subgrains, as illustrated in Figure 2.1. Subgrain boundaries contribute to recovery in three ways; by the formation of subgrains, by annihilating intruding free dislocations and by subgrain migration. Subgrains remain approximately equiaxed during deformation, unlike grains whose shapes depend on deformation[7].

Subgrain formation requires dislocation climb and cross slip to occur and is therefore a thermally activated process. Subgrains are not free of internal strains[7]. In metals with a high Stacking Fault Energy (SFE) such as aluminium, dislocation climb and cross slip can occur more easily and occurs extensively at high temperatures, and is often the only form of dynamic restoration[8].

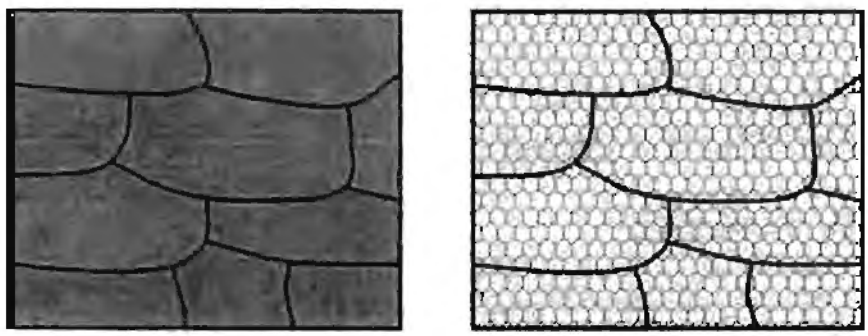

Figure 2.1 Stages of recovery: subgrains develop though annihilation and rearrangement of dislocations (after Humphreys and Hatherly[8]).

During the initial stages of deformation there is an increase in the flow stress as the dislocations interact and multiply. This initial work hardening is independent of temperature and strain rate[9]. However, as the dislocation density rises, so the driving force and hence the rate of recovery increases and during this period a microstructure of low angle grain boundaries and subgrains develops[10]. At a certain strain, dependent on temperature, the rates of dislocation initiation and annihilation reach equilibrium and the dislocation density remains constant, resulting in a steady state flow stress.

Aluminium is a Face Centred Cubic (FCC) metal that typically permits severe plastic deformation during processing without failure such as cracking or tearing. This is primarily due to the high SFE, which facilitates dynamic recovery during deformation.

2.2.1.2 Recrystallization

Following recovery, recrystallization takes place by the nucleation and growth of new strain free grains at the expense of the recovered structure. Preferred nucleation sites predominantly occur in a relatively small volume, where the amount of lattice distortion is large. The relatively strain free grains then grow and consume the recovered grains, resulting in a new grain structure with a lower dislocation density. The driving force for recrystallization is the unreleased portion of the stored energy after recovery has taken place[8]. The stages of recrystallization are illustrated in Figure 2.2.

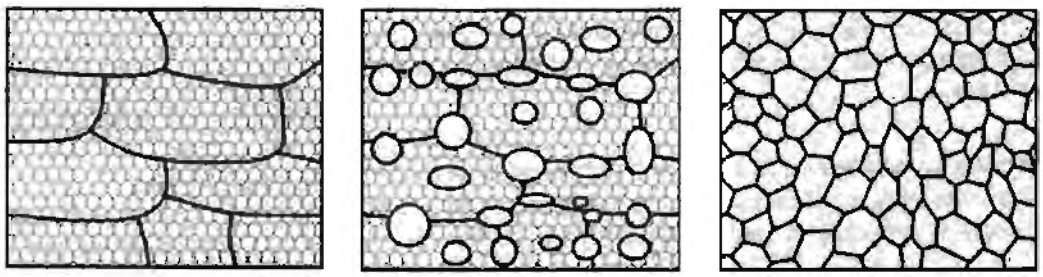

Figure 2.2 Stages of recrystallization (after Humphreys and Hatherly[6]). Nucleation occurring in regions of high misorientation, the newly forming grains impinge upon one another, after which grain growth will occur.

2.2.2 Microstructural Evolution during Hot Rolling

During hot rolling, the deformation is applied in a series of passes, which are separated by interpass times in which the metal will remain at rolling temperatures. Industrial multipass hot rolling of aluminium takes place at temperatures of between 300 and 500 °C and at strain rates of between 0.1 and 50 sec^{-1} [11]. The microstructural and textural development that take place during the rolling of aluminium are a result of complex interactions between thermal, mechanical and metallurgical phenomena[12]. Since the mechanical properties are dependent on the developed microstructure, it is necessary to predict the microstructural evolution during rolling in order to predict the mechanical properties of the final product.

At hot rolling temperatures, thermally activated deformation and restoration processes occur, and the microstructural evolution will depend on the strain, strain rate and temperature of deformation. By varying these parameters it has been possible to quantify deformation and annealing behaviour as a function of these parameters[5,13,14]. The Zener-Hollomon parameter (Z) is used to describe the deformation variables, and is given in Equation 2.1. Z is also known as the temperature compensated strain rate and is used to cover a range of thermo-mechanical variables by assuming that the temperature of deformation can be compensated by changes in strain rate or that the strain rate can be compensated by changes in temperature.

Equation 2.1 $$Z = \dot{\varepsilon} \exp\left(\frac{Q_{def}}{RT_{def}}\right)$$

Where Q is the activation energy of deformation for the material, R is the gas constant, T the deformation temperature and $\dot{\varepsilon}$ the strain rate.

During industrial hot rolling the thermo-mechanical parameters for each pass are not identical, and therefore the Zener-Hollomon parameter between passes is different. Furthermore, for each pass the strain and temperature distribution through the thickness and along the length of the workpiece is not homogeneous, thereby leading to a variation in Zener-Hollomon within the workpiece. This would lead to variations in microstructural evolution within the workpiece, thus resulting in variations in mechanical properties.

2.2.3 Success in Modelling Microstructural Evolution During Rolling of Aluminium

Static recrystallization and the recrystallized grain size are strongly influenced by strain, strain rate and temperature of deformation. The effect of the thermo-mechanical deformation parameters on static recrystallization can be represented by Equation 2.2, which characterises the time taken for 50% by volume of the material to recrystallise.

Equation 2.2

$$t_{0.5} = C\varepsilon^a Z^b d_0^c \exp\left(\frac{Q_{rex}}{RT_{rex}}\right)$$

The thermo-mechanical variables being incorporated by the ε and Z terms, ε being the prior strain and Z the Zener-Hollomon parameter given in Equation 2.1. Industrial hot rolling models should however include constitutive laws for both deformation and interpass stages to characterise microstructural evolution. The kinetics of static recrystallization is usually modelled using the Johnson-Mehl-Avrami-Kolmogrov (JMAK) approach. However, it has been found that equations that have been successfully used on steels have been less successfully used for aluminium alloys[2,11]. A more sophisticated description of the microstructural evolution is required for aluminium alloys, which considers recovery and textural evolution during deformation. Pure aluminium exhibits very high rates of dynamic recovery, which is expected to inhibit dynamic recrystallization.

2.3 Plane Strain Compression Testing

2.3.1 The Plane Strain Compression Test

The necessity to understand and predict grain size and texture development during thermo-mechanical processing requires a reproducible laboratory scale technique, to which PSC testing has proven adequate[15,16,17]. As part of an investigation of the hot working characteristics of aluminium, PSC testing is used to provide specimens for metallographic evaluation.

The PSC test is a method used to simulate the deformation conditions of plate rolling on a laboratory scale, namely that of plane strain. The PSC test allows control over thermo-mechanical variables, such as strain, strain rate and temperature and can therefore be used to describe the effect of these thermo-mechanical process variables on the microstructural evolution. In this way PSC testing can be used to quantify deformation and annealing behaviour as a function of strain and the Zener-Hollomon parameter.

2.3.2 The Origin of the Plane Strain Compression Test

The PSC test was suggested by Orowan[18] as a compression test method that might simulate the yielding condition of metals during rolling by inhibiting lateral spread. The plane strain condition results in a measured yield stress equal to 1.155 σ_0 (where σ_0 is the yield stress for homogeneous compression) according to the von Mises criterion. PSC testing has since been used to obtain material flow curve data and to examine the influence of deformation parameters on microstructural evolution.

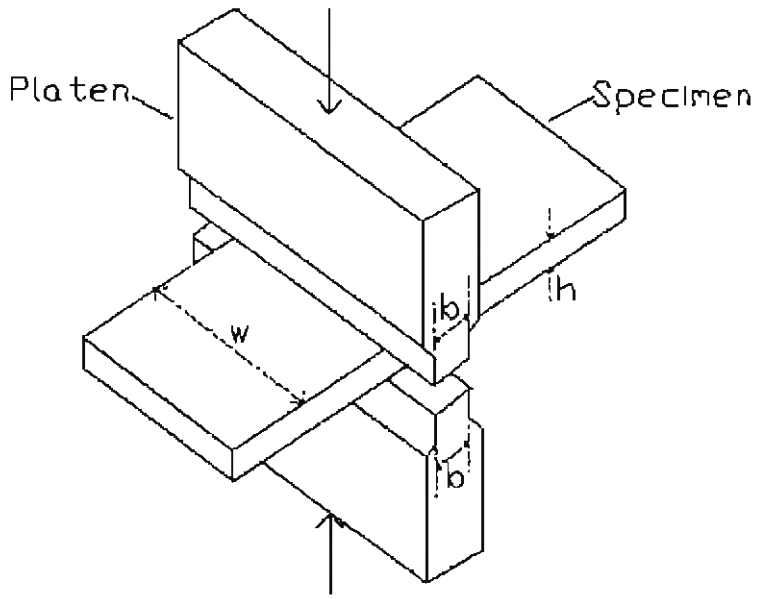

Figure 2.3 PSC test assembly (after Duckham[15]).

2.3.3 Strain Distribution

The strain distribution in the material between the anvils results from the material flow during compression. The material flow is governed by the prevailing slip line field, which represents a solution to the geometry configuration at a particular strain contained within the volume under the tools[19]. Slip line field theory was first demonstrated by Hill *et al*[19] who considered the problem of compression of a rectangular block of material between rough parallel anvils illustrated in Figure 2.4. Since the volume of the plastic-rigid material does not change, each incremental distortion in a state of plane strain consists of pure shear. It is therefore expected that the corners of the platens experience stress singularities and plastic zones will initiate at the sharp edges of the anvils as shown in Figure 2.4 (a). The shear lines will spread inwards until they meet in the geometric centre of the block[20]. The slip line field is then the portion of the material that is straining at any moment[21].

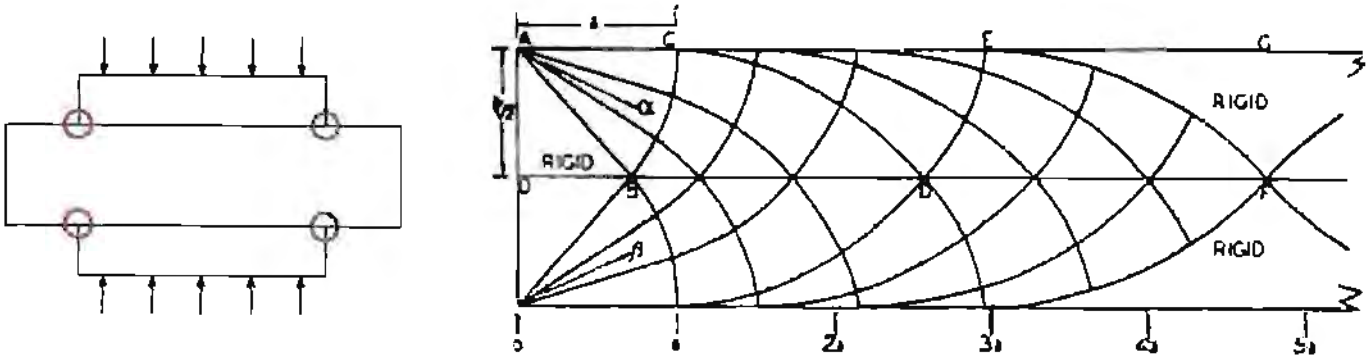

(a) (b)

Figure 2.4 (a) Area of strain singularity and (b) slip line field for compression between rough rigid platens (after Hill *et al*[19]).

The analysis of deformation patterns during PSC testing was originally proposed by making a distinction between compression between rough anvils[19] and compression between parallel smooth anvils[20]. These approaches contributed to the understanding of slip line field theory and it has been shown that different slip line fields develop for different friction conditions between anvil and specimen. The most simple slip line field arises when there is no friction, in which the slip lines in the specimen meet the anvil surfaces at 45° and the field consists of a series of straight-line crosses, which intersect at

the specimen mid-thickness plane. The number of crosses increases according to the tool width to specimen height ratio (b/h) as deformation occurs, starting with a single cross when b/h is equal to one[15].

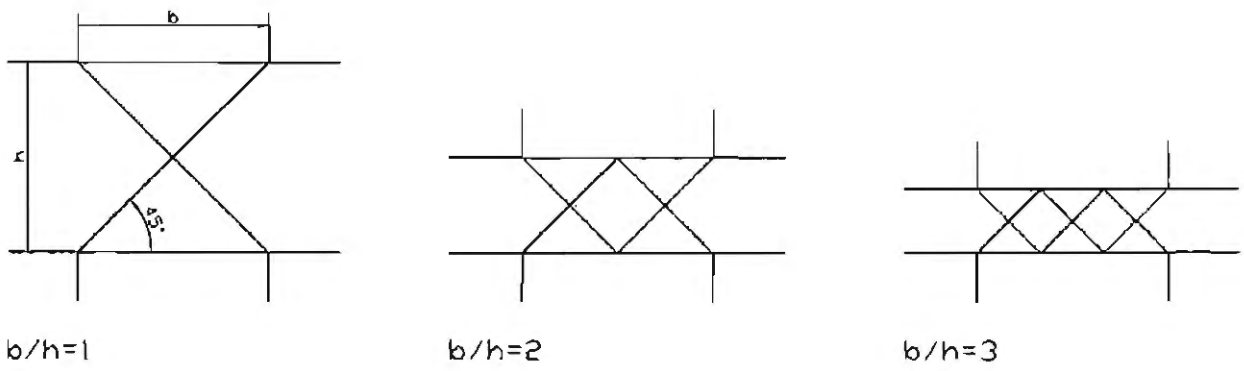

Figure 2.5: Slip line field for different geometry configurations assuming frictionless conditions.

Slip line field theory has been applied to PSC for various b/h ratios and has shown that the pattern of deformation is sensitive to b/h, in particular when the ratio is greater than one[20,22]. The deforming material initially passes through local shear zones forming a 'single cross' (for b/h = 1), but as deformation proceeds, the pattern changes to a 'double cross', and material passing through these shear zones will have received a variable amount of strain depending on its position in the specimen.

Measurements of the strain distribution during PSC testing show that the nominal strain does not change the pattern of strain developed during the test or the average value of strain in the active slip fields. It seems to depend on the b/h ratio, which determines the number of "crosses" in the slip line field[21].

2.3.4 The Limitations of Slip Line Field Theory

Slip line field theory assumes that the flow stress of the material is insensitive to strain, strain rate and temperature, and that the material suffers an instantaneous shear at a slip line. In practice, flow stress is sensitive to strain, strain rate and temperature, and the slip line field patterns consist of zones of localised shear rather than lines[21]. The use of PSC testing to simulate thermo-mechanical processing is further complicated by the fact that the strain distribution and corresponding variations in local temperature are particularly important for highly strain, strain rate and temperature sensitive processes such as static or dynamic recovery and recrystallization[21]. Advances in numerical simulation has however, allowed a more accurate determination of the slip line field accounting for all phenomena causing inhomogeneity.

2.3.5 Friction

In metal forming operations it is necessary to know the friction condition that exists between the tool and workpiece if calculation of strain and strain rate is required. This has been found to be of particular importance to PSC testing, where friction has been shown to have a profound effect on the strain distribution in the deformation zone of the specimen[23].

The presence of unavoidable friction forces at the specimen-anvil interfaces modifies the forces required to carry out straining, which results in an inaccurate determination of the stress-strain data. Alexander[23] and Shi *et al*[24] have noted that the surface conditions of the tool and work piece during PSC testing affect the nominal stress-strain curve due to variations in coefficient of friction. These effects mean that the measured effective stress is not equal to the anticipated value. An accurate prediction of the friction condition is therefore required for a numerical model to accurately predict the strain distribution in the specimen and force-displacement results.

Gelin[25] conducted PSC tests, which have shown that the increase in sample width with increasing strain depends on the specimen geometry (initial width in the transverse direction w_0 and initial height h_0) and lubrication condition. Gelin[25] used this method to estimate the coefficient of friction for PSC tests using a Coulomb friction model for PTFE film lubrication. In the investigation, numerous tests were conducted to different nominal strain values in order to obtain measurements of the transverse spread and the platen deformation distance. The correlation between spread and friction could then be determined independently through the use of a three-dimensional finite element model to approximate the friction condition.

2.3.6 Adiabatic Heating

Heat is generated by plastic deformation during high strain rate deformation, resulting in thermal softening. If the deformation occurs slowly, as in quasi-static loading conditions, most of the generated heat is conducted and/or convected away from the slowly deforming regions and the body remains in an isothermal condition[26,27].

Hot rolling is carried out at relatively high mean strain rates ($> 1\ sec^{-1}$), which may result in adiabatic heating. In order to investigate the influence of thermo-mechanical process variables on the microstructural evolution, PSC testing should simulate similar thermo-mechanical process conditions experienced during industrial rolling operations. During PSC testing the strains and strain rates are not homogeneous through the section of the workpiece. Therefore, the heat generated by deformation will result in localized through-thickness variations in temperature during deformation. Heat will also be lost at the specimen surfaces when the specimen is heated internally to temperatures above the temperatures of the anvils. Since the material flow is strain rate and temperature sensitive, the inhomogeneity of conditions within the specimen will usually increase with strain. Such localized variations in thermo-mechanical parameters are important because of the relationship between the deformation condition and the resulting microstructure.

During deformation most of the mechanical work is converted into heat, producing an average temperature rise, ΔT. In the absence of any changes in internal energy, this is given by Equation 2.3.

Equation 2.3
$$\Delta T = \frac{1}{\rho c}\int_{0}^{\varepsilon'} \sigma d\varepsilon - H(T_O, T_S)$$

Where ρ is the density, c the specific heat of the deforming material, ε' is the maximum strain, and $H(T_0,T_s)$ is a function of the external temperature and surface temperature of the material which represents the heat loss. The above equation assumes that all energy generated by plastic work is converted into heat.

Timothy *et al*[16] investigated the adiabatic temperature rise and assumed that 95% of the plastic work per unit volume is dissipated as heat and that the adiabatic heating results in a temperature change of:

Equation 2.4 $$\Delta T < 0.95\sigma_{ss}\frac{\varepsilon}{\rho c}$$

Where σ_{ss} is the steady state flow stress during hot working, ε is the equivalent plastic strain, ρ is the density and c is the specific heat capacity of the material.

2.4 Finite Element Analysis

The Finite Element Method (FEM) was part of an overall effort by both engineers and mathematicians to discritize continuum problems. The FEM appeared in the metal forming field in the seventies, and has since been used extensively in metal plasticity studies with the aid of sophisticated Finite Element (FE) programs. The use of the FEM in metal plasticity problems can provide accurate approximations to the real solution.

2.4.1 The Finite Element Method

The FEM is a numerical procedure for analysing structures and continua, and is used to solve problems that are too complicated to be solved satisfactorily by classical analytical methods[28]. The FEM has been stated as follows: "The FEM is a computer-aided mathematical technique for obtaining approximate numerical solutions to the abstract equations of calculus that predict the response of physical systems subjected to external influences"[29].

The practical benefits of the FEM are usually associated with problems involving complex geometry in 2D, 3D, or highly nonlinear behaviour. This is because the governing differential equations of these problems do not lend themselves to be solved by analytical methods[30]. The FEM is extensively used in the fields of solid mechanics (elasticity, plasticity, statics and dynamics), heat transfer (conduction, convection and radiation) and fluid mechanics (flow fields).

The FEM models a structure as an assemblage of small elements. Each element is of simple geometry and is therefore more easily analysed than the complete structure. The FEM result is an approximation to a real solution by a model that consists of a piece-wise continuous solution[28].

In determining the piece-wise solution of elements, the FEM focuses on particular points or 'nodes' in the solution region. The element is derived by assuming an element stiffness, which is dependent on internal nodal displacements[30]. The FEM often requires the evaluation of surface integrals, that is the regions of integration between subdivisions of the solution region. Matrix algebra is the method of assembly of the linear algebraic equations that are used in the FEM formulation, which are conveniently used in computer algorithms. Similar to Hooke's law for a spring, a matrix of coefficients becomes the "stiffness matrix" that relates the external forces to the nodal displacements.

Equation 2.5 $$\{F\} = [K]\{d\}$$

Where, F, K and d are the force vector, stiffness matrix and displacement vector respectively.

In summary the FEM is a discritization procedure of continuum problems posed by mathematical statements[31]. Zienkewicz[31] summarises the FEM as follows:

1. The continuum is separated by imaginary lines into a number of 'finite elements'.
2. The elements are assumed to be interconnected at a discrete number of nodal points. The displacements of these nodal points are the unknown parameters of the problem.
3. A set of functions is chosen to define the state of displacement within each 'finite element' and on its boundaries in terms of nodal displacements.
4. The displacement functions now define the state of strain within an element by evaluation of the nodal displacements. These strains, together with any initial strains and the constitutive properties of the material, will define the state of stress throughout the element and its boundaries.

2.4.2 The FEM and PSC

PSC tests are most often performed when the rheological parameters of a material in a metal forming operation need to be determined. PSC testing has the advantage over tensile testing in that nominal strain values of up to 2.5 can be achieved. However, due to the heterogeneous deformation of the PSC test, interpretation of the results is complex[17]. The heterogeneous deformation is due to friction between tool and specimen, and tool and specimen geometry. FEM simulation of plastomeric tests allows the prediction of the real state of deformation, accounting for phenomena causing the inhomogeneity.

Traditional interpretation of compression tests results is based on the assumption of homogeneous strain and temperature distribution in the deformation zone. By considering the inhomogeneity of deformation caused by friction, tool geometry and nonuniform temperatures resulting from deformation heating, the FEM would allow approximation of the strain, strain rate and temperature. Application of the FEM to the simulation of the PSC test enables a consideration of real state of deformation by the evaluation of the local values of strains, strain rates and temperatures.

Kowalski[17] used the FEM to investigate the mechanical variables during PSC testing and concluded that the full interpretation of the results of the PSC test presented serious difficulties, since the test involves significant inhomogeneity of deformation, resulting in local strain, strain rate and temperature variation from nominal values.

Numerical modelling also allows the external variables to be varied to find out what effect they may have on the result, which can be used to justify approximations. This process mimics the actions which the experimenter might take. The internal variables, such as friction and material properties, are not under the control of the experimenter, but their values will affect the conclusions to be drawn from modelling[27].

2.4.3 The Use of the FEM for Metal Plasticity Problems

The FEM has attracted extensive use in the field of metal plasticity with a wide range of FEM codes that incorporate specialized and general metal plasticity capabilities.

The purpose of the FEM is to create a numerical model that behaves mathematically like the system that is being modelled. This requires that material properties, loads and boundary conditions of the system be accurately incorporated into the numerical model in order for the model to approximate the behaviour of the system.

When using the FEM to approximate a solution, it is necessary to evaluate the accuracy and detail to afford the analysis. It is often necessary or possible to make approximations or assumptions to be used in the analysis. Assumptions and approximations should be made to ensure that acceptable results are obtained. A Finite Element Analysis (FEA) will generally always contain assumptions that will lead to errors in the predictions of nodal displacements, and consequent errors in the result. It is therefore necessary to investigate the sensitivity of the solution to these parameters.

2.4.4 The Nonlinear Analysis

In structural mechanics a problem is considered to be nonlinear if the stiffness matrix or load vector is dependent on displacement. Nonlinearity of structural systems can be classed as material nonlinearity, which is associated with changes in material properties, or geometric nonlinearity, which is associated with changes in structural configuration. For a problem stated in Equation 2.5 as $\{F\}=[K]\{d\}$, in a linear analysis $[K]$ and $\{F\}$ are independent of $\{d\}$, whereas in a nonlinear analysis $[K]$ and/or $\{F\}$ are functions of $\{d\}$[28]. The classifications "linear" and "nonlinear" are artificial in that a solution can be satisfactorily approximated by linear solution methods[28].

2.4.4.1 Material Nonlinearity

A material is called nonlinear if the stresses {σ} and strains {ε} are related by a strain-dependent matrix rather that a matrix of constants. Thus the computational difficulty is that equilibrium equations must be written using material properties that depend on strains, but strains are not known in advance[28]. Figure 2.6 illustrates a typical flow curve for a metal. It can be seen that the stiffness changes for increasing strain, which is illustrated by tangent stiffness lines at different strain values.

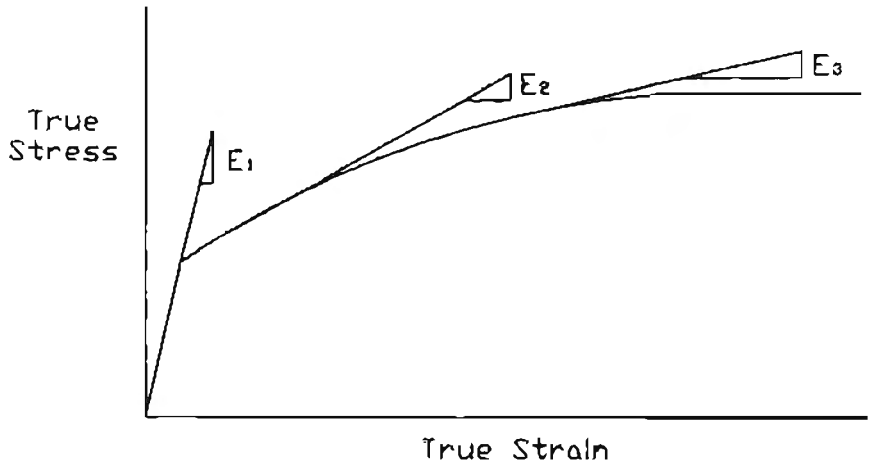

Figure 2.6 Material nonlinearity, illustrating the tangent stiffness at different strain values ($E_1 > E_2 > E_3$).

2.4.4.2 Geometric Nonlinearity

Geometric nonlinearity arises due to deformations that significantly alter the location or distribution of forces, therefore equilibrium equations must be written with respect to the deformed geometry, which is not known in advance[28]. The use of a geometric nonlinear algorithm attempts to obtain equilibrium between the deformed structure and the applied loads. Geometric nonlinearity is illustrated in Figure 2.7, where initially the stiffness of the rod is independent of geometry; however, once a critical force is reached the rod begins to deflect. The force required to produce further deformation is dependent on the geometry of the deforming structure.

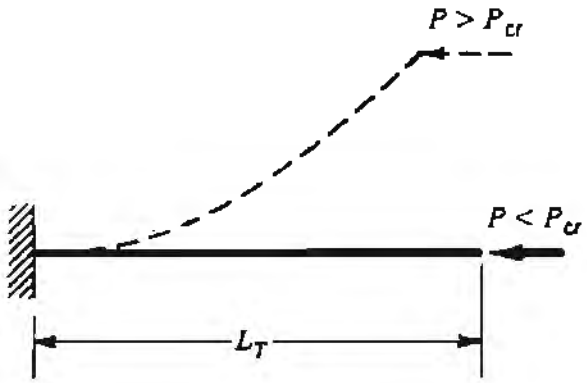

Figure 2.7 Geometric nonlinearity arising from changes in geometry of the beam as the load P is increased above a critical value P_{cr} (after Cook *et al*[28]).

2.4.4.3 Nonlinear Solution Methods

A time-independent nonlinear problem as stated in Equation 2.5, $\{F\}=[K]\{d\}$, where $\{F\}$ is known and $[K]$ is a function of $\{d\}$, can be calculated for a given $\{d\}$. In order to simulate a nonlinear problem, the stiffness $[K]$ is composed of a constant term $[K_O]$ and a term $[K_{NL}]$, which depends on nodal displacements. Therefore, displacement $\{d\}$ is caused by load $\{F\}$ and is given by $\{F\}=[[K_O] + [K_{NL}]]\{d\}$. It is assumed that $[K_{NL}]$ is known in terms of $\{d\}$, and therefore $\{F\}$ can be calculated in terms of $\{d\}$. Since the nodal displacements are not known in advance an explicit solution for $\{d\}$ in terms of $\{F\}$ is not possible. Instead, an iterative method is required to determine $\{d\}$[28].

2.4.5 The Friction Condition and the FEM

Friction is an important factor that must be considered during metal forming processes. The surface characteristics of both the workpiece and the tool influence the frictional behaviour during the forming process. Determination of the friction condition is important in order to produce an accurate model for numerical simulation. For a FEM model, an accurate determination of the friction condition will improve the quality of the numerical results. During a forming process the load is transferred from the tool to the workpiece, with friction influencing the direction of the resultant force at the surface of the workpiece. Furthermore, the applied forces change the surface structure, which would lead to differential friction conditions during the forming operation.

For metal forming operations the friction condition depends on several variables, namely contact pressure, sliding speed, workpiece and tool material, surface roughness and lubricant. The friction condition affects the material flow and therefore the strain and strain rate distribution during the forming process.

2.4.6 Material Properties

Constitutive equations that relate the flow stress of a material with a known initial microstructure to strain, strain rate and temperature are an essential input for numerical modelling of thermo-mechanical processing operations[32]. For metals and alloys that undergo dynamic recovery the stress-strain relationship should fulfil several important conditions, which have been summarized by Kocks[33]. First, the flow stress curve of the annealed material must display a finite yield stress at the onset of plastic flow. Second, the initial work hardening rate should be independent of both temperature and strain rate, whereas the work hardening behaviour at large strains should be strongly dependent upon these parameters. Third, it is important that the stress-strain relationship be able to predict the achievement of a saturation stress once sufficiently large strains have been applied to the material[9].

These conditions impose severe restrictions to the form of the stress-strain relationship, the most commonly used being of the exponential saturating form as proposed by Sah[34].

Equation 2.6

$$\sigma = \sigma_{ss} - \left(\sigma_{ss} - \sigma_0\right) \exp\left(-\frac{\varepsilon}{\varepsilon_r}\right)$$

Equation 2.7

$$\sigma = \sigma_0 + \left(\sigma_{ss} - \sigma_0\right)\left[1 - \exp\left(-\frac{\varepsilon}{\varepsilon_r}\right)\right]^n$$

Equation 2.8

$$\sigma = \left[\sigma_{ss}^2 - \left(\sigma_{ss}^2 - \sigma_0^2\right)\exp\left(-\frac{\varepsilon}{\varepsilon_r}\right)\right]^{\frac{1}{2}}$$

In the above equations, σ_0 represents the initial flow stress at the onset of plastic deformation, σ_{ss} is the steady state flow stress and ε_r the relaxation strain, which is the strain required to achieve some particular value of hardening fraction $(\sigma-\sigma_0)/(\sigma_{ss}-\sigma_0)$. σ and ε represent the effective stress and effective strain and constant n represents a strain-hardening exponent taken as 0.5.

The correlation of σ_0 and σ_{ss} with temperature and strain rate was suggested by Sellars and Tegart[35] based on the hyperbolic sine relationship and the Zener-Hollomon parameter, Z:

Equation 2.9

$$Z = \dot{\varepsilon} \exp\left(\frac{Q}{RT}\right) = A\left[\sinh\left(\alpha\sigma_p\right)\right]^{m'}$$

Where $\dot{\varepsilon}$ represents the effective strain rate, Q the experimental deformation activation energy, R the universal gas constant, A the pre-exponential constant, α and m' the stress-sensitivity parameters to be correlated to experimental data.

2.5 Visioplasticity

Visioplasticity is a test method used to determine the deformation path within a workpiece during large deformation forming operations. The technique consists of placing a grid on the surface of the workpiece and measuring the distortion of the grid after an incremental deformation as shown in Figure 2.8. The displacements, strains and strain rates can then be determined. In visioplasticity investigations it is assumed that each nodal point moves in a straight line to its final point, and the displacement of each node is obtained by a subtraction of the original co-ordinates from its final co-ordinates. Visioplastic results can then be compared with FEM predictions.

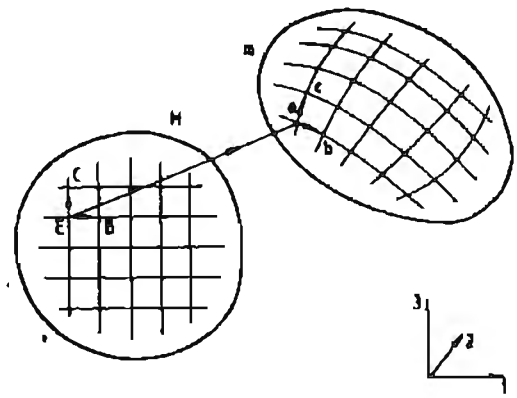

Figure 2.8 Visioplastic grid used to obtain incremental strain (after Beynon and Sellars[36]).

The ability to reproduce the complex strain history is based on the physical significance of equivalent strain. Equivalent strain is an invariant function used to simplify a complex state of strain by combining shear and compressive/tensile strains as a single scalar parameter. It is then possible to determine the variation in total equivalent strain through the thickness of the specimen and to simulate the deformation process.

Visioplasticity has been used successfully by Colas and Sellars[21], and Beynon and Sellars[36], in the analysis of the strain distribution during PSC testing. The method involved splitting the specimen on the longitudinal axis of symmetry, scribing a grid on the cross-sectional surface, clamping the half specimens together and performing the test. Using this technique the calculation of the equivalent strain can be obtained.

2.6 Hardness-Strain Correlation

During metal working processes, the workpiece strain hardens as a result of plastic deformation. Hardness measurements can therefore be used to gauge the level of plastic strain of the deformed workpiece. In cold deformation processes the effects of recovery and recrystallization are negligible and the strain hardening of the workpiece is preserved. Therefore, microhardness measurements can be used to quantify the local accumulated plastic strain.

Tensile and microhardness tests can be used to establish a correlation between the plastic strain and hardness. In this way, microhardness measurements can be performed on the cold worked specimens to obtain a strain distribution pattern within the deformation zone. The measured strain distribution can then be compared to FEM approximations. Matching the measured and predicted strain verifies the FEM model.

Tseng *et al*[37] used the hardness-strain correlation in the analysis of the strain distribution during the rolling of steels. However, elevated temperature testing could not be used due to extensive softening occurring during deformation, resulting in little variance in hardness measurements in the deformation zone.

CHAPTER THREE - EXPERIMENTAL METHOD

Given the complexity of determining the microstructural evolution during industrial hot rolling, it is necessary to start from high purity alloys, for which precipitate structures do not evolve during deformation, and to carry out laboratory controlled experiments as industrial trials are not feasible. Laboratory tests must involve simple deformation paths that reproduce the deformation characteristics of hot rolling. It is generally accepted that PSC testing is a satisfactory test method to fulfil these conditions.

The following chapter describes the experimental method and procedures used to interpret the PSC test.

3.1 Material

3.1.1 Chemical Composition

The alloy employed in this investigation is an aluminium alloy, AA1200, which is a commercial purity aluminium containing minor additions of Si and Fe which are known to reduce recovery of purity aluminium alloys[3]. The chemical composition limits of the alloy is indicated in Table 2.1.

Cu	Si + Fe	Mn	Zn	Ti	Balance
0.05	1.0	0.05	0.1	0.05	0.15

Table 2.1 Maximum chemical composition limits (in wt%), aluminium 99.00-wt% minimum[1].

3.1.2 Material History

The material was supplied by Hulett Aluminium Rolled Products (Pty) Ltd., Pietermaritzburg, South Africa, in the form of transfer bar ex foilstock process (23.3 mm gauge). The microstructure of the as received material is indicated in Figure 3.1. The retained rolled microstructure illustrates elongated grains in the rolling direction. It was therefore necessary to perform an annealing treatment in order to obtain a homogeneous equiaxed grain structure. The material was annealed for 30 minutes in an air furnace at a temperature of 400 °C with the intention of producing a finer equiaxed recrystallized grain structure. An annealing time of 30 minutes was consistently used, as it is known that the homogenisation treatment can markedly influence the degree of recrystallization during subsequent annealing treatments following deformation.

The microstructure of the as received and annealed material is illustrated in Figure 3.1 (a) and Figure 3.1 (b) respectively. Figure 3.1 (a) reveals a partially recrystallized microstructure.

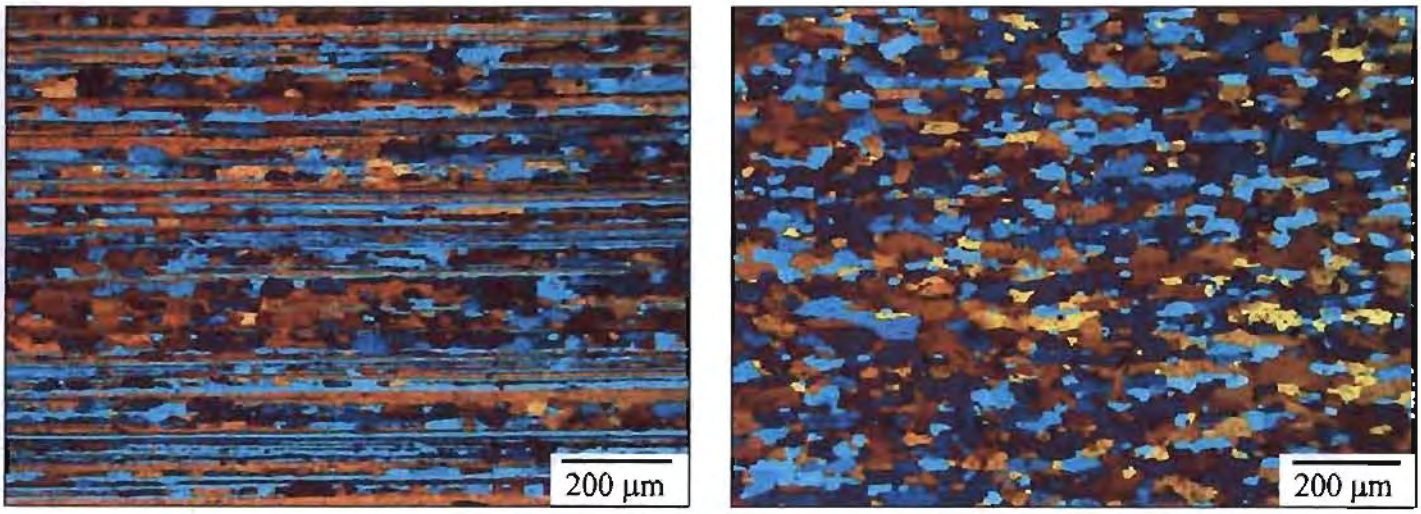

(a) (b)

Figure 3.1 The (a) as received and (b) annealed microstructures.

3.2 Plane Strain Compression Testing

3.2.1 The Plane Strain Compression Apparatus

A typical PSC testing assembly is illustrated in Figure 3.2. A specimen of width (w) and thickness (h) is compressed between two platens of breadth (b). As crosshead movement of the platen occurs, the specimen thickness is reduced, with material flow in the length direction (rolling direction) and minimal flow in the width direction (transverse direction). PSC testing attempts to simulate the deformation condition of plate rolling, namely that of plane strain. However, the plane strain condition requires that negligible deformation should occur in the width direction. The PSC geometry and specimen geometry established by Duckham[10,15] were used in the present investigation. For a detailed description of the PSC rig used in the present investigation shown in Figure 3.3, as well as the testing capabilities and testing procedures, refer to Duckham[10].

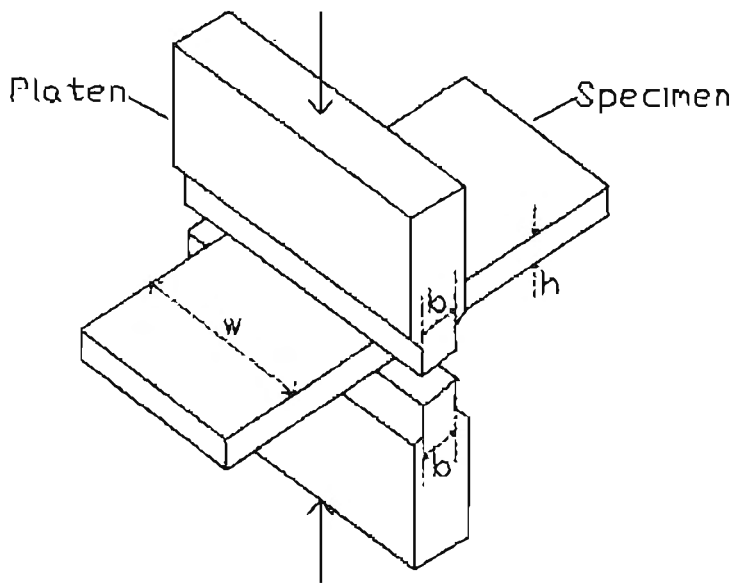

Figure 3.2 PSC testing assembly (after Duckham[10]).

(a)

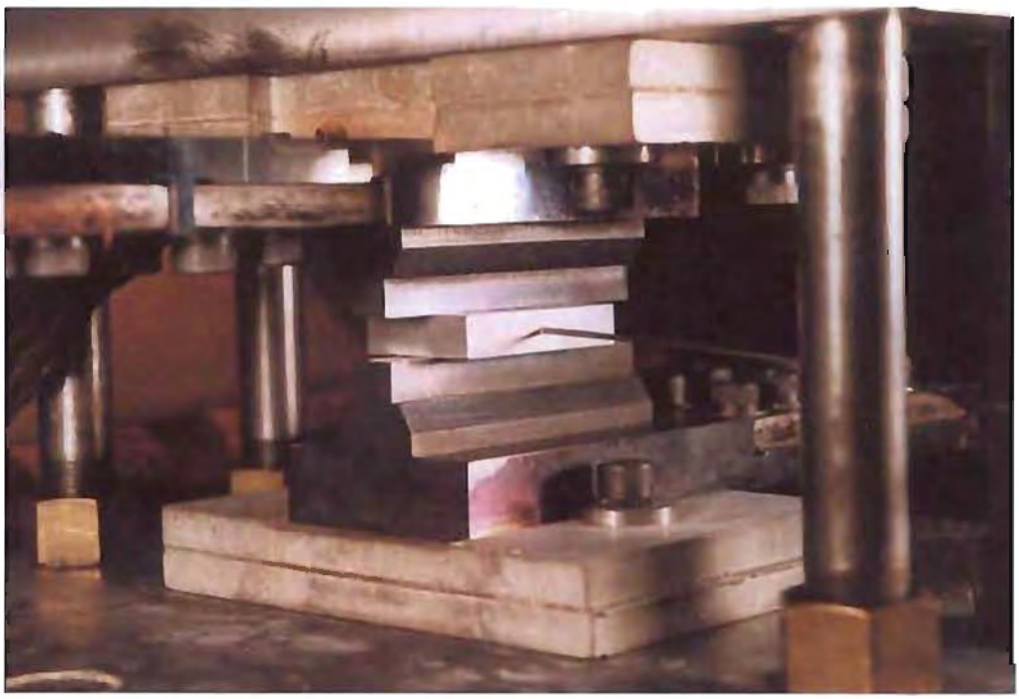

(b)

Figure 3.3 PSC rig: (a) general view of apparatus, (b) close up of a specimen before being compressed between the anvils.

For a rigid plastic material, deformation under plane strain conditions is pure shear strain. Applying the von Mises stress criterion, the stress and strain are given by:

Equation 3.1 $$\sigma = \frac{2}{\sqrt{3}}\sigma_0$$

Equation 3.2 $$\varepsilon = \frac{\sqrt{3}}{2}\varepsilon_0$$

Where σ and ε are the stress and strain measured in plane strain compression respectively, and σ_0 and ε_0 are the stress and strain measured in homogeneous compression respectively.

3.2.2 Specimen Geometry

Plane strain compression specimens of 10 mm thickness, 33 mm width and 52 mm length were machined from the as received transfer bar (AA1200 foilstock material). The as received material had a gauge of 23.3 mm. In order that specimens are symmetric with respect to the initial microstructure, specimens were machined from the centre thickness of the hot rolled plate. The specimen orientation was such that the simulated rolling direction coincided with the plate rolling direction, as shown in Figure 3.4.

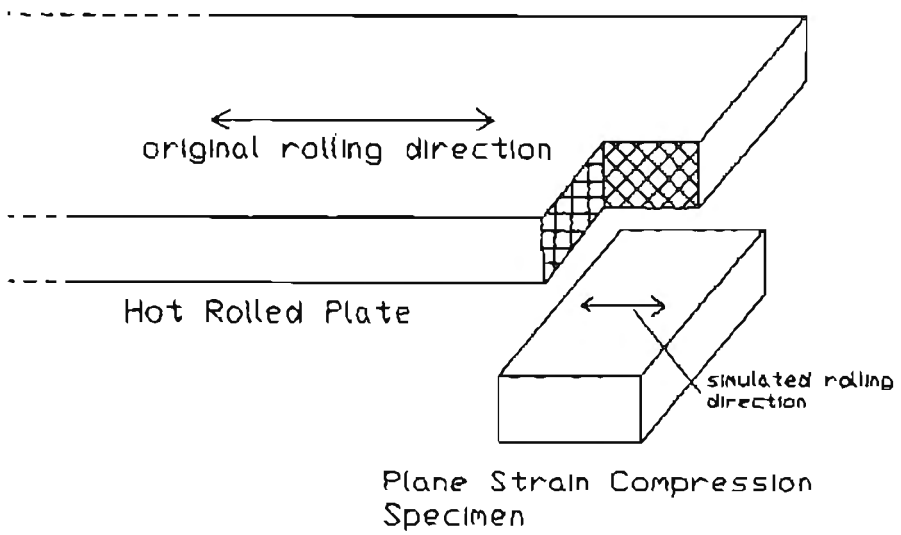

Figure 3.4 PSC specimen orientation with respect to rolled plate (after Duckham[10]).

3.2.3 Specimen Heating

Direct electrical resistance heating was used to heat specimens for high temperature testing. High amperage current is passed through the specimen in contact with the anvils. The specimen is in turn heated due to the material's resistance to current. The temperature of the specimen is measured by a thermocouple inserted in a hole drilled into the side of the specimen as shown in Figure 3.3 (b).

Electrical resistance heating on this particular PSC rig has previously been investigated both experimentally and using a coupled thermal-electrical analysis[38]. The results of the investigation concluded that the temperature distribution before compression was homogeneous. However, the temperature of the anvils was found to have a varying temperature distribution resulting in heat being conducted away from the specimen surface during compression. This would therefore need to be considered in the FEA of high temperature PSC testing.

3.2.4 Friction Condition

The aluminium specimens were lubricated with a graphite lubricant spray and graphite powder, which allows for electrical conduction for heating of the specimen. Specimens were ground to a 1200 grit finish on silicon carbide paper before lubrication was applied. The graphite powder and spray combination was effective; however, the lubrication appeared to break down at temperatures above 400 °C. The breakdown of the lubrication is therefore investigated in this work as it causes variations in strain distribution within PSC specimens. A varying friction condition is thus another variable to consider when determining the strain distribution within the PSC specimen.

3.2.5 Quenching of Specimens

Immediately following deformation the specimens were quenched in water to prevent static annealing of the deformed microstructure. This was achieved by manually removing the specimen from the PSC testing apparatus and placing the deformed specimen into water at room temperature. It was possible to quench specimens consistently within 1 second following deformation.

3.2.6 Heat Treatments

In order to study the recrystallization behaviour, deformed PSC specimens were subjected to various annealing treatments in a salt bath at temperatures between 300 and 460 °C. The salt bath was used, as opposed to an air furnace, to enable rapid heating of specimens, and would allow short annealing treatments to be performed in order to produce partially recrystallized microstructures. The partially recrystallized microstructures would be a direct indicator of the stored energy to be used for verification and validation of the FEM model.

3.3 Finite Element Analysis

The present investigation is an attempt to establish the thermo-mechanical variables for PSC testing of aluminium on the apparatus designed by Duckham[10] at the University of Cape Town, South Africa. A coupled thermal-displacement analysis is used to approximate the thermo-mechanical parameters within the PSC specimen during testing. The model is based on implementing a model using ABAQUS[39] 6.21 Standard, an implicit general-purpose module that can solve a wide range of linear and nonlinear problems.

3.3.1 Brief Review of a FEM Model

The first step of a FEM simulation is to discritize the actual geometry of the structure using a collection of finite elements. Each element represents a discrete portion of the physical structure and is joined by a set of nodes. The collection of nodes and finite elements is called the mesh. The displacements of the nodes are fundamental variables calculated by ABAQUS[39] during a stress analysis. Once the nodal displacements are known, the stresses and strains in each element can be determined.

3.3.2 Geometry of the Model

The particular geometry used to model the PSC test is representative of the PSC test (see Figure 3.5), as symmetry allows an eighth model to be used for both the specimen and the anvils. This is because the model behaviour is assumed to be symmetric about the centre line of the Normal Direction (ND), Rolling Direction (RD) and Transverse Direction (TD).

Figure 3.5 Eighth model of the PSC specimen.

3.3.3 Element Selection

Eight noded reduced integration continuum elements were used to model the specimen, whilst the anvils were approximated to be perfectly rigid. These elements were used for reduced computational expense, but at the same time providing a fine mesh. ABAQUS[39] recommends the use of a fine mesh of linear, reduced integration elements for large mesh distortions, and since in general it is better to use first-order elements for those parts of the model that will form the slave surface in contact analyses. The slave surface being the specimen surface.

3.3.4 Analysis Type

Coupled thermal-displacement analysis using ABAQUS 6.21 Standard. Standard is a general purpose FEA module that can solve a range of linear and nonlinear problems.

3.3.5 Material Properties

Constitutive equations that relate the flow stress of a material with a known initial microstructure to strain, strain rate and temperature are an essential input for numerical modelling of a thermo-mechanical processing operation. The investigation uses the relationship for equivalent flow stress, σ, as a function of equivalent strain, ε, as proposed by Sah *et al*[84] and used by Shi *et al*[82] in determining constitutive equations for commercial purity aluminium.

Equation 3.3

$$\sigma = \sigma_0 + \left(\sigma_{ss} - \sigma_0\right)\left[1 - \exp\left(-\frac{\varepsilon}{\varepsilon_r}\right)\right]^n$$

Where σ_0 is the initial flow stress, σ_{ss} is the steady state flow stress, ε_r is the transient strain constant, and n is a constant, which from the relationship between stress and dislocation density is expected to be 0.5.

The parameters σ_0, σ_{ss} and ε_r must be expressed in terms of strain rate ($\dot{\varepsilon}$) and temperature (T), and for this purpose the Zener-Hollomon parameter (Z) combines the effects, where R is the gas constant and Q is activation energy for deformation. The relationship is given in Equation 3.4, where the use of the hyperbolic sine is used to cover the range of stresses.

Equation 3.4

$$Z = \dot{\varepsilon}\exp\left(\frac{Q_{def}}{RT_{def}}\right) = A\left[\sinh\left(\alpha\sigma_p\right)\right]^{n'}$$

The constitutive equations proposed by Shi *et al*[42] for commercial purity aluminium combined with tensile, compression and PSC testing of the material under investigation allowed determination of constants A, α and m', given in Table 3.2. The constants were determined by varying the values determined by Shi *et al*[42] to approximate experimental flow curve data. In Table 3.2 original constants determined by Shi *et al*[42] are indicated by a *.

σ	α	m'	A
σ_0	0.1	11.0	4.00×10^{11}
σ_{01}	0.0445 *	4.5	1.52×10^{11} *
σ_c	0.027	5.0	1.96×10^{11} *

Table 3.2 Constants for constitutive flow stress relationship for experimental alloy.

The Young's Modulus used in the FEA is 70 Gpa. Temperature dependence is not used since the elastic strain is negligible in comparison to the plastic strain.

3.3.6 Adiabatic Heating

Heat is generated by plastic deformation during high strain rate deformation, resulting in thermal softening. Hot rolling is carried out at relatively high mean strain rates (>1 sec^{-1}), which may result in adiabatic heating. In order to investigate the influence of thermo-mechanical process variables on the microstructural evolution, PSC testing should simulate similar thermo-mechanical processing conditions experienced during industrial hot rolling. During PSC testing the strain distribution is not homogeneous through the thickness of the specimen, which may result in localized heating. This would result in a variation in thermo-mechanical variables within the PSC specimen, which can in turn be related to the Zener-Hollomon parameter to predict microstructural evolution. The material properties used in the FEA to investigate adiabatic heating during PSC testing are given in Table 3.3. The values of thermal conductivity, specific heat and density were selected from generalised material properties of aluminium.

Inelastic Heat Fraction	Thermal Conductivity (W/m.K)	Specific Heat (J/kg.K)	Density (kg/m^3)
0.95	200	910	2700

Table 3.3 Inelastic heat fraction and material properties used in FEM model[16,40].

3.3.7 Boundary Conditions

Boundary conditions must be applied to the FEM model in order that the model behaviour is assumed to be representative of the PSC test.

3.3.7.1 Displacement and Rotation

Displacement and rotation boundary conditions were applied to the symmetry planes of the PSC specimen in the RD, ND and TD so that deformation would be symmetric and that the one-eighth model approximation would be valid.

Displacement and rotation boundary conditions were similarly applied to the anvil in order that one-eighth symmetry be maintained and that the anvil crosshead speed is adjusted for constant strain rate deformation.

3.3.7.2 Thermal

For elevated temperature simulation the temperature of the PSC specimen before deformation was assumed to be homogeneous as determined by Jahajeeah[38]. A temperature boundary condition was applied at the specimen-anvil interface, with conduction occurring to the anvil where the temperature at the anvil-specimen interface is the initial test temperature during the test.

3.3.7.3 Surface Interaction

A Coulomb friction model was used to approximate the friction condition between contacting surfaces as given in Equation 3.5.

Equation 3.5 $$F = \mu N$$

3.3.8 Solution Procedure

ABAQUS[39] uses a Newton-Raphson iterative method to obtain solutions for nonlinear problems. In a nonlinear analysis the solution cannot be calculated by solving a single system of equations, as would be done in a linear analysis. Instead, the solution is found by applying the specified loads gradually and incrementally working toward the final solution. Therefore the simulation is broken down into a number of load increments and finds the appropriate equilibrium configuration at the end of each load increment. It therefore often takes several iterations to determine an acceptable solution to a given load increment. The sum of the incremental responses is the approximate solution for the nonlinear analysis.

3.3.9 The Plane Strain Condition

In PSC testing, there is always some spread in the TD. If the initial breadth is not large, the spread is not negligible and the stress and strain in the specimen are significantly affected. Figure 3.6 shows the strain in the TD for a corresponding nominal strain for the chosen specimen geometry detailed in Section 3.2.2. The nominal strain was calculated assuming plane strain compression and the von Mises criterion was used to obtain an equivalent plastic strain[21]. The average strain in the TD is 0.09 per unit strain in the ND for the test data in Figure 3.6. Since a true plane strain condition does not exist, it is therefore necessary to determine whether a plane strain FEM model would accurately approximate the PSC test or whether a three-dimensional model should be used.

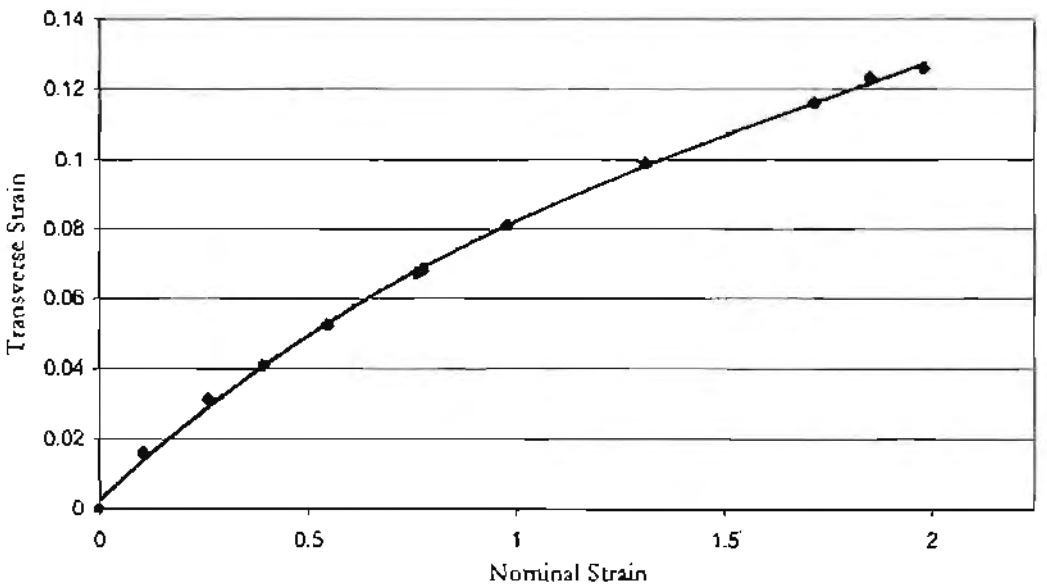

Figure 3.6 Nominal normal strain vs. nominal transverse strain for tests performed at room temperature at a strain rate of 0.1 sec^{-1}, for the chosen specimen geometry detailed in Section 3.2.2.

3.3.10 FEA Type

In order to determine whether the strain in the TD is negligible for the PSC testing technique and that the plane strain condition exists, a comparison of a plane strain and three-dimensional analyses was required. In the plane strain analysis the strain in the TD is assumed to be negligible in comparison to the strain in the ND, whereas the three-dimensional analysis models the PSC test accounting for the spread in the TD. Figure 3.7 (a) and (b) illustrate the variation in Peak Equivalent Plastic Strain (PEEQ) along a path along the centre line in the RD and ND for the plane strain and three-dimensional analysis at 250 °C at nominal strains of 0.5 and 1.

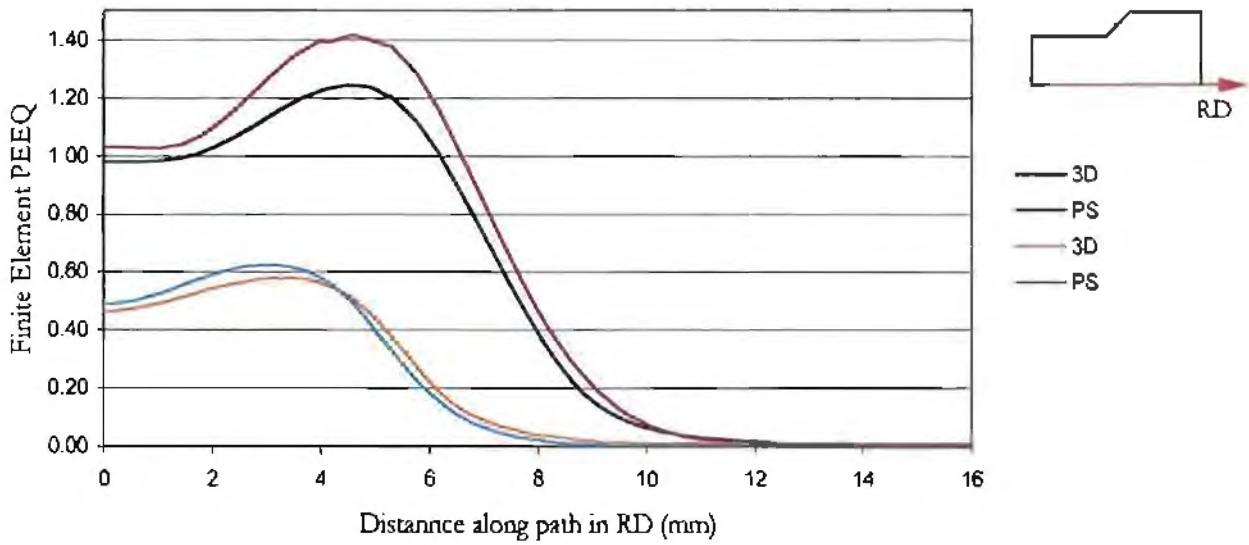

(a)

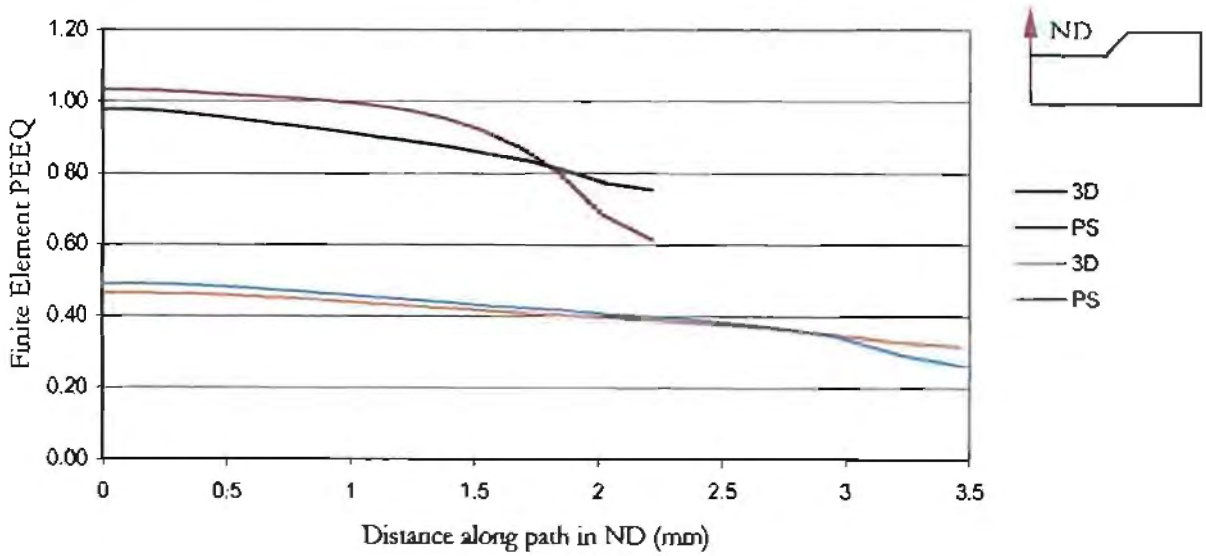

(b)

Figure 3.7 Three-dimensional and plane strain FEM predictions of PEEQ along centre line in the (a) RD and (b) ND for specimens deformed to a nominal strain of 0.5 and 1.

It is apparent that the plane strain model does not approximate the three-dimensional model and that the lateral spread in the width direction must be considered, which results in the plane strain approximation giving an over estimate of the PEEQ. Locking of nodes at the anvil corner, as will be discussed in Section 3.3.11, occurs in the plane strain model leading to the drop in PEEQ below the surface of the anvil as shown in Figure 3.7 (b). A three dimensional model is therefore used in the FEM study.

3.3.11 Parametric Study

A FEA solution is an approximation, since the solution has some error relative to the exact solution. A sufficiently refined mesh should be used to ensure that the results for the simulation are adequate, as a coarse mesh can yield inaccurate results. The numerical solution provided by a model will tend toward a unique value as the mesh density is refined. The mesh is said to have converged when further refinement produces a negligible change in the solution. It is therefore necessary to perform mesh convergence studies, where the problem is simulated with a progressively finer mesh and the results compared. It is also rarely necessary to use a uniformly fine mesh throughout the structure being analysed. A fine mesh should be used in areas of high stress gradients and a coarser mesh used in areas of low stress gradients or where the magnitude of the stress is not of interest.

First-order reduced integration elements are prone to hourglassing with sufficient mesh refinement minimizing the problem[39]. Estimation and improvement is accomplished by repeating the entire analysis using a different mesh of the same type of element (n-analysis) or by keeping the same mesh but changing the type of element (p-analysis), and then observing the differences between the solutions. A parametric study also allows the determination of an optimal computational time for a desired accuracy of result.

Since first-order elements are to be used in the analysis an n-refinement analysis was performed. Since a three-dimensional model is used in the analysis of the PSC test, n-analysis is performed in the three co-ordinate axis directions due to the simplicity of the geometry. The result of the parametric study is the mesh illustrated in Figure 3.8. The sufficiently refined mesh has been found to give accurate approximations with computational time of primary importance. The parametric study is detailed in Appendix A.

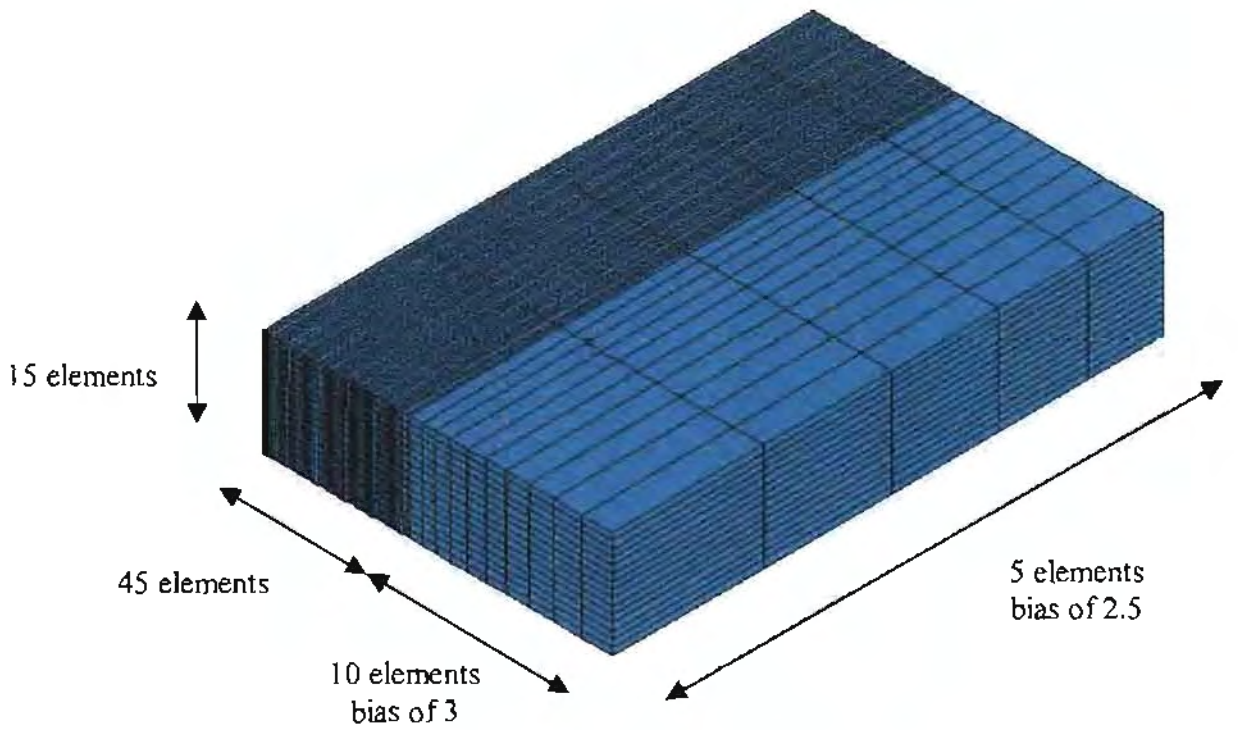

Figure 3.8 Mesh to be used in 3D FEA of PSC test.

In the formation of the FEM model it is necessary to use a refined mesh for the specimen/anvil surface. This is because the FEM applies loads at nodes and not along the surface of the element between the nodes. At the anvil corner the distortion of the elements should simulate the material flow; however, if a coarse mesh is used the nodes become locked in by the anvil corner, as illustrated in Figure 3.9. It is therefore necessary to use a refined mesh to reduce the locking effect. It was also necessary to add a radius of 0.25 mm to the anvil corner, which had negligible effect on the FEM model. Furthermore, a radius is created from the cleaning of the anvils with a 1200 grit paper before each test.

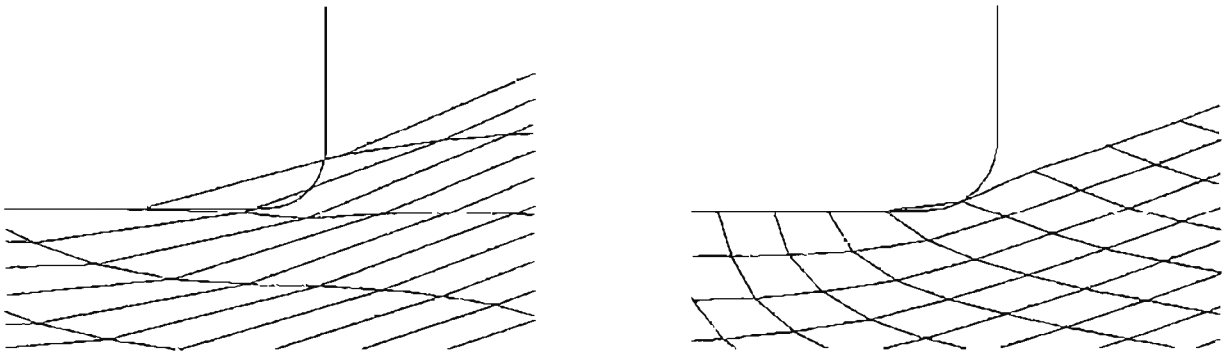

Figure 3.9 (a) Coarse and (b) fine mesh showing locking of nodes at anvil corner during deformation.

3.3.12 Derivation of FEA Results

The results obtained from the FEA are a piecewise approximation and it is therefore necessary to illustrate from which elements the FEA results were obtained, and used in the subsequent Results and Discussion.

The material at the centre of the PSC specimen is likely to receive approximate plane strain deformation. Unless otherwise stipulated the FEA results used in Chapter Four, were obtained from the elements at the centre of the FE mesh, as shown in Figure 3.10. The RD, ND and TD are shown in Figure 3.10 which are referred to in Chapter Four. The RD, ND and TD refer to node paths along the centre lines in the FE principal axes 1, 2 and 3 directions respectively. Two-dimensional FEM contours are presented in Chapter Four, with the contours being obtained from the 1-2 plane at the centre of the PSC specimen. Since metallographic investigation is carried out at the centre of the RD/ND plane of deformed PSC specimens, the strain and strain rate at the centre of the PSC specimen, discussed in Chapter Four, is obtained by calculation of the average strain and strain rate in the six elements at the geometric centre of the PSC specimen.

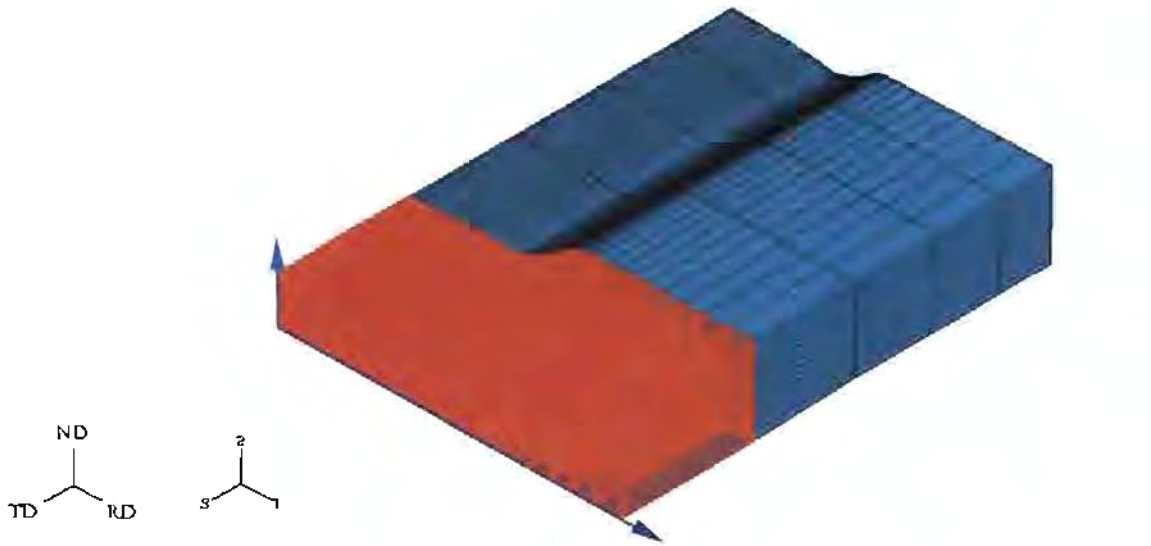

Figure 3.10 FE mesh illustrating the elements and the node paths used to obtain the results presented in Chapter Four.

In Chapter Four the equivalent plastic strain is compared with the nominal strain of the PSC test. The nominal strain refers to the nominal strain assuming homogeneous PSC, given by Equation 3.6.

Equation 3.6 $$\varepsilon_{nom} = 1.155 \ln\left(\frac{h_0}{h_f}\right)$$

Where h_0 is the initial specimen height and h_f the specimen height after deformation.

3.4 Visioplasticity

Visioplasticity was used to validate the FEM model using the technique described by Beynon and Sellars[36]. The PSC specimen is split along the central plane from which material does not flow in the TD, and a grid scribed on one of the exposed faces, as illustrated in Figure 3.11. The two halves are then clamped together as shown in Figure 3.12 and the test performed. This allows calculation of the strain. The important features of the derivation are that a logarithmic strain term is used and that each grid intersection is assumed to move in a straight line.

It is considered that grids deformed in a finite step cannot be used in visioplasticity analyses if the deformation is nonuniform, as points do not have straight line trajectories[41]. However, the purpose of this study is to use the technique to quantify the strain distribution during PSC testing using large finite steps. The patterns would

therefore be able to be compared to the FEM predictions and give guidance about local deformation conditions in relation to microstructural changes during hot working.

The grid was scribed using a vernier calliper as illustrated in Figure 3.11. The lines in the RD and ND are 0.75 mm apart. The coordinates of the intersections of the lines were obtained before and after testing using the Reflex Microscope No.1, Reflex Measurements LTD, at the Biomedical Imaging Centre at the University of Cape Town, South Africa. This allowed the calculation of the equivalent plastic strain.

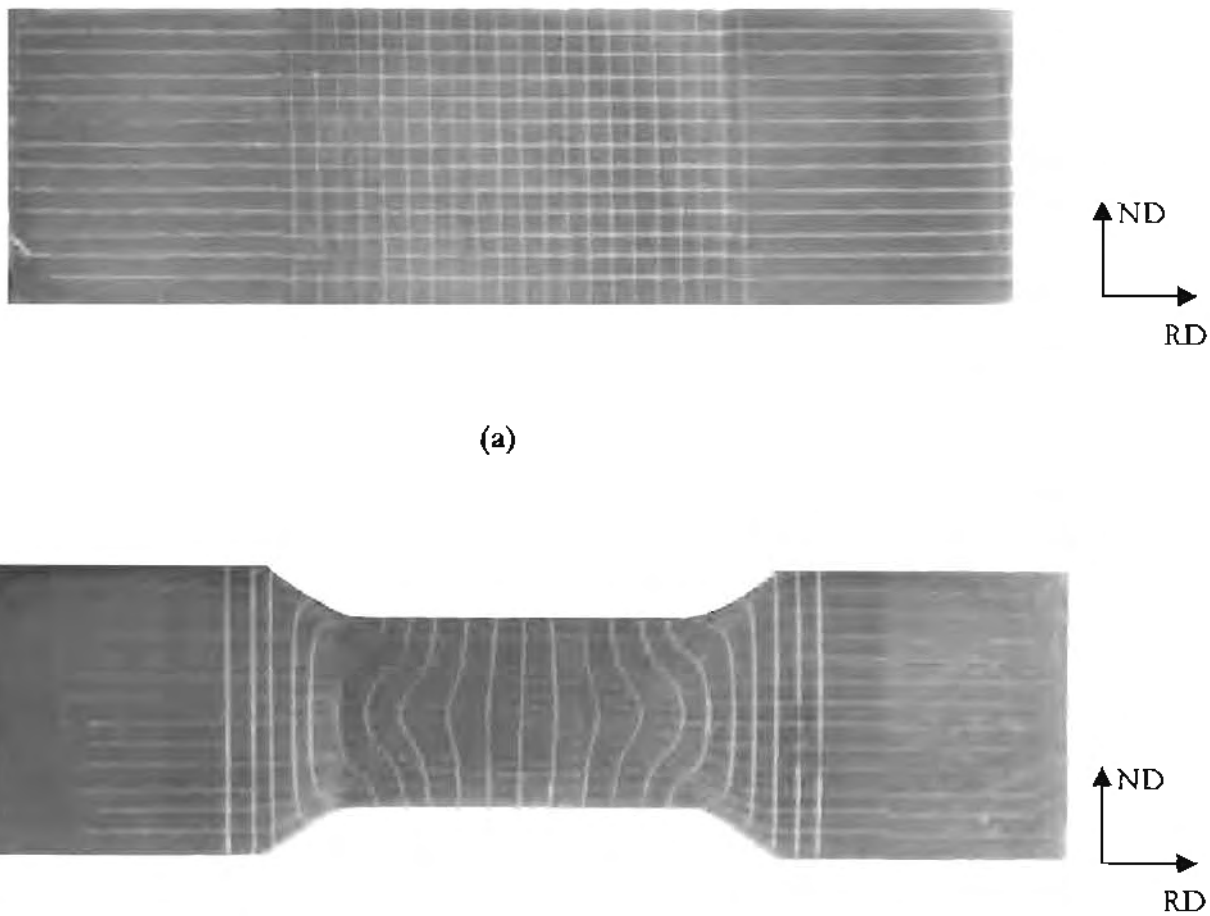

Figure 3.11 Visioplastic grid (a) before and (b) after testing.

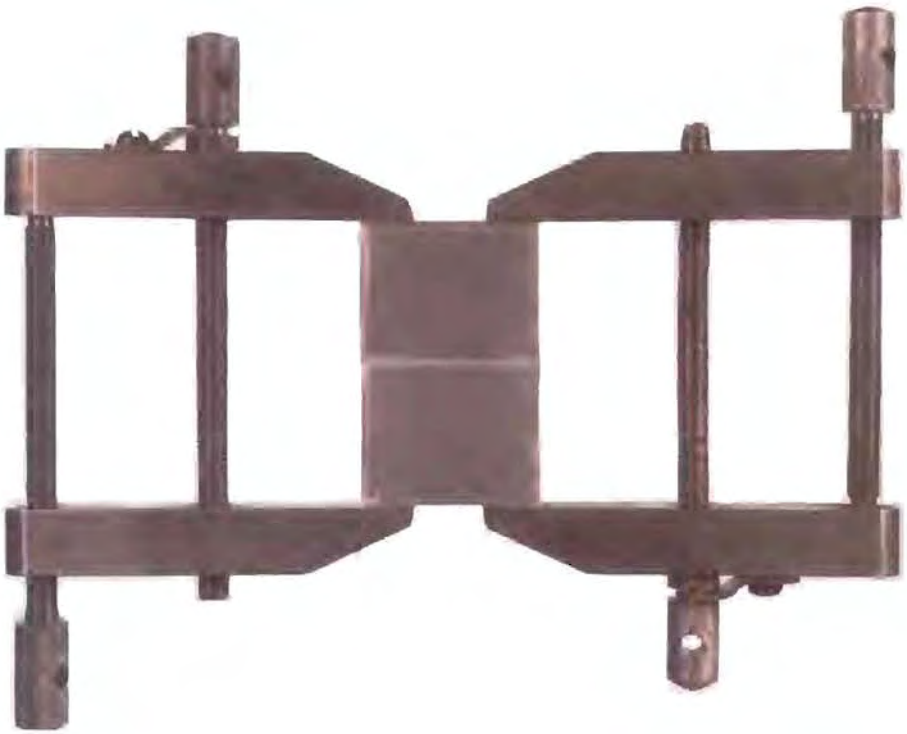

Figure 3.12 Clamped half specimens before testing.

3.4.1 Calculation of Equivalent Strain

Consider a two dimensional rectangular grid as shown in Figure 3.13, with the coordinate axes parallel to the initial state. As element M is deformed to m the equivalent strain can be obtained by combining the effects of principle and shear strain terms, as described by Beynon and Sellars[36].

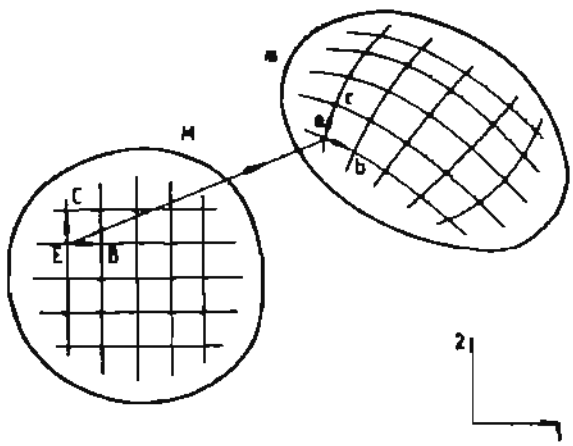

Figure 3.13 Deformed visioplastic grid from which the equivalent strain can be calculated (after Beynon and Sellars[36]).

The strain in the 1 and 2 directions is given by:

Equation 3.7 $$e_1 = \ln\frac{|eb|}{|EB|} \quad \text{and} \quad e_2 = \ln\frac{|ec|}{|EC|}$$

The shear strain is defined as half the angle of shear in the 1-2 plane, which is the decrease in the angle between **EB** and **EC**.

Equation 3.8 $$e_{12} = \gamma_{12}/2 = 0.5\left(\pi/2 - \theta\right)$$

Where θ is the angle between **eb** and **ec**, which can be obtained by taking the dot product of the two vectors.

Equation 3.9 $$\theta = \cos^{-1}\left[\frac{eb \cdot ec}{|eb||ec|}\right]$$

An equivalent strain can then be obtained. Note that the strain in the 3 direction is omitted.

Equation 3.10 $$\bar{e} = 2/3\left(e_1^2 - e_1e_2 + e_2^2 + 3e_{12}^2\right)^{1/2}$$

The visioplastic analysis ignores the error incurred by assuming that each point travels in a straight line to its final position, with a rectangular hyperbolic path more likely[36]. This is acceptable since the visioplastic analysis is directly compared with FEM approximations along symmetry lines or at symmetry points, therefore theoretically along or at points with straight line trajectories.

The visioplastic results are illustrated by equivalent strain contour plots using Surfer, a commercial windows based contour and map viewing program.

3.5 Strain-Hardness Correlation

Tensile and axisymmetric compression tests were performed at room temperature to determine a relationship between hardness and strain, as illustrated in Figure 3.14, which could then be used to determine the strain distribution for PSC tests performed at room temperature. At room temperature the effects of recovery during deformation are considered negligible and the strain hardening of the work piece preserved. A strain-hardness correlation at hot working temperatures (above 200 °C) could not be obtained due to the effects of dynamic recovery resulting in little variance in hardness with increasing strain.

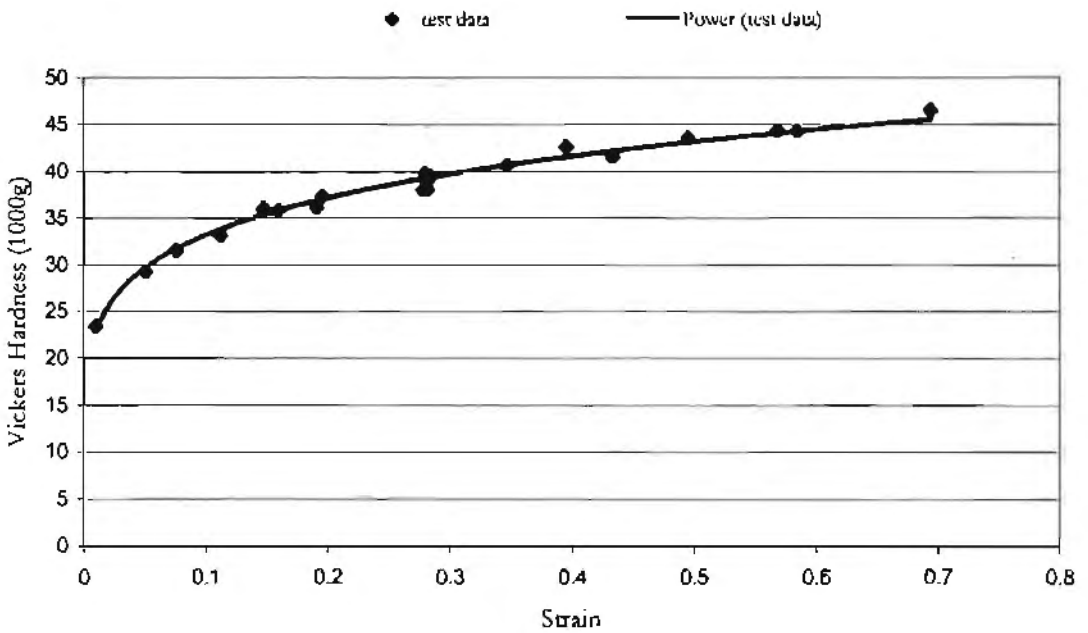

Figure 3.14 Strain vs. Vickers hardness with power law trendline, determined from tensile and axisymmetric compression tests performed at room temperature at a strain rate of 0.1 sec^{-1}.

A power law trendline was used to correlate strain and hardness. The power law is appropriate since it is often used in the description of the flow curve determination of aluminium alloys. The equation that describes the trendline is used to convert hardness values to strain and is given by Equation 3.11, where HV is Vickers hardness (1000 g) and ε the corresponding strain.

Equation 3.11 $$\varepsilon = (6.024 \times 10^{-11}) HV^{6.063}$$

The strain-hardness results are illustrated by strain contour plots using Surfer, a commercial windows based contour and map viewing program.

3.6 Optical Microscopy

3.6.1 Specimen Sectioning

Specimens were sectioned along the longitudinal plane for microscopical investigations. The longitudinal plane is the plane that contains the ND and RD. Shi *et al*[24] approximated the plane strain condition to exist in the central (w-b) part of the specimen, therefore 8 mm from each end of the specimen was discarded.

3.6.2 Preparation

Following sectioning, the specimens were cold mounted in an epoxy resin for grinding and polishing. Specimens were ground on 500 grit silicon carbide paper until plane. Specimens were then mechanically polished using diamond polish with a finishing polish using a suspension of fine colloidal silica. Specimens were then anodised electro-chemically using Barkers reagent (2.5 % Fluoroboric Acid in H_2O). Anodising conditions used were approximately 60 seconds, 17 volts, at room temperature.

3.6.3 Microscopy

The anodic layer deposited on the specimens is anisotropic due to varying grain orientations at the surface of the specimen, which allowed grain contrasts to be viewed under polarised light. Specimens were viewed using the Reichert Mef3A incident light microscope with the objective of 10X employed.

CHAPTER FOUR - RESULTS AND DISCUSSION

4.1 Context of the Research Project

4.1.1 Context of the Investigation of Thermo-Mechanical Variables during Plane Strain Compression Testing

PSC testing is widely accepted as a mechanical test used to simulate hot rolling on a laboratory scale. The PSC test is used extensively in metallurgical investigations and in determination of recrystallization kinetics, where thermo-mechanical variables are used to fit experimental data to analytical recrystallization models. The strain and strain rate, however, are not homogeneous through the thickness of the PSC specimen during testing and due to the inhomogeneity of strain distribution, adiabatic heating may occur at strain rates greater than 1 sec^{-1}. Therefore, nominal values of strain and strain rate cannot be used to approximate the actual strain and strain rate in the volume of material being analysed. Furthermore, at elevated temperatures lubrication breakdown occurs, resulting in increased friction between the anvils and the specimen. The friction condition affects the strain and hence strain rate distribution through the thickness of the specimen.

In view of the above, in order to more accurately determine the recrystallization kinetics of a discrete volume of material within the PSC specimen, a better understanding and determination of the thermo-mechanical variables during PSC testing is required.

4.1.2 Finite Element Analysis and Visioplasticity Investigation

Although the FEM can provide accurate approximations to the strain and strain rate in a specific volume of material during PSC testing, it is necessary to investigate the validity of the FEM results. Visioplastic experiments were used to verify and validate the FEM predictions of strain and strain rate during PSC testing. Once the FEM model is validated the model can be used to simulate an infinite number of mechanical or thermo-mechanical process variables within the range of experimental validation. The validated FEM results can then be used to more accurately predict the strain and strain rate in the volume of material being analysed, therefore improving predictions of analytical recrystallization models.

4.2 Determination of the Mechanical Variables during PSC Testing

4.2.1 Effect of Temperature and Strain Rate on the Strain Distribution in FE Model

The strain distribution, assuming slip line field theory, is independent of strain rate and temperature. The constitutive equations used in the description of the flow curve data in the present study, however, incorporate strain rate and temperature dependencies. Therefore, different flow curves are associated with different thermo-mechanical variables of deformation.

It has been found that due to the low work hardening rate of aluminium at temperatures above 200 °C, the assumption of slip line field theory being independent of strain rate and temperature is valid in describing the strain and strain rate distribution across the RD/ND plane of the PSC specimen. This is shown in Figure 4.1, which indicates the PEEQ at the geometric centre of the PSC specimen for deformation temperatures of 200 and 400 °C, and for strain rates of 10 and 0.1 sec^{-1}. Figure 4.1 shows negligible variation in strain at the centre of the PSC specimen for increasing strain rate or increasing temperature for a specific coefficient of friction. The strain distribution and therefore strain rate distribution are not affected by changes in strain rate or temperature during PSC testing. The assumption of slip line field theory being independent of temperature and strain rate is therefore valid.

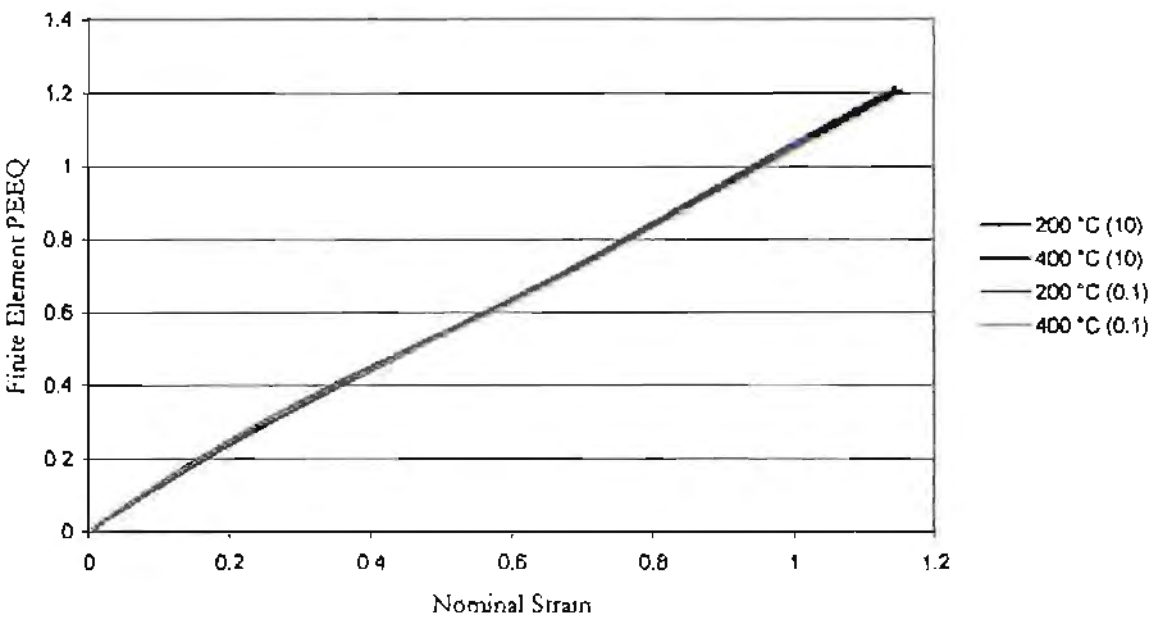

Figure 4.1 FEM PEEQ at the centre of the PSC specimen for simulations at 200 and 400 °C at strain rates of 0.1 and 10 sec^{-1} for a coefficient of friction of 0.06, showing that the strain and strain rate at the centre of the PSC specimen in the RD/ND plane are independent of strain rate and temperature of deformation.

In contrast, at cold working temperatures the assumption of slip line field theory being independent of strain rate and temperature is not valid. Comparison of the strain at the centre of the PSC specimen for FEM simulations performed at 25 and 250 °C reveals a significant variation in strain, particularly at nominal strains greater than 0.4. Figure 4.2 illustrates the PEEQ at the centre of the PSC specimen for tests performed at 25 and 250 °C, and deformed at strain rates of 0.1 sec^{-1}. The FEM prediction agrees well with actual visioplastic results that are included in Figure 4.2. The variation in strain at the centre for deformation temperatures of 25 and 250 °C is attributed to the work hardening characteristics of AA1200. At 25 °C the material work hardens to a greater extent than at 250 °C due to limited recovery, which consequently leads to a change in the strain distribution within the PSC specimen.

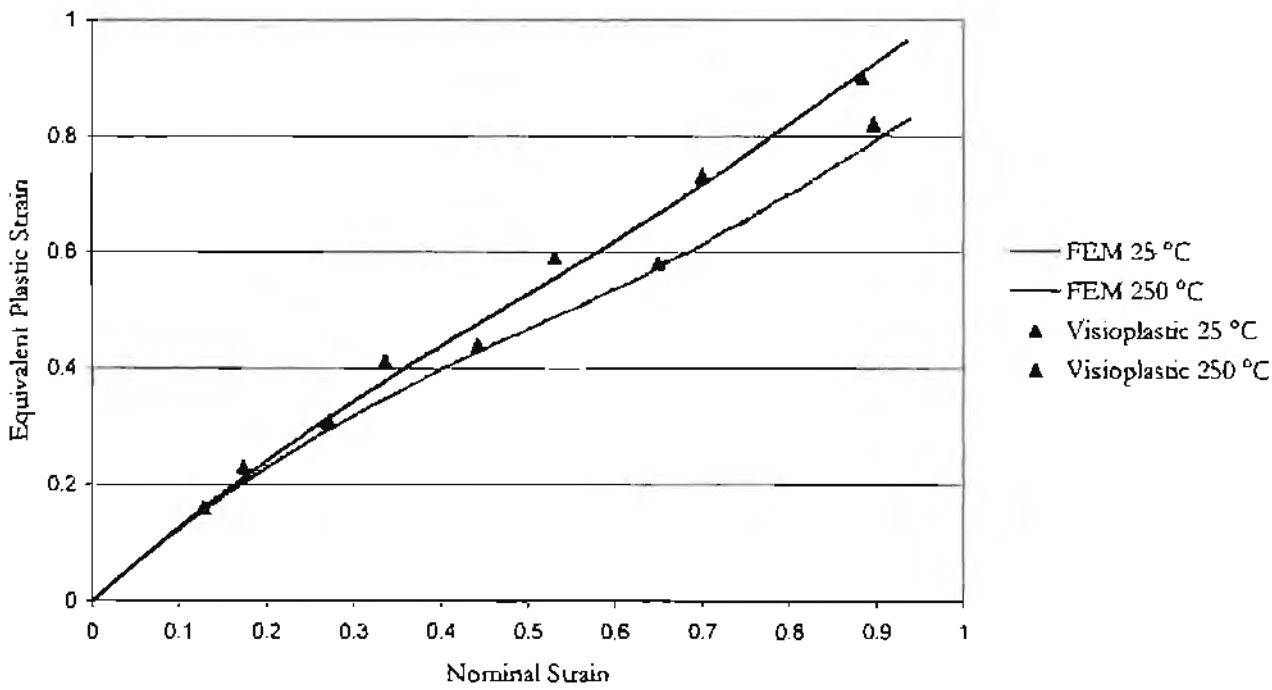

Figure 4.2 Equivalent strain at the centre of the PSC specimen for visioplastic experiments and FEM prediction assuming a coefficient of friction of 0.05 performed at 25 and 250 °C at a strain rate of 0.1 sec^{-1}. The strain and hence strain rate at 25 and 250 °C differ considerably.

4.2.2 The Friction Condition

It has been shown from an earlier study that breakdown of the graphite lubricant occurs at temperatures above 400 °C during PSC testing of aluminium[10]. The breakdown in lubrication results in an increase in the coefficient of friction between the specimen and the anvils, which is known to change the strain distribution through the thickness of the PSC specimen. Beynon and Sellars[37] used graphite lubrication for PSC testing and found an increase in the coefficient of friction above 300 °C. Since the strain and strain rate distribution is sensitive to the friction condition between the specimen and the anvils, determination of the coefficient of friction at elevated temperatures is required to accurately predict the strain and strain rate distribution within the PSC specimen using the FEM. Initial FEA showed that the strain distribution within the PSC specimen is significantly affected by variations in the coefficient of friction, as shown in Figures 4.3 and 4.4, which subsequently changes the strain rate distribution within the specimen.

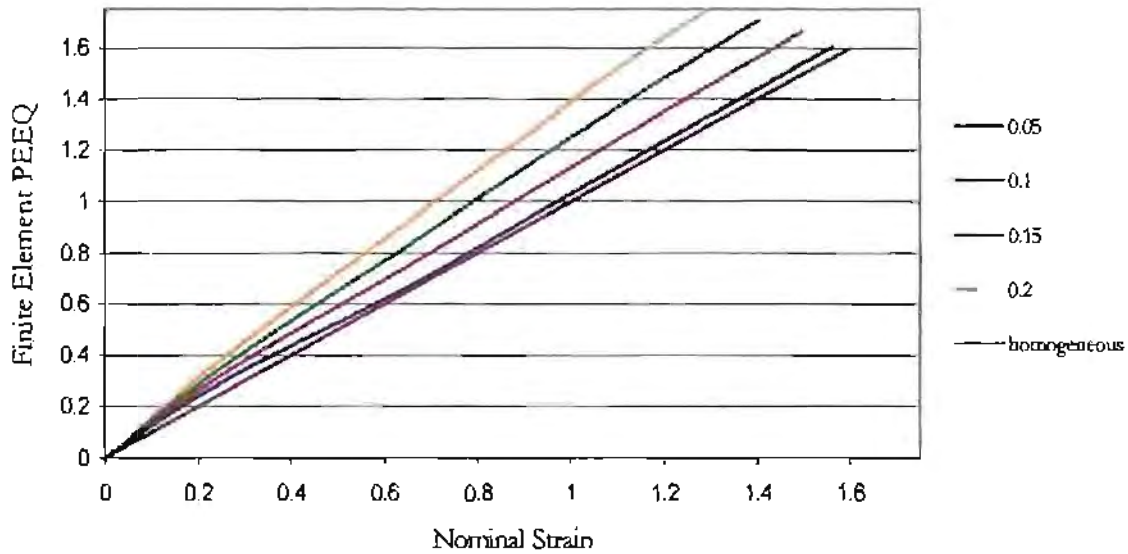

Figure 4.3 FEM approximation of the PEEQ at the centre of PSC specimen for different coefficients of friction, showing a variation in predicted strain at the centre of the PSC specimen. The homogeneous line indicates the strain assuming homogeneous plane strain compression (i.e. homogeneous across the RD/ND plane).

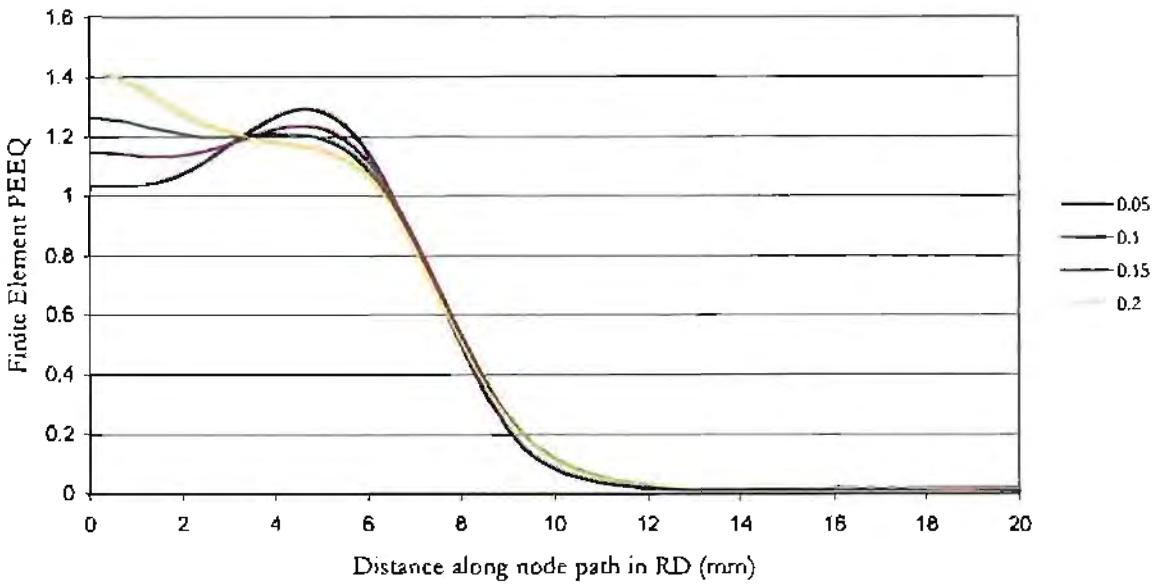

(a)

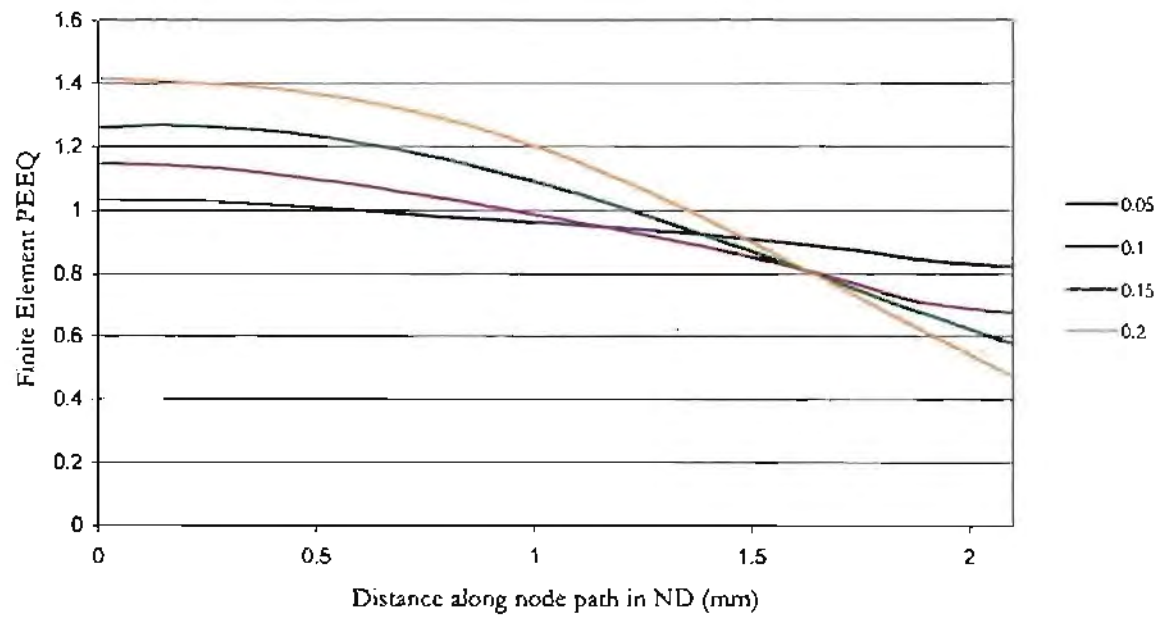

(b)

Figure 4.4 PEEQ distribution along node paths along the centre line in the (a) RD and (b) ND, showing variations in strain distribution with changes in coefficient of friction.

4.2.3 The Effect of the Friction Condition on the Strain Distribution

The strain distribution for the FEM simulations has been shown to be sensitive to small variations in the coefficient of friction. Figures 4.5 and 4.6 illustrate the influence of strain distribution on lubrication breakdown at 440 °C. Figures 4.5 and 4.6 plot equivalent strain contours for visioplastic PSC specimens deformed at 250 and 440 °C respectively, to nominal strains of 0.42 at a strain rate of 10 sec^{-1}.

A change in strain distribution is indicated for the specimen deformed at 440 °C and is attributed to lubrication breakdown resulting in an increased coefficient of friction between the specimen and the anvils. For the visioplastic specimen deformed at 440 °C the strain is localized in the central region as a result of an increased 'dead zone' resulting from an increased coefficient of friction. The 'dead zone' being the volume of material near the surface of the PSC specimen beneath the anvils. The material does not strain as would be predicted by slip line field theory for frictionless conditions, hence the volume of material is termed the 'dead zone'. The increased 'dead zone' increases material flow at the centre of the specimen resulting in a measured strain of 0.46 and 0.58 at the centre for specimens deformed at 250 and 440 °C respectively.

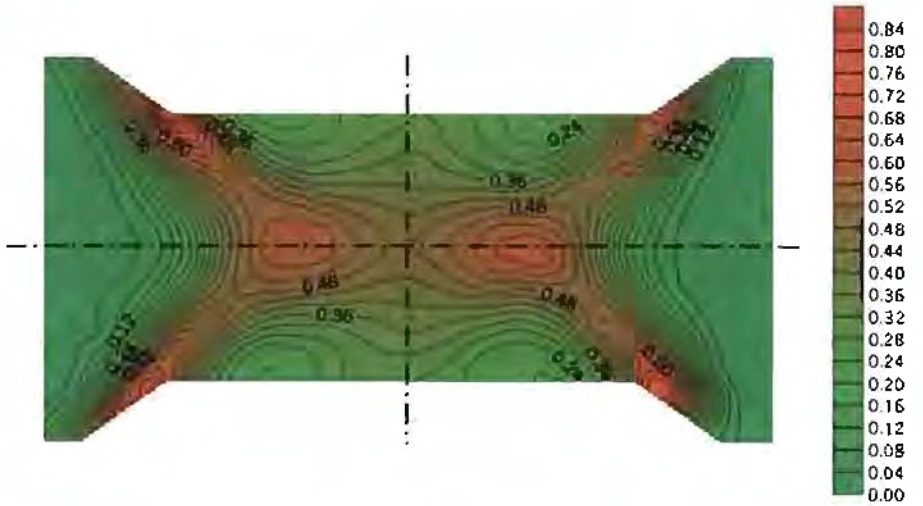

Figure 4.5 Visioplastic equivalent strain contour for specimen deformed at 250 °C to a nominal strain of 0.42 at a strain rate of 10 sec^{-1}, showing a measure strain of 0.46 at the centre of the RD/ND plane.

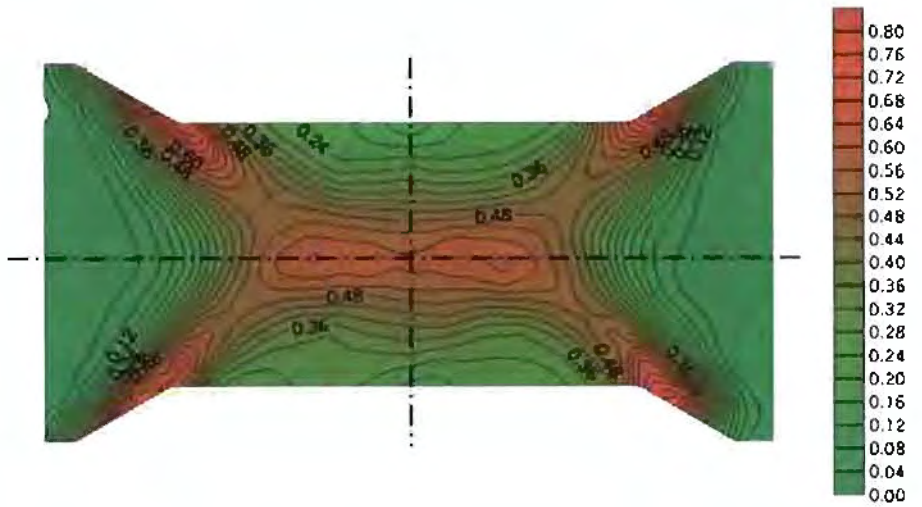

Figure 4.6 Visioplastic strain contour for specimen deformed at 440 °C to a nominal strain of 0.42 at a strain rate of 10 sec^{-1}. The contour plot clearly shows a variation in strain distribution as a result of lubrication breakdown when compared to Figure 4.5. The strain contour shows a strain of 0.58 at the centre of the RD/ND plane.

To illustrate the FEM predictions of the strain distribution for elevated temperature PSC testing, FEM simulations of tests performed at 250 and 440 °C are illustrated in Figure 4.7 (a) and (b) respectively. A coefficient of friction of 0.05 and 0.15 is used in the FEM simulations at 250 and 440 °C respectively. The values of coefficient of friction were chosen to approximate the friction condition at the specific test temperature, which is further discussed in Section 4.2.4. The FEM PEEQ contours show similar characteristics to the visioplastic strain contours shown in Figure 4.5 and 4.6. The increased coefficient of friction for the simulation at 440 °C changes the strain distribution with increased material flow at the centre as a result of an increased 'dead zone' area.

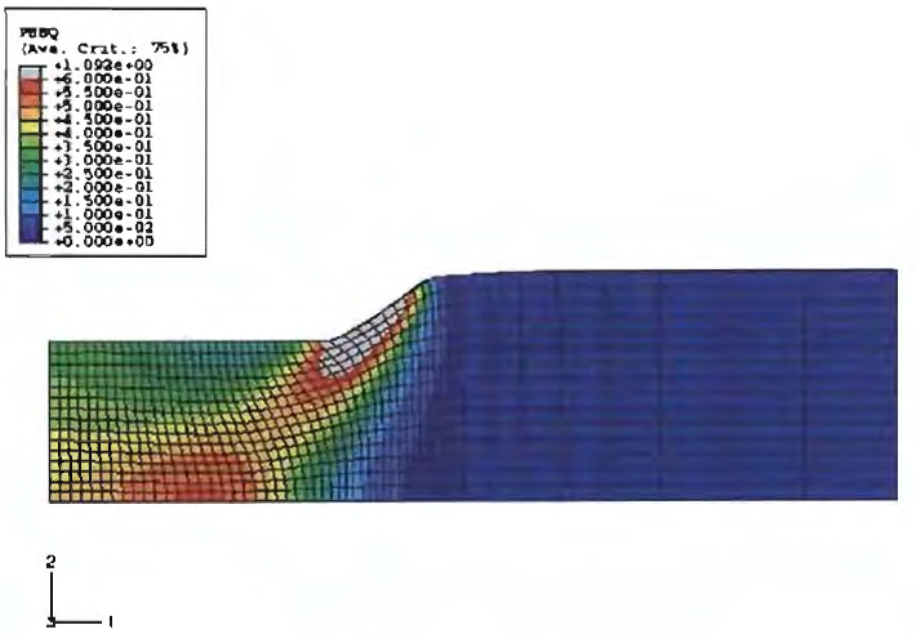

(a)

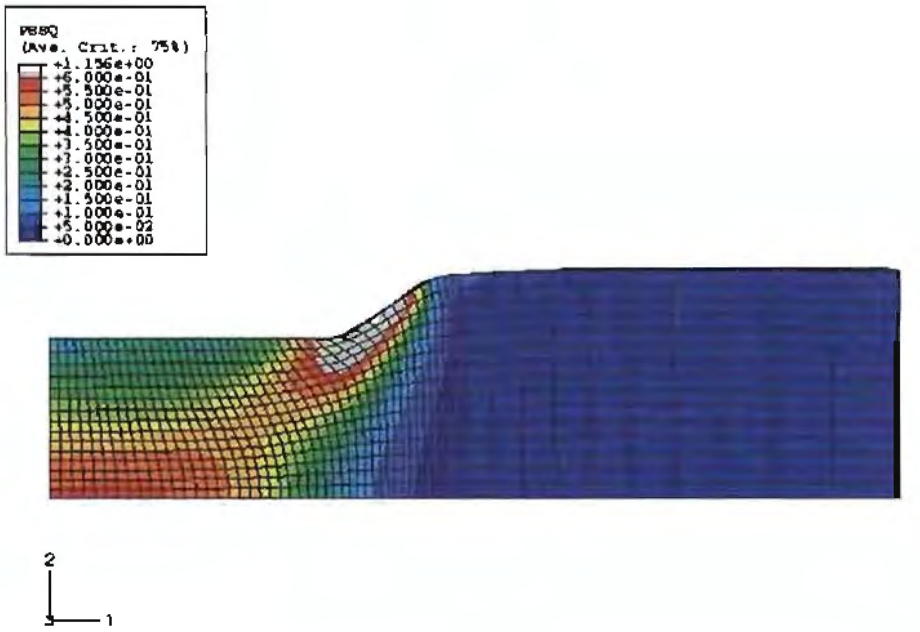

(b)

Figure 4.7 FEM PEEQ contour plot of PSC specimens deformed at (a) 250 and (b) 440 °C at strain a strain rate of 10 sec^{-1} to a nominal strain of 0.42, showing a change in the strain distribution as a result of different simulated coefficients of friction. The coefficients of friction are 0.05 and 0.15 respectively.

4.2.4 Determination of the Friction Condition

4.2.4.1 Friction - Method I

At temperatures between 300 and 400 °C lubrication breakdown occurs resulting in increased friction with increasing test temperature. The increase in coefficient of friction changes the strain and strain rate distribution through the thickness of the PSC specimen as discussed in Section 4.2.3. Visioplastic specimens were therefore deformed at 25, 250, 325, 350, 375, 400 and 440 °C to investigate lubrication breakdown. Once the coefficient of friction for each test is determined, the coefficient of friction can then be approximated for any temperature between 25 and 440 °C. The coefficient of friction for a specific test temperature can then be used in a FEM model to more accurately predict the strain and strain rate at the centre of the PSC specimen.

For visioplastic PSC specimens deformed at 25, 250, 325, 350, 375, 400 and 440 °C the coefficient of friction is approximated by plotting the measured visioplastic strain at the centre of the PSC specimen at different nominal strain values and compared with FEM PEEQ predictions for different simulated friction conditions as shown in Figures 4.8, 4.9, 4.10 and 4.11.

In Figures 4.8, 4.9, 4.10 and 4.11 the nominal strain refers to the strain assuming homogeneous PSC, and the equivalent strain refers to the measured visioplastic equivalent strain and the FEM PEEQ prediction. The visioplastic equivalent strain, however, does not consider the strain in the transverse direction. The visioplastic strain therefore includes a transverse strain value, which is approximated to be of 0.1 per unit nominal normal strain. The value of 0.1 transverse strain per unit nominal normal strain is obtained by assuming the transverse strain to be homogeneous along the length of the PSC specimen in the TD. The FEM is used to investigate the plane strain condition as will be discussed in Section 4.2.8, to which the transverse strain was found to be approximately constant and equal to 0.1 per unit nominal normal strain along the length of the PSC specimen in the TD.

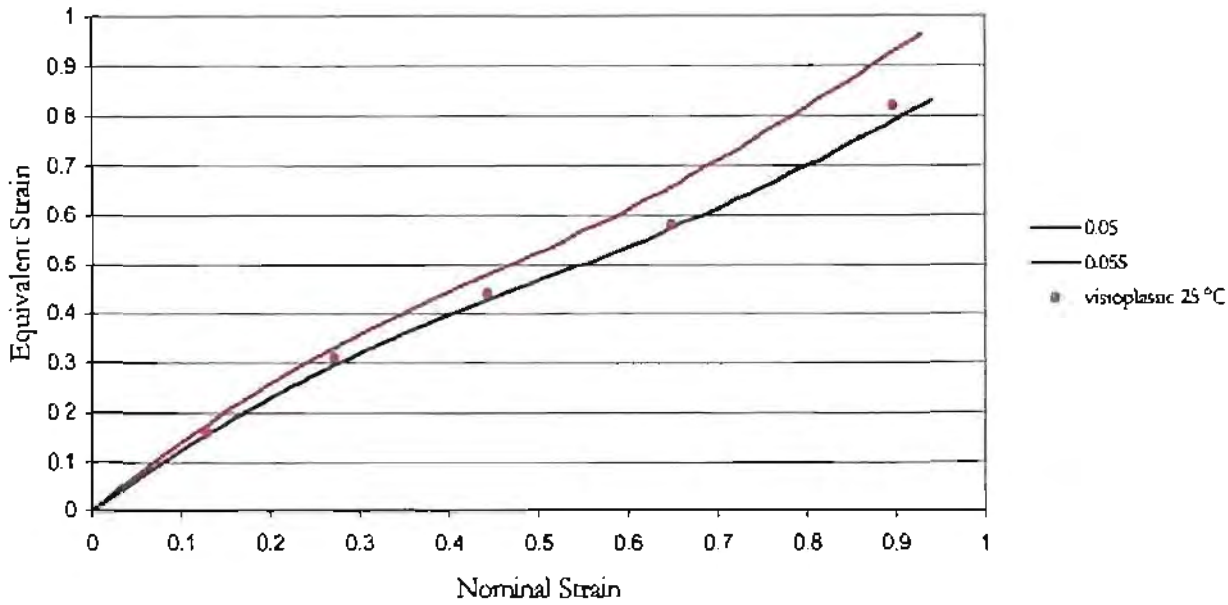

(a)

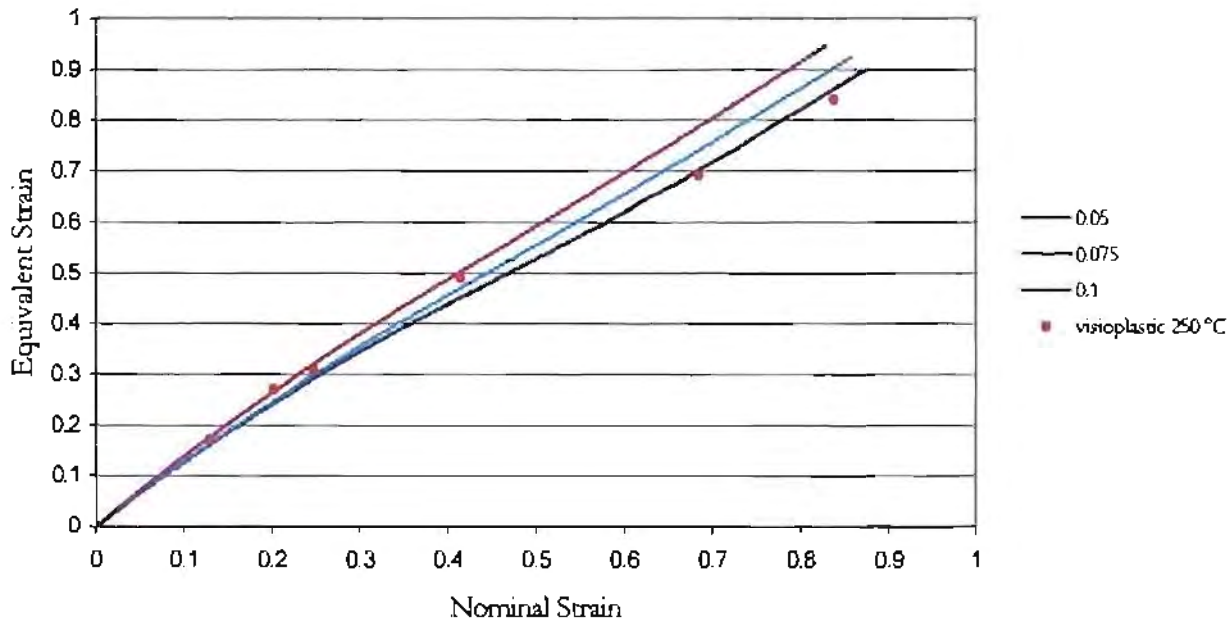

(b)

Figure 4.8 Visioplastic strain at the centre of the PSC specimen and FEM approximation for tests performed at (a) 25 and (b) 250 °C at a strain rate of 10 sec^{-1}, showing an approximate coefficient of friction of 0.05 for deformation temperatures of 25 and 250 °C.

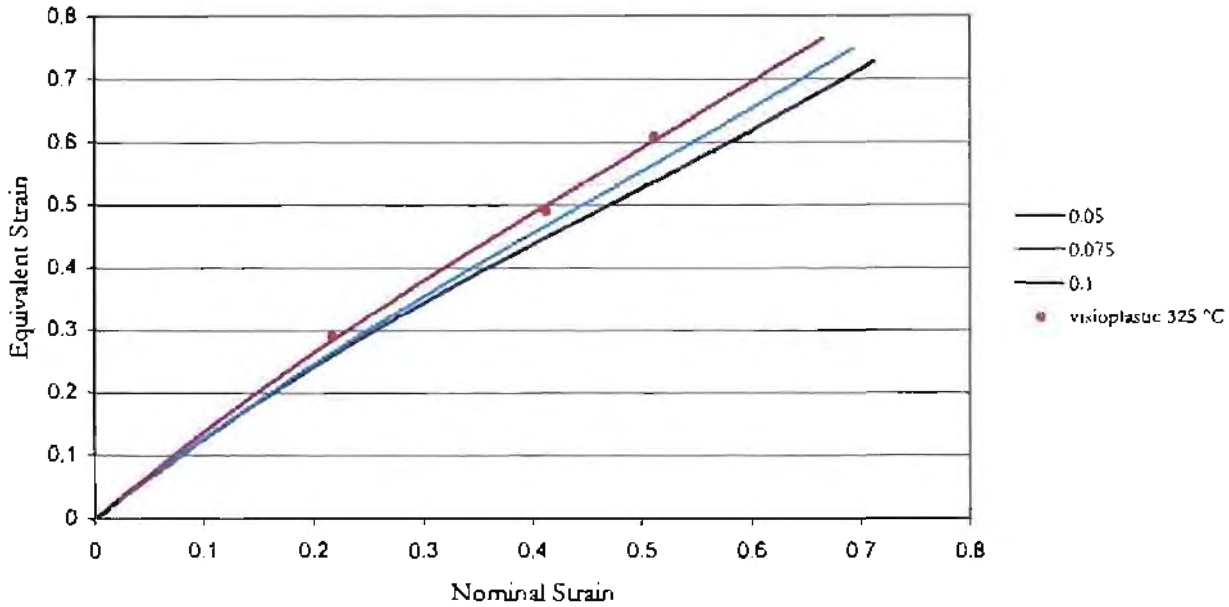

(a)

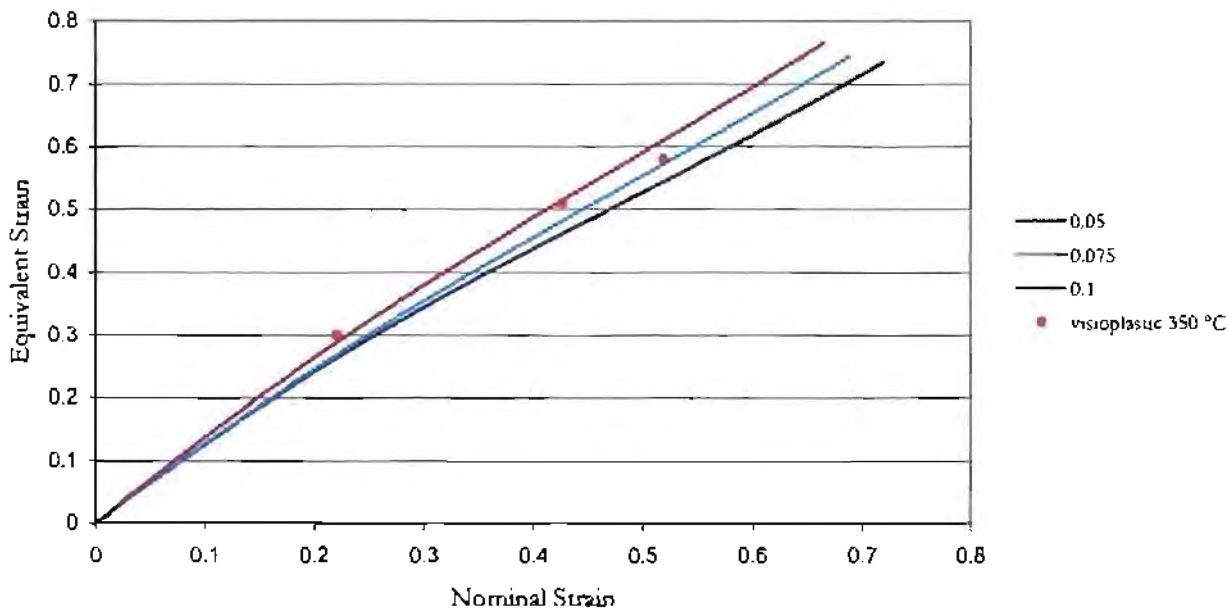

(b)

Figure 4.9 Visioplastic strain at the centre of the PSC specimen and FEM approximation for tests performed at (a) 325 and (b) 350 °C at a strain rate of 10 sec^{-1}, showing an approximate coefficient of friction of 0.1 for deformation temperatures of 325 and 350 °C.

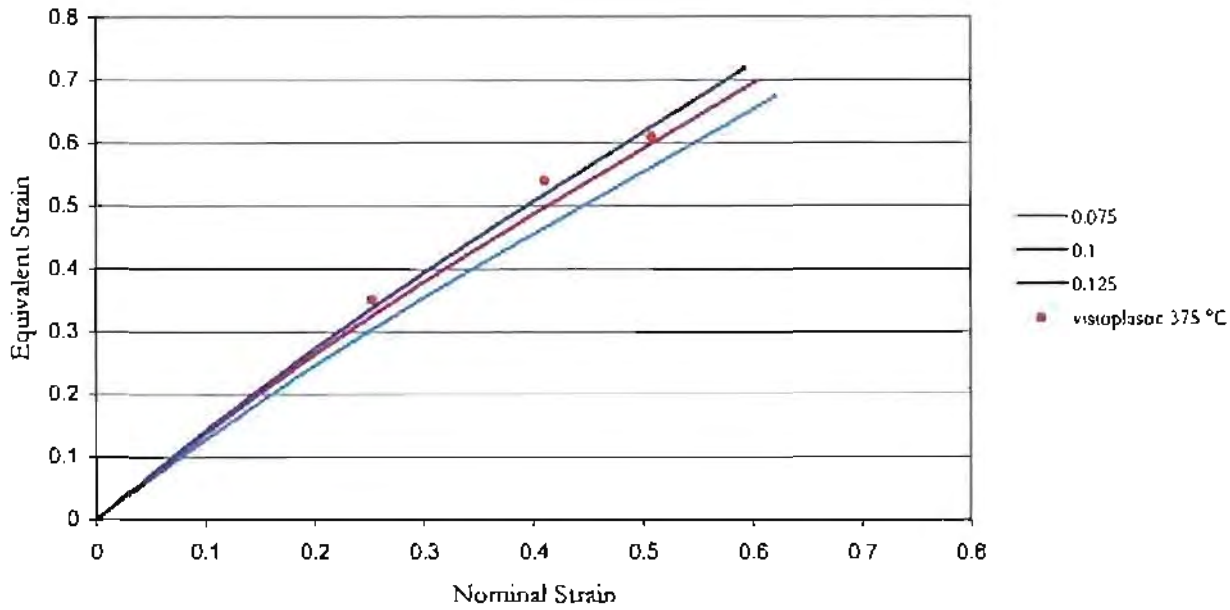

(a)

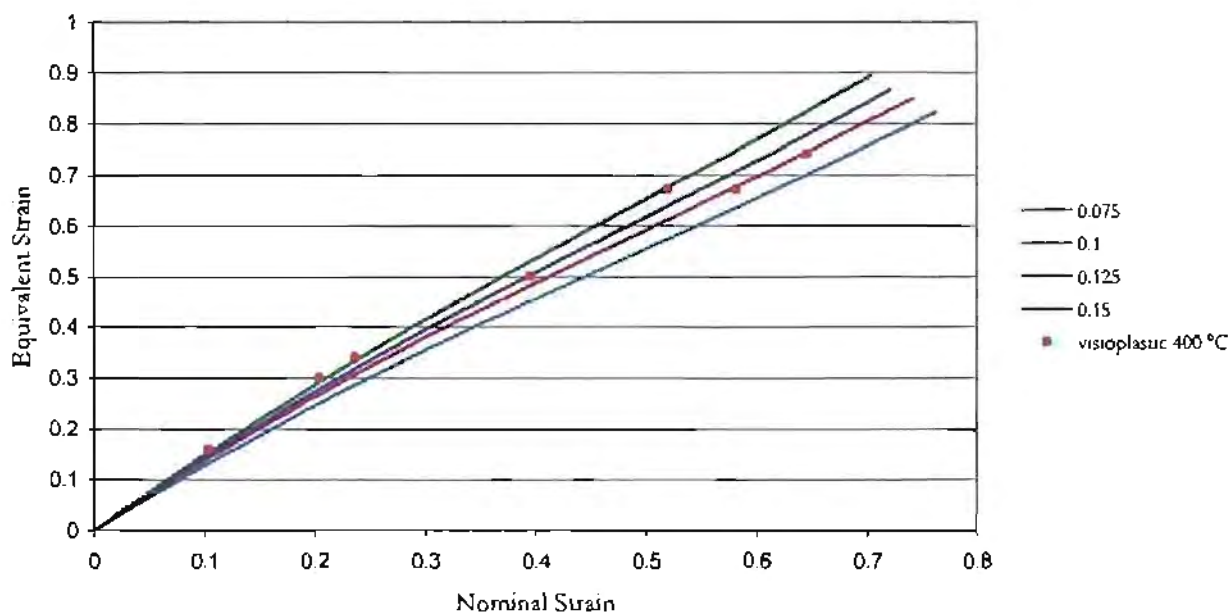

(b)

Figure 4.10 Visioplastic strain at the centre of the PSC specimen and FEM approximation for tests performed at (b) 375 and (b) 400 °C at a strain rate of 10 sec^{-1}, showing an increased coefficient friction when compared to the 250 °C visioplastic tests. At 400 °C there is a significant variation in measured strain, with lubrication possibly breaking down during one test but not in another (see for example nominal strains of 0.52 and 0.57).

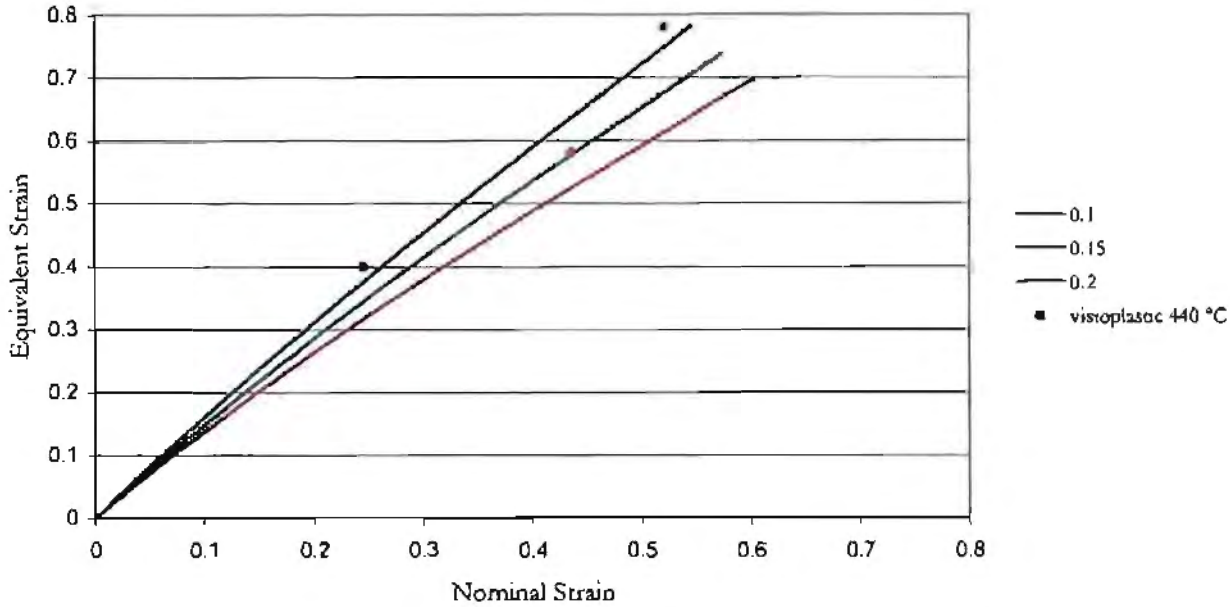

Figure 4.11 Visioplastic strain at the centre of the PSC specimen and FEM approximation for tests performed at 440 °C, showing an increase in coefficient of friction when compared to Figures 4.10 (a) and (b).

This method gives a good approximation of the coefficient of friction and illustrates the variation in strain at the centre of the visioplastic specimen attributed to changes in friction condition. It is also evident from Figures 4.10 (b) and 4.11 for tests performed at 400 and 440 °C that the lubricant breaks down more in one test than in another, therefore affecting the strain and strain rate distribution at the centre of the PSC specimen differently. The visioplastic equivalent strain at the centre of the PSC specimen for specimens deformed to different nominal strains therefore does not approximate similar coefficients of friction. The variation in friction condition at constant temperature would need to be considered when determining a strain range which the material at the centre is likely to have received during elevated temperature testing.

4.2.4.2 Friction – Method II

In determining the coefficient of friction it was found that the coefficient of friction could be more accurately approximated in combination with Friction Method I by directly comparing the FEM and visioplastic equivalent strain along a path from the centre of the PSC specimen in the ND. As the coefficient of friction is increased the slope of the distance-strain curve increases as shown in Figure 4.12 (a) for simulated coefficients of friction from 0.05 to 0.2. Therefore, by comparing the average slope of the FEM and visioplastic curves shown in Figure 4.12 (a) and (b) a more accurate determination of the coefficient of friction is obtained.

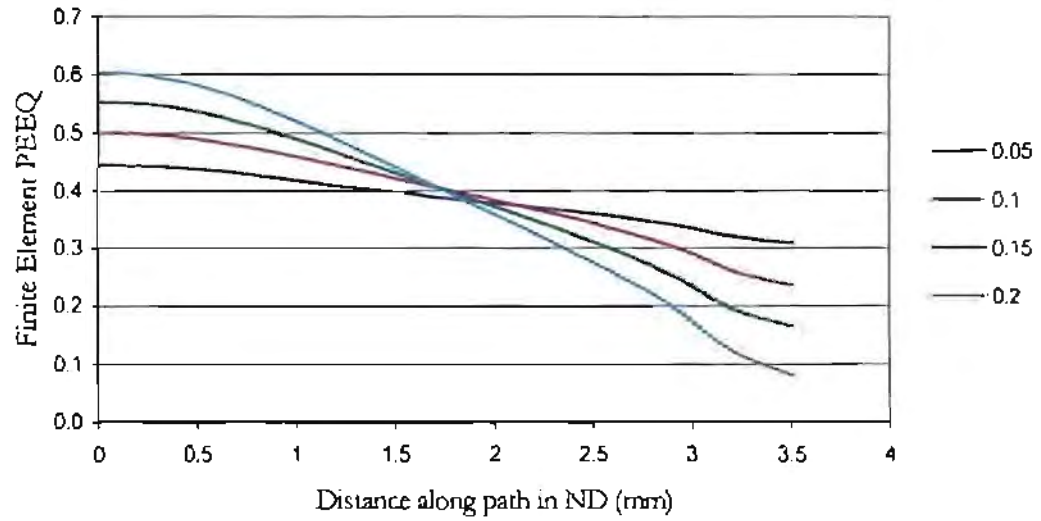

(a)

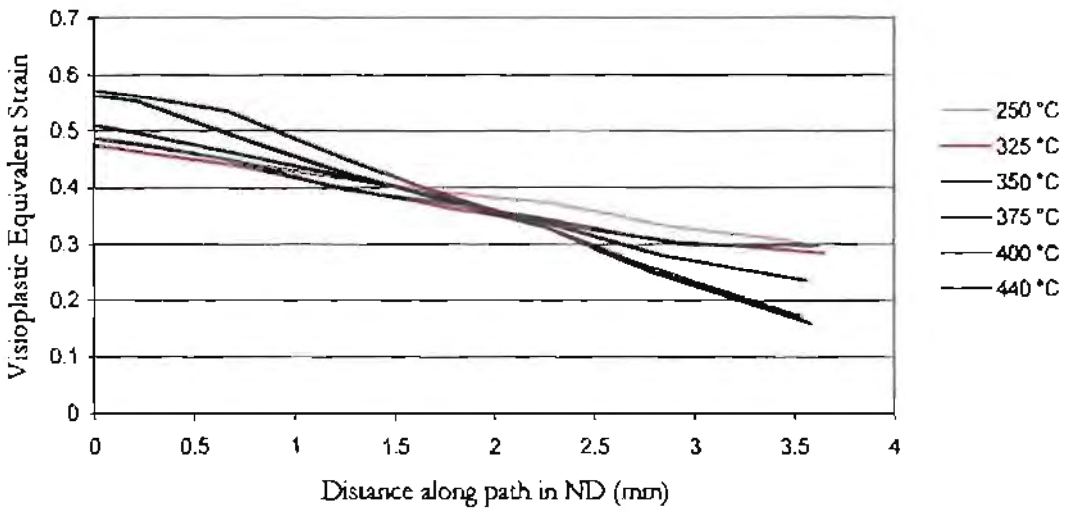

(b)

Figure 4.12 (a) FEM and (b) visioplastic equivalent strain along a node path in the ND used to calculate the coefficient of friction from the average slope of the graphs at a nominal strain of 0.42 deformed at a strain rate of 10 sec^{-1}.

The visioplastic PSC specimens deformed at 250, 325, 350, 375, 400 and 440 °C deformed to nominal strains of 0.22, 0.42 and 0.6 at a strain rate of 10 sec^{-1} were used to find the relationship between the deformation temperature and coefficient of friction using the average gradient of the FEM solution. In Figure 4.13 and 4.14 the average gradient for the visioplastic specimens are plotted as bars with horizontal lines indicating the FEM average gradient for simulated coefficient of friction. The negative of the average gradient is used for ease of graphical representation.

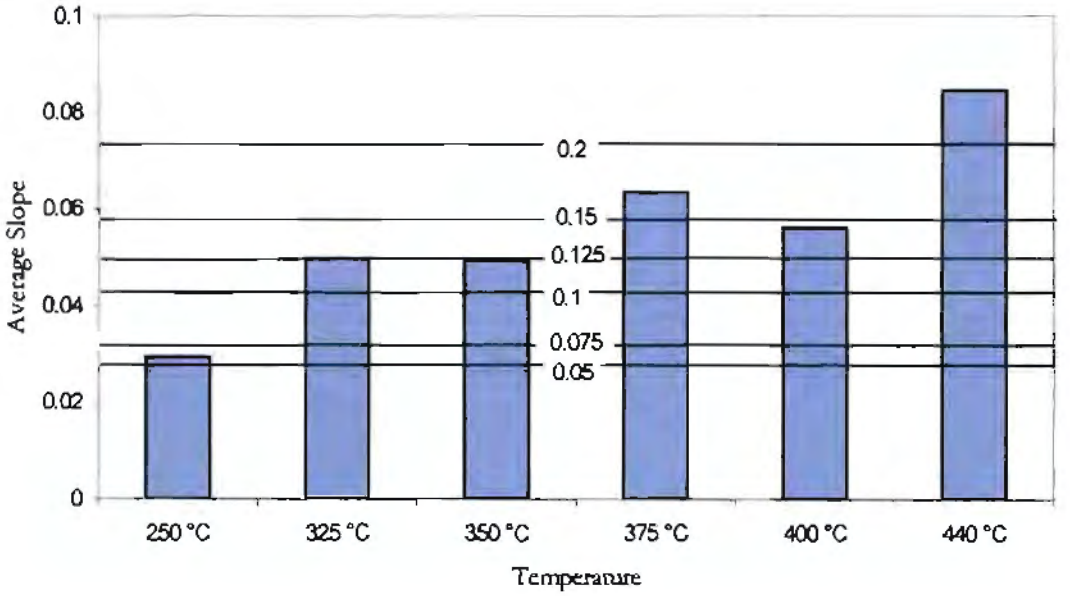

(a)

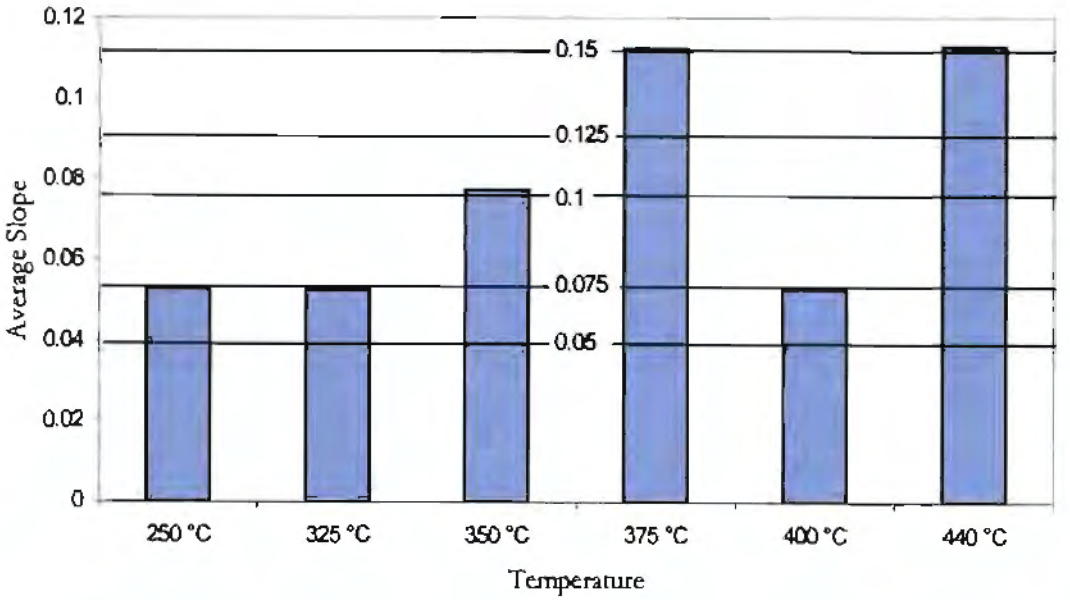

(b)

Figure 4.13 Visioplastic average gradient indicated by bars with FEM prediction of average gradient indicated by horizontal lines, for visioplastic tests performed to a nominal strain of (a) 0.22 and (b) 0.42 at a strain rate of 10 sec^{-1}.

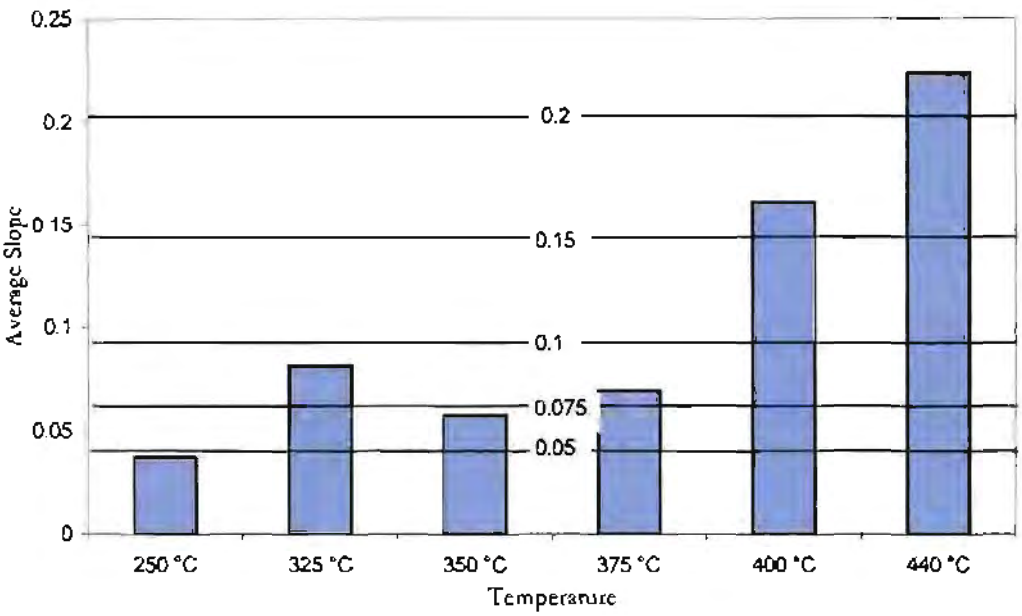

Figure 4.14 Visioplastic average gradient indicated by bars with FEM prediction of average gradient indicated by horizontal lines, for visioplastic tests performed to a nominal strain of 0.6 at a strain rate of 10 sec^{-1}.

As discussed in Section 4.2.4.1, the coefficient of friction appears to breakdown in one test but not in another. This is consistently illustrated in Figure 4.13 and 4.14 at a deformation temperature of 400 °C. The coefficient of friction approximated to be 0.14, 0.075 and 0.17 for nominal strain values of 0.22, 0.42 and 0.6 respectively.

4.2.4.3 Variation in Coefficient of Friction at Constant Deformation Temperature

The strain distribution patterns obtained from the visioplastic investigations show that there can be a large variation in the strain distribution due to variations in the coefficient of friction for tests performed at the same initial deformation temperature, as discussed in Section 4.2.4.1 and 4.2.4.2. This is further illustrated in Figure 4.15 by the visioplastic strain contours for deformation at 400 °C and has been graphically shown in Section 4.2.4.1 and 4.2.4.2. It appears that the lubrication breakdown occurs more in the one test than in the other.

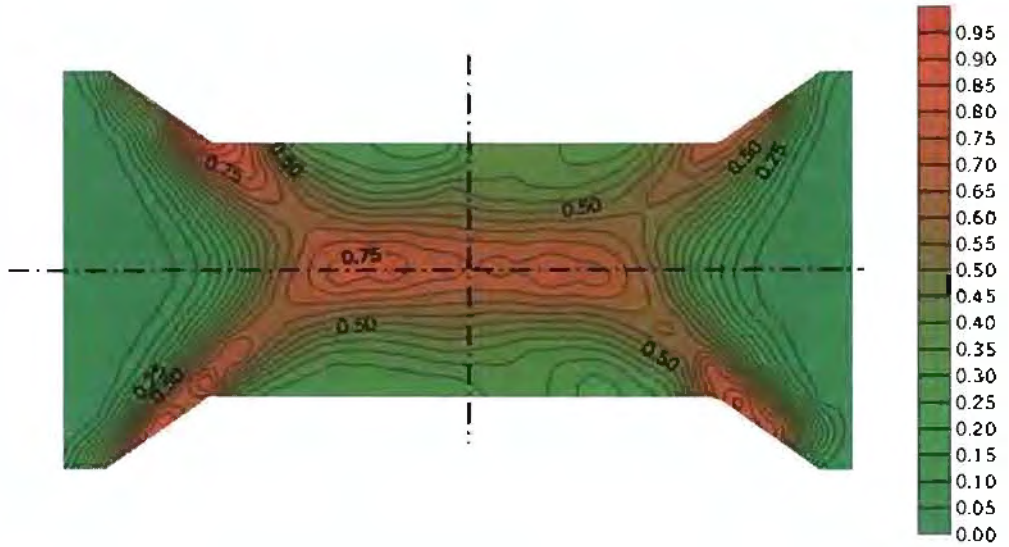

(a)

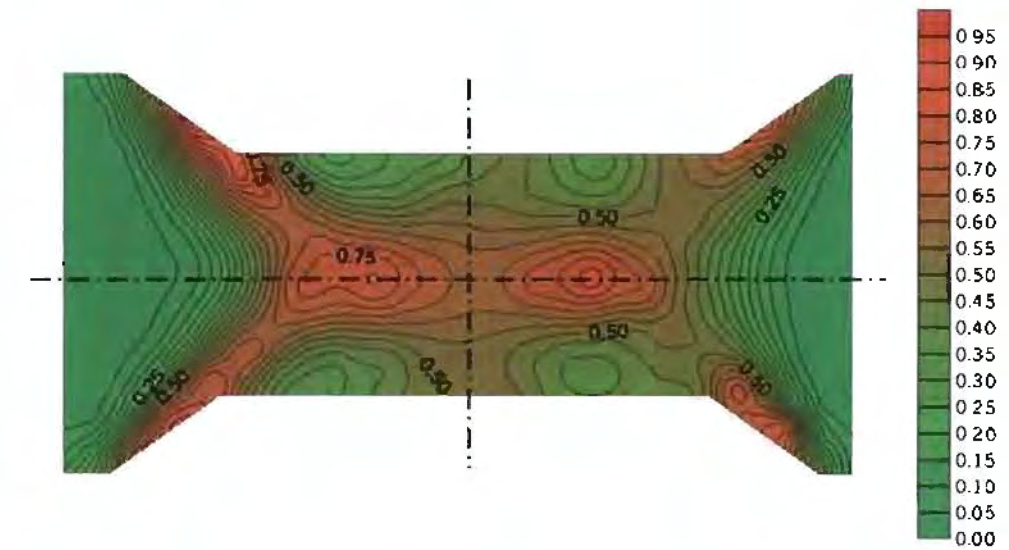

(b)

Figure 4.15 Visioplastic strain distribution contours for specimen deformed at 400 °C to a nominal strain of (a) 0.52 and (b) 0.57 at a strain rate of 10 sec^{-1} showing variations in strain contours for deformation at the same initial test temperature.

The strain distribution patterns indicate that the coefficient of friction is greater in Figure 4.15 (a) than in (b) as there is an increased 'dead zone' in (b) compared to (a). The increased friction results in increased material flow at the centre of the PSC specimen and the shear lines become less pronounced.

The variation in the coefficient of friction is further illustrated in Figure 4.16, where the visioplastic equivalent strain along a path from the centre of the PSC specimen in the ND is plotted for the two tests. Figure 4.16 shows that the gradient of the equivalent strain-distance curve is different for each test, which represents different friction conditions. The curve for the test performed to a nominal strain of 0.52 (Figure 4.15 (a)) shows an increased negative gradient when compared to the gradient for the test performed to a nominal strain of 0.57 (Figure 4.15 (b)). It is therefore apparent that the coefficient of friction is greater for the specimen deformed to a nominal strain of 0.52 than for the specimen deformed to a nominal strain of 0.57. The approximate variation in the coefficient of friction between the two specimens is 0.08 and 0.14 for (a) and (b) respectively, as determined in Section 4.2.4.1.

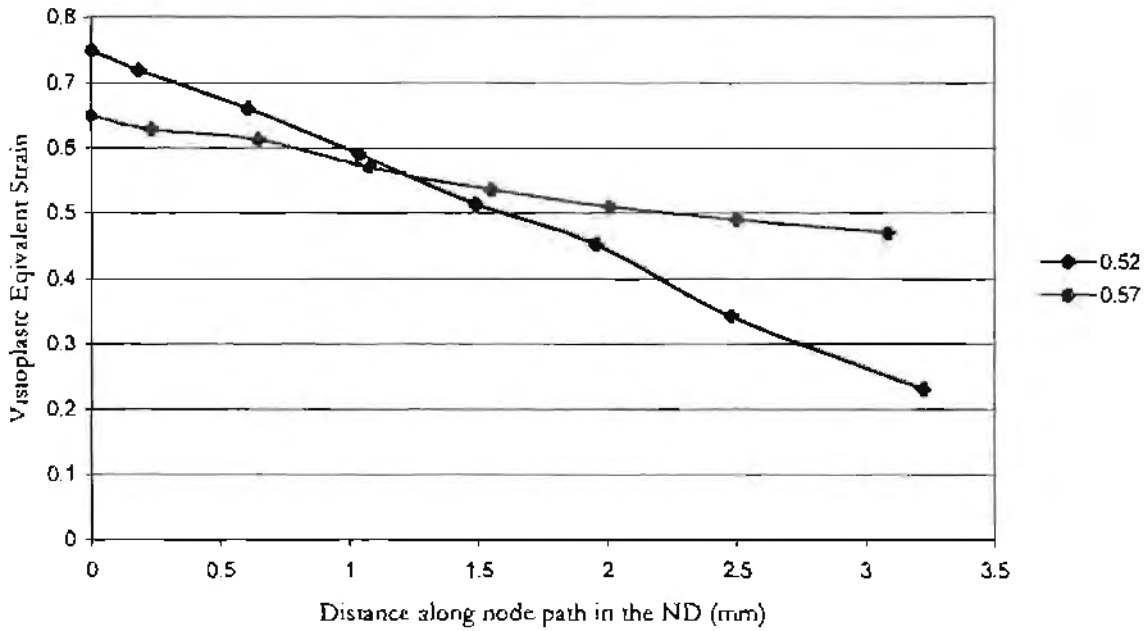

Figure 4.16 Visioplastic equivalent strain in the ND for specimens deformed to nominal strains of 0.52 and 0.57 at 400 °C at a strain rate of 10 sec^{-1}. The graphs clearly show a variation in gradient, which represents a variation in coefficient of friction between the two tests.

In determining the equivalent strain at the centre of the PSC specimen, a range of strain values should be considered within the temperature range where lubrication breakdown occurs. Exact determination of the equivalent strain is not possible as there will always be a significant variation in strain between PSC tests performed at the same deformation temperature because of the sensitivity of strain distribution to lubrication breakdown for aluminium PSC specimens.

4.2.4.4 Characterisation of Friction Condition

Interpretation of the result of Methods I and II allows the coefficient of friction to be determined at a specific temperature, which includes an approximate error. The range of coefficients of friction for each test temperature is used to determine a mean value and an approximate error. This is shown in Figure 4.17, which shows lubrication break down occurring progressively above 300 °C, which is consistent with the work of Beynon and Sellars[36] who estimated graphite lubrication to breakdown above 300 °C.

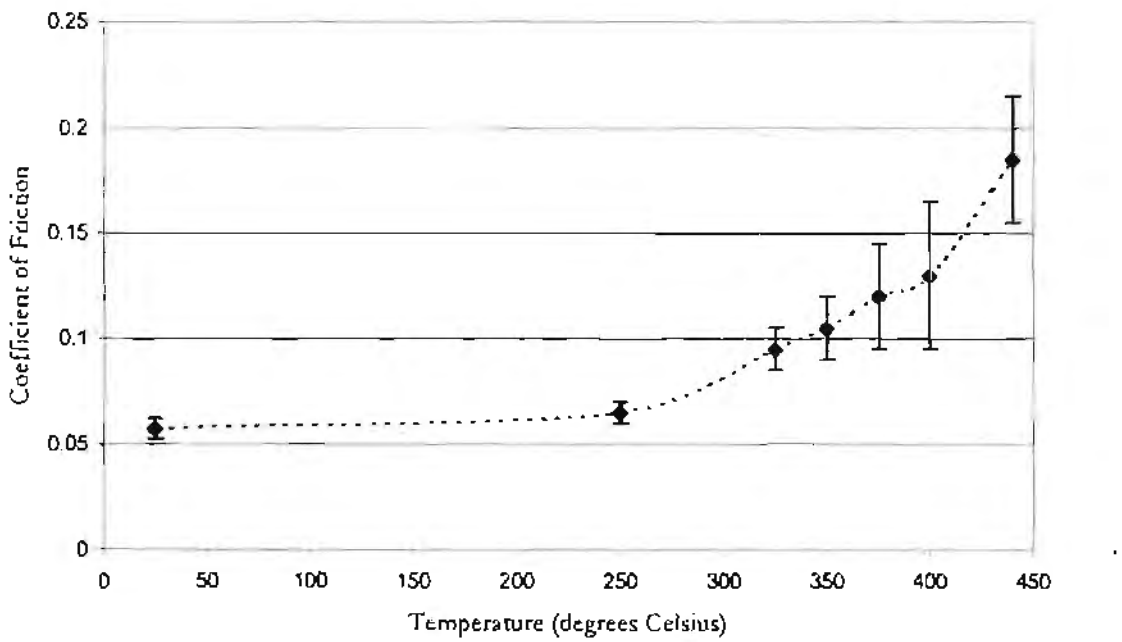

Figure 4.17 Effect of temperature on coefficient of friction as a result of breakdown in lubrication, showing lubrication breakdown occurring progressively above 300 °C.

A quadratic best-fit trendline of the coefficients of friction shown in Figure 4.17 allows the coefficient of friction to be determined within the range of deformation temperatures investigated. The coefficient of friction for the specific test temperatures investigated is given in Table 4.1 using the trendline approximation.

25	250	325	350	375	400	440
0.05	0.06	0.09 ± 0.01	0.1 ± 0.02	0.12 ±0.02	0.14 ±0.03	0.18 ±0.03

Table 4.1 Approximation of coefficient of friction values for the test temperatures investigated.

From the present study, equations have been derived from experimental and numerical results in which the coefficient of friction can be approximated within the range of deformation temperatures investigated. The coefficient of friction can then be incorporated into a FEM model to more accurately predict the strain and strain rate distribution within the PSC specimen for a specific test temperature.

For test temperatures between 25 and 250 °C the coefficient of friction is approximately constant at 0.05. The coefficient of friction at 250 °C given in Figure 4.17 is 0.06; however, a variation of coefficient of friction of 0.01 has little effect on the strain distribution at 250 °C. For temperatures from 25 to 250 °C the coefficient of friction is given by equation 4.3.

Equation 4.3 $\mu = 0.05$

For temperatures above 250 °C the coefficient of friction is determined by Equation 4.4.

Equation 4.4 $\mu = 2.4 \times 10^{-6} T^2 - 1.04 \times 10^{-3} T + 0.1746$

Where T is the temperature at which the PSC test is performed in degrees Celsius. Since lubrication breakdown occurs progressively above 300 °C, an approximate error of 15 % above and below the value of the coefficient of friction is required above 300 °C. The 15% error is used to determine the strain range the material at the centre of the PSC specimen may have received.

4.2.5 The Effect of Rate of Deformation on the Friction Condition

The surface interaction between contacting surfaces can be slip rate dependent with lower coefficients of friction being associated with faster slip rates. The slip rate being the rate at which the contacting surfaces slide over one another. Therefore, higher slip rates will be associated with higher nominal strain rates of the PSC test. Visioplastic analysis was performed at 250 and 400 °C at strain rates of 0.1 and 10 sec^{-1} to investigate the effect slip rate on friction condition. Figure 4.18 (a) and (b) show the effect of strain on the rate of deformation, clearly showing that no significant variation occurs.

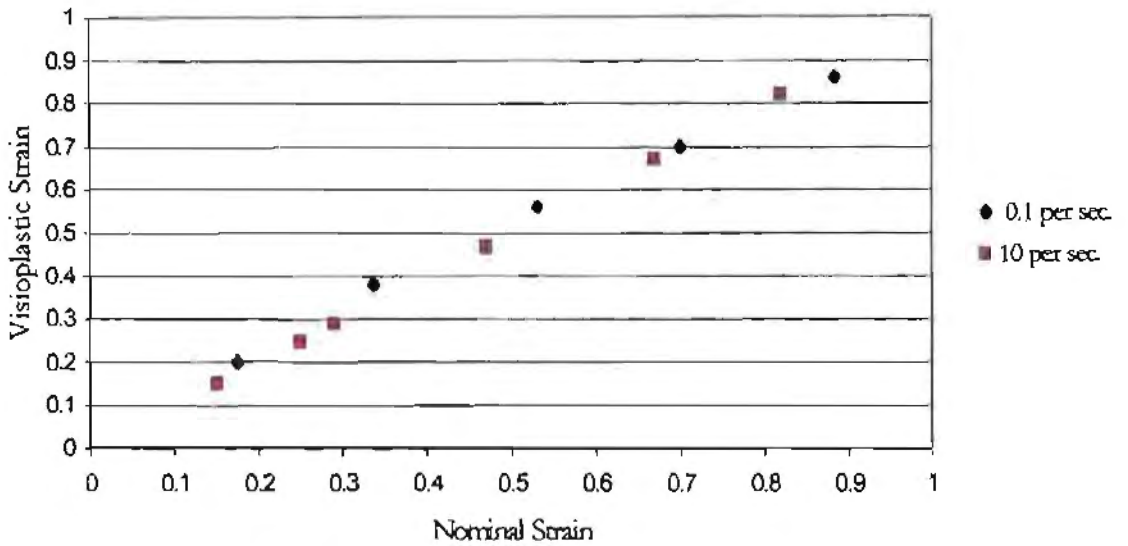

(a)

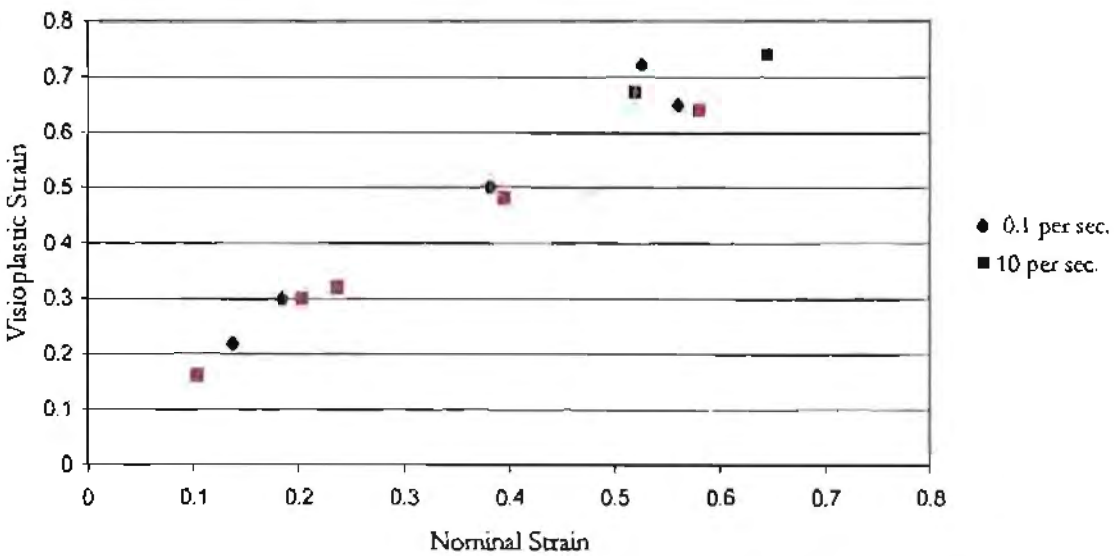

(b)

Figure 4.18 Equivalent strain at the centre of visioplastic PSC specimen deformed at (a) 250 and (b) 400 °C showing no significant variation in measured strain at the centre of the PSC specimen.

4.2.6 The Strain Rate During PSC Testing

The PSC rig designed by Duckham[10] uses a displacement control algorithm to adjust the anvil speed in order to simulate a constant nominal deformation rate of the PSC specimen. This is achieved by incrementally lowering the anvil crosshead speed during deformation to compensate for the reduction in thickness of the specimen. Strain rate compensation was therefore incorporated into the FEM model to simulate a constant nominal plane strain strain rate. Figure 4.19 illustrates PEEQ vs. time for a test performed at 250 °C at a strain rate of 10 sec^{-1}. The coefficient of friction, assuming Coulomb friction, is varied between 0.05 and 0.1. Figure 4.19 indicates that the strain rate is approximately constant at the centre of the PSC specimen. The variation in strain rate is approximately 3% and 12 % of the nominal strain rate for coefficients of friction of 0.05 and 0.1 respectively. It must be noted that for tests performed above 300 °C lubrication break down occurs as discussed in Section 4.2.4, therefore changing the strain and strain rate at the centre of the PSC specimen.

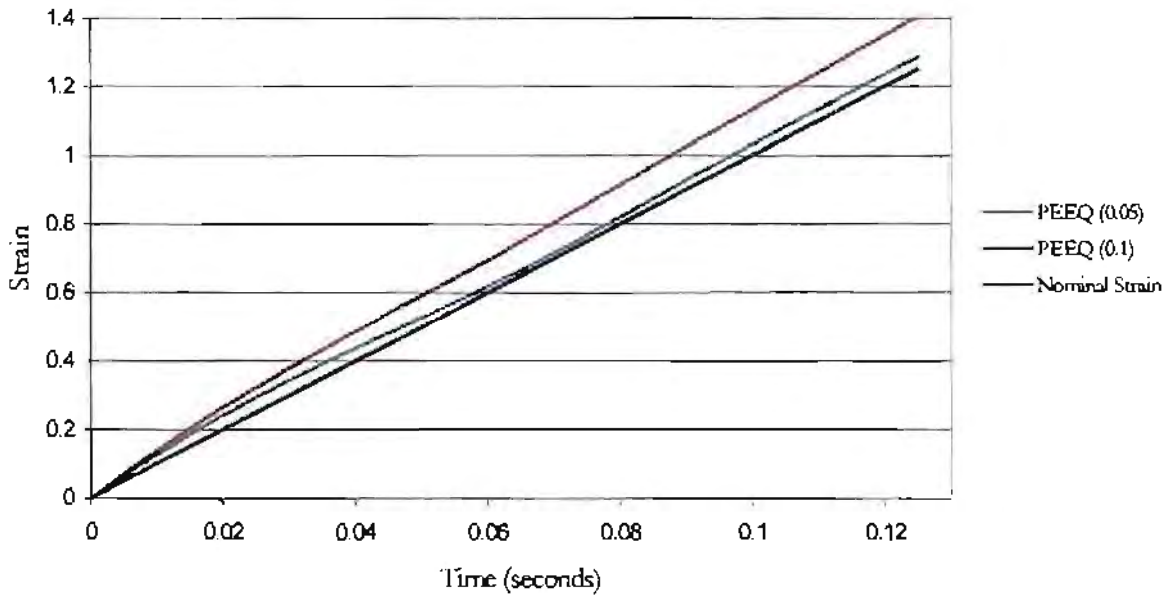

Figure 4.19 PEEQ vs. Time FEM predictions, showing approximately constant deformation rate at the centre of PSC specimen.

The Zener-Hollomon parameter is used to describe the influence of strain rate and temperature during deformation on the constitutive equations that relate deformation conditions to the microstructural evolution during subsequent annealing treatments. From Equation 2.2 it can be seen that the dependence of strain rate on Zener-Hollomon parameter is less significant than the effect of temperature. An increase in strain rate of up to 5% would be negligible in relation to the constitutive equations used to describe recrystallization kinetics when approximating the temperature of the test within 5 °C or when adiabatic heating occurs. However, the strain rate predicted by the FEM simulation is a better approximation of the strain rate that the material is receiving, as opposed to the nominal strain rate, and should be used in fitting experimental data to analytical microstructural models.

4.2.7 Slip Line Fields

The material flow in the volume of material under the anvil during PSC testing is governed by the prevailing slip line field, which is determined by the specimen and anvil geometry. Figures 4.20 and 4.21 are used to simulate the slip line fields produced during PSC testing at different nominal strain values for a coefficient of friction of 0.05.

Figure 4.20 illustrates the strain singularity at the corner of the anvil upon initial deformation. The shear lines then spread inwards towards the centre of the specimen at an angle of approximately 45°. As deformation proceeds the ratio of anvil breadth to specimen height (b/h) changes, resulting in a progressive change in the slip line field. This is illustrated in Figures 4.20 and 4.21, where the number of crosses changes from approximately 1 in Figure 4.20 to 3 in Figure 4.21 (b).

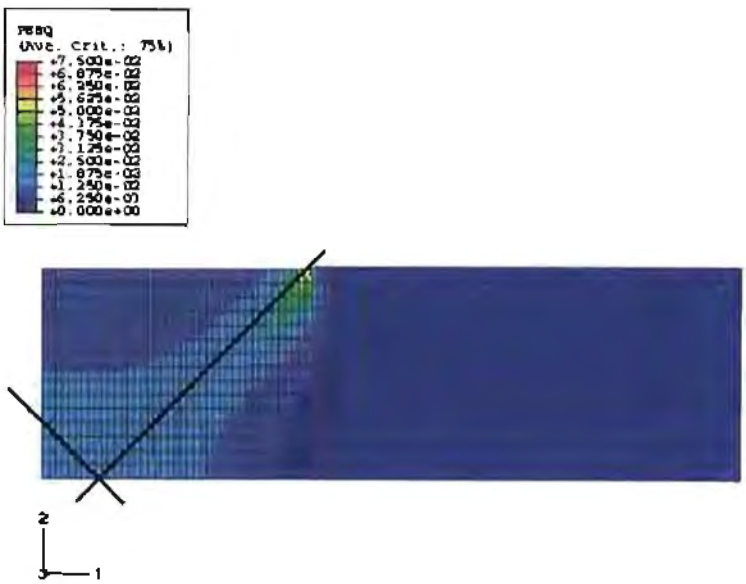

Figure 4.20 FEM PEEQ contour upon initial deformation illustrating strain singularity at the anvil corner and shear lines at 45°.

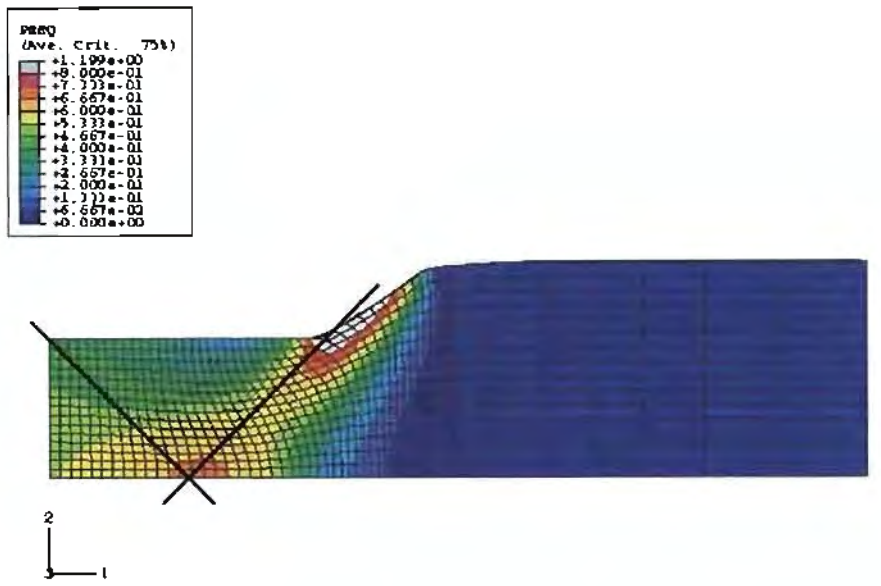

(a)

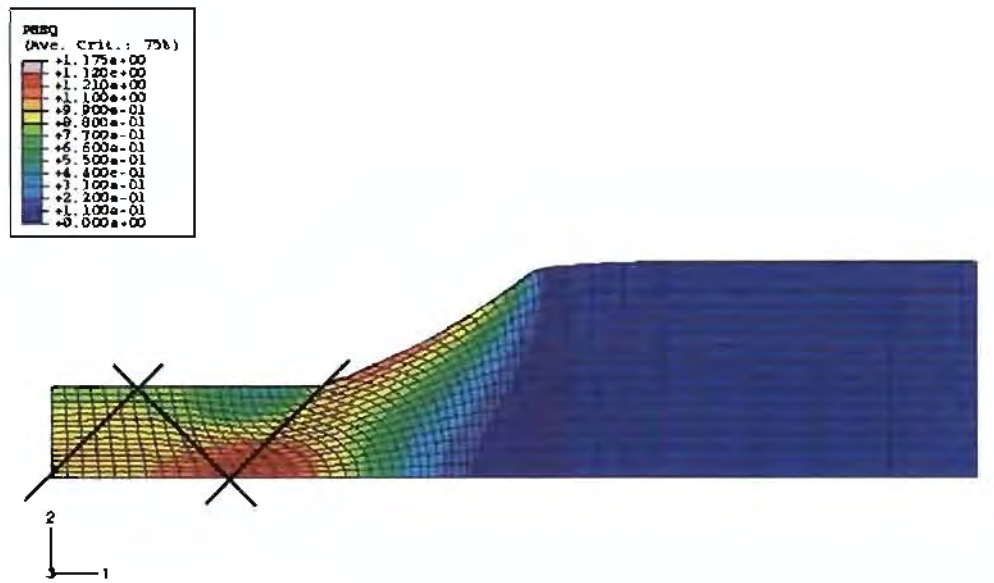

(b)

Figure 4.21 FEM PEEQ contour for 250 °C simulation at a strain rate of 10 sec^{-1}, slip lines drawn at 45° for b/h ratios of (a) 2 and (b) 3, showing that the strain distribution becomes more homogeneous across the RD/ND plane at b/h ratios greater than 2.

Figure 4.21 (b) does not show distinct slip lines. As deformation proceeds the b/h ratio changes, consequently the prevailing slip line field changes during deformation. The change in slip line field results in a more homogeneous strain distribution for b/h ratios greater than 2 (nominal strains greater than 0.97 in this case).

The above results are consistent with the visioplastic analysis. It is noted that the slip line field generated during deformation changes for temperatures above 300 °C. This is due to the breakdown in lubricant resulting in increased friction. From visioplastic analysis the increased friction creates an increased 'dead zone' beneath the anvil. The increased friction at temperatures above 300 °C results in increased material flow at the centre of the specimen, changing the strain distribution. As lubrication breakdown occurs the friction increases, the slip lines become less pronounced and a band of localized strain at the centre of the PSC specimen is produced as illustrated in Figure 4.7 (b).

4.2.8 Plane Strain Deformation

As suggested by Shi *et al*[25], it has been found that an approximate plane strain condition exits in the central (w-b) part of the deformed specimen, as illustrated in Figure 22 (a), w being the specimen length in the TD and b the anvil width. This is because the material at both ends of the specimen is equally free to move in both the length and width directions (TD and RD). Therefore, the deformation at each end of the specimen is more like axisymmetric compression and the approximate plane strain condition does not exist over this part of the specimen. The plane strain condition is investigated by analysing the PEEQ and the principal strains along the node path from the geometric centre of the PSC specimen in the TD as illustrated in Figures 4.22 (b) and 4.23. The FEM model is for a specimen deformed at 400 °C at a strain rate of 10 sec^{-1} to a nominal strain of 1 using a coefficient of friction of 0.1 and 12 elements were used in the TD.

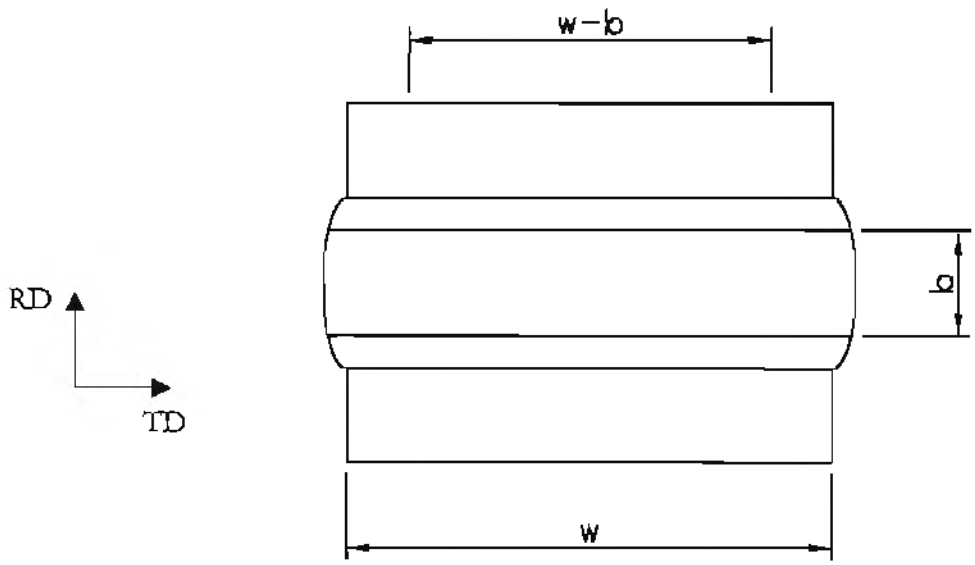

(a)

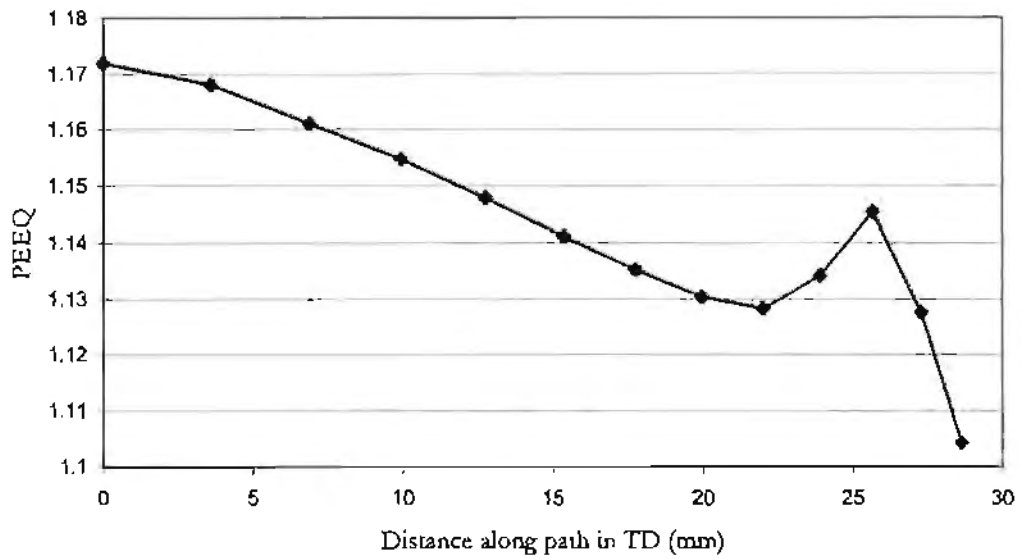

(b)

Figure 4.22 (a) Schematic diagram illustrating central (w-b) part of a deformed PSC specimen. (b) FEM PEEQ along node path in the TD, 0 being the centre of the PSC specimen, showing that the approximate plane strain condition breaks down at approximately 20 mm from the centre of the PSC specimen.

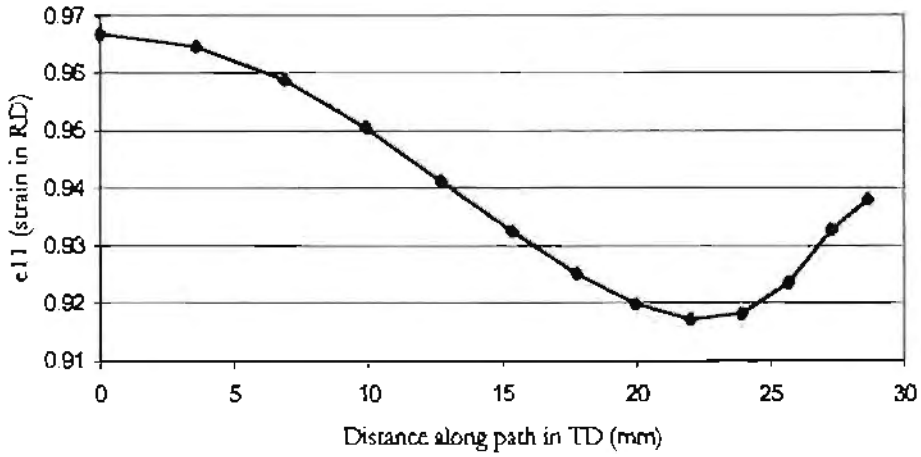

(a)

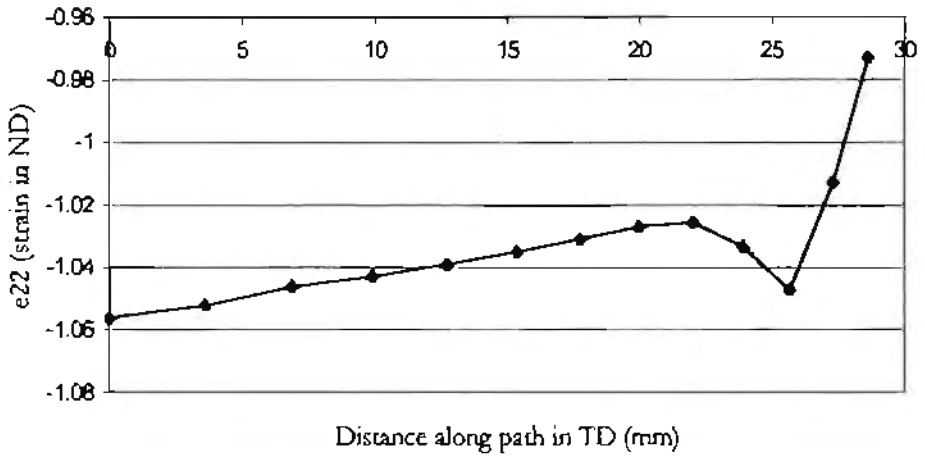

(b)

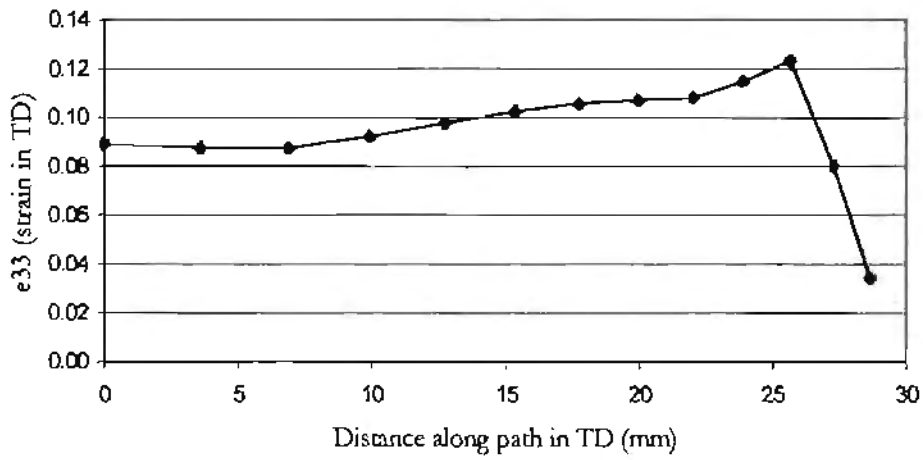

(c)

Figure 4.23 Principal plastic strain along node path in TD, (a) e11, (b) e22 and (c) e33 indicating variations in strain towards the end of the PSC specimen and (c) showing that a true plane strain condition does not exist during PSC testing.

Figure 4.22 (b) illustrates the PEEQ plot at a nominal strain of 1, which illustrates the variation in strain in the TD from the centre of the PSC specimen showing a steady drop in strain towards the end of the specimen with a discontinuity occurring at approximately 20 mm from the centre. Figure 4.23 (a), (b) and (c) show similar trends for the principal strain values at 20 mm from the centre of the PSC specimen. It is also apparent from Figure 4.23 (c) that a true plane strain condition does not exist during PSC testing with an average strain in the TD (e33) of approximately 0.1 per unit nominal strain in the ND. However, the result of Figures 4.22 (b) and 4.23 show that material receiving approximate plane strain deformation is the central (w-b) volume of material.

Figure 4.22 (b) shows a variation of 0.04 strain in the central (w-b) part of the deformed specimen. This variation is negligible but should be considered when determining the strain range in the centre part of the PSC specimen for deformation temperatures between 25 and 440 °C, as the variation in friction condition will result in a range of PEEQ values at the centre of the PSC specimen. The coefficient of friction does not change the approximate plane strain condition in the central (w-b) part of the deformed specimen but changes the strain magnitude.

4.2.9 Finite Element Mesh Distortion

At nominal strains greater than 1.4 mesh distortion occurs resulting in the mesh instability known as hourglass mode. Hourglass mode is illustrated in Figure 4.24 (b), showing mesh distortion. The instability arises because of shortcomings in the evaluation of the stiffness equations when using low order Gauss-Quadrature. The instability can be overcome by mesh refinement or by using a higher-order Gauss-Quadrature rule; however, computation time would increase. The hourglass mode instability was acceptable for the range of nominal strains investigated; however, the instability should be considered for nominal strain values greater than 1.4. For nominal strains greater than 1.4 the strain and strain rate at the centre of the PSC specimen can be extrapolated from FEM predictions as the strain and strain rate increase approximately linearly with incremental change in nominal strain.

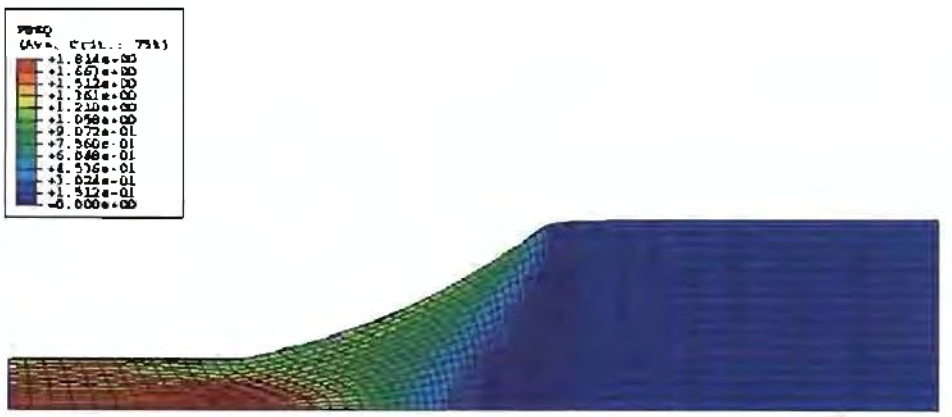

(a)

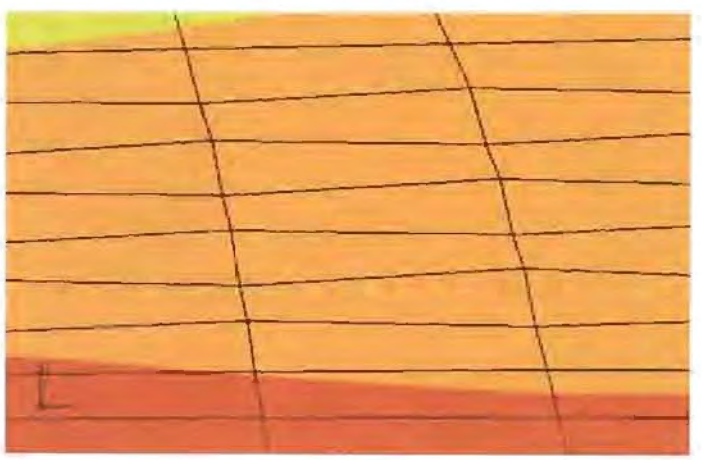

(b)

Figure 4.24 FE mesh distortion showing hourglassing for (a) nominal strains greater than 1.4 at (b) approximately the centre of the PSC specimen.

4.2.10 Strain-Hardness Correlation

The strain-hardness correlation determined from tensile and axisymmetric compression tests was used to obtain a strain contour to be used for direct comparison with FEM approximations for validation. Figure 4.25 shows a strain contour plot for a PSC specimen deformed at 25 °C at a strain rate of 0.1 sec^{-1} to a nominal strain of 0.28.

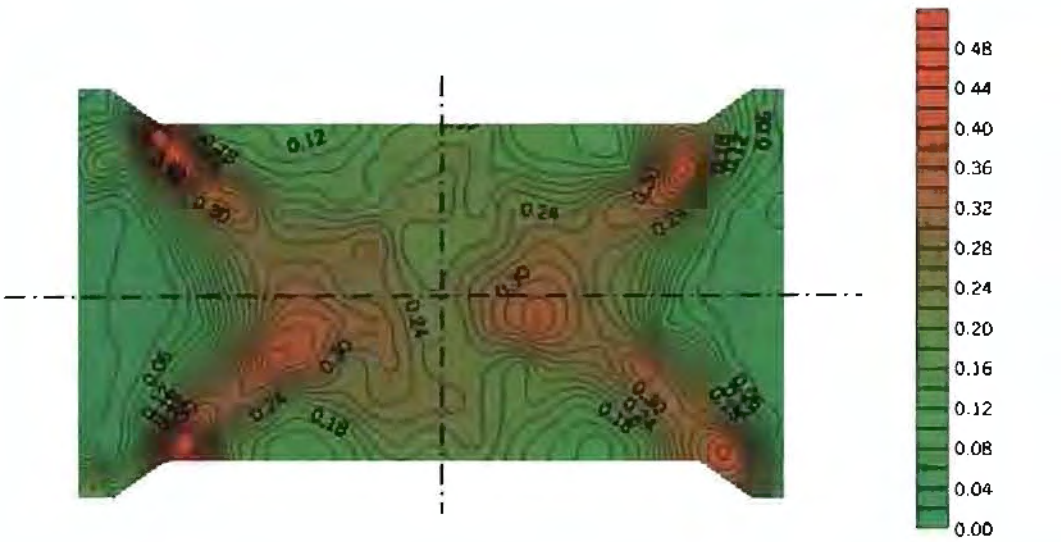

Figure 4.25 Strain contour using strain-hardness correlation for PSC specimen deformed at 25 °C at a strain rate of 0.1 sec^{-1} to a nominal strain of 0.28.

The strain contour contains discontinuities in strain distribution as a result of variations in hardness measurements. At higher nominal strains the hardness correlation does not approximate to the accuracy of the FEM or visioplasticty results with discontinuities becoming prevalent. At high strain values there is little variation in hardness with increase in strain, the strain-hardness correlation was therefore unsuccessful in determining a strain distribution during PSC testing at room temperature. Furthermore, the technique could not be used at elevated temperatures because of dynamic recovery resulting in little variation in hardness measurements.

4.2.11 Comparison Between Present and Past Research

Determination of the mechanical variables during PSC testing has been investigated for steel[21] and aluminium[36] using visioplastic analysis and it is apparent from previous and the present research that an exact determination of the mechanical parameters is complex, and that a range of mechanical parameters is applicable. A range of mechanical variables is more applicable for PSC testing of aluminium since the strain and strain rate distribution is sensitive to small changes in friction condition. This is attributed to the low work hardening of aluminium. Whereas for steel, which has a higher work hardening rate, the strain distribution is less sensitive to variations in friction condition. This is because the change in stress for incremental change in strain is greater, leading to greater segregation between areas of high and low strain. Therefore, the low work hardening of aluminium results in a more homogeneous strain distribution compared to that of steel, but is sensitive to small variations in friction.

4.3 Determination of Thermal Variables during PSC Testing

4.3.1 Recrystallization Study

The microstructural evolution during post deformation annealing reveals inhomogeneous recrystallization within PSC specimens across the RD/ND plane, as shown in Figure 4.26, which consistently occurs for deformation temperatures between 25 and 460 °C at strain rates of 10 sec^{-1} to nominal strains of 1.

Previous work by Jahajeeah[38] concluded that the temperature distribution prior to testing at hot working temperatures was homogeneous. At a strain rate of 10 sec^{-1} the PSC test is performed in 0.1 seconds to a nominal strain of 1, in which heat loss to the anvils is considered negligible. PSC specimens were deformed at 25, 250 and 440 °C at strain rates of 10 sec^{-1} to approximate nominal strains of 1. Figure 4.26 shows recrystallization initiating near the surface of the specimen with the centre material requiring longer annealing times to fully recrystallise for specimens deformed at 25, 250 and 440 °C. The driving force for recrystallization is the stored energy of the deformed microstructure, which can be directly associated with microstructural models in terms of strain and the Zener–Hollomon parameter.

(a)

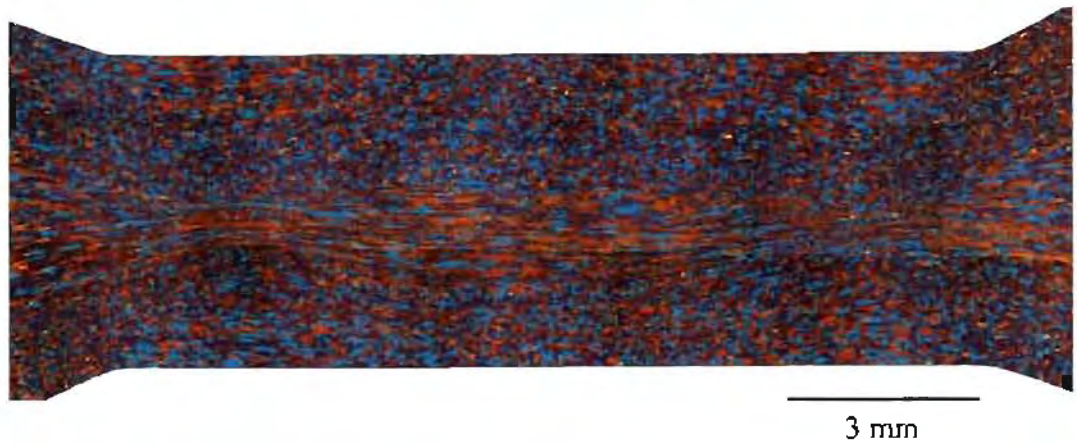

(b)

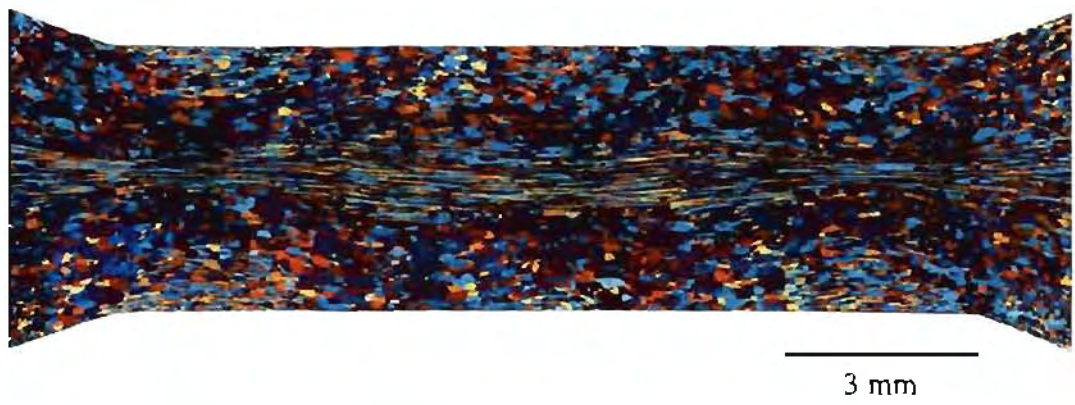

(c)

Figure 4.26 Polarized light micrographs showing recrystallization initiating at the surface of PSC specimens deformed at test temperatures of (a) 25, (b) 250 and (c) 440 °C. PSC tests performed at a strain rate of 10 sec^{-1}, to nominal strains of approximately 1. Annealing treatments performed at 300 °C for 20 seconds, 350 °C for 10 seconds and 440 °C for 15 seconds respectively.

From Section 4.2.3, it is evident that the strain and strain rate at the centre of the specimen are greater than at the surface. Figure 4.27 illustrates the true stress-true strain flow curve at 440 °C at a strain rate of 10 sec^{-1} showing that at a strain of 1 the stress-strain relationship has reached a steady state stress, where an increase in strain causes a negligible change in stress level. This is due to the dislocation initiation being equal to the dislocation annihilation as a consequence of recovery, resulting in a steady state stored energy being obtained. Therefore, assuming homogeneous temperature and strain rate distribution of the deformed PSC specimen; flow curve data can be used to evaluate the resultant recrystallization for any thermo-mechanical deformation parameters by considering the variation in strain distribution across the RD/ND plane of the PSC specimen.

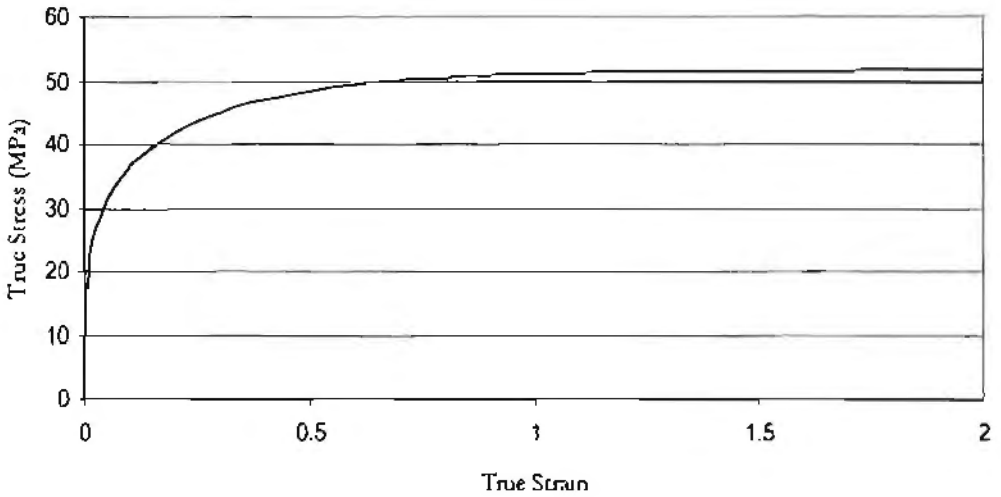

Figure 4.27 Flow curve for deformation at 440 °C at a strain rate of 10 sec^{-1}, showing steady state stress above approximately a strain of 1.

As discussed in Section 4.2.3, the strain at the centre of the deformed PSC specimen is greater than in the material near the surface. Therefore, considering homogeneous temperature distribution, the stored energy due to strain is greater at the centre than at the surface of the PSC specimen. The increased strain at the centre means the centre material is experiencing a higher strain rate, which results in a variation in the Zener-Hollomon parameter through the thickness of the PSC specimen. Furthermore, the increased friction at temperatures above 300 °C, as discussed in Section 4.2.4, would result in a higher strain and subsequent strain rate at the centre of the specimen. Therefore, considering homogeneous temperature distribution within the PSC specimen, recrystallization is expected to initiate at the centre of the PSC specimen.

For tests performed at a strain rate of 1 sec^{-1} the inhomogeneity of the recrystallization reaction over the RD/ND plane of the PSC specimen was not pronounced. Therefore, the thermo-mechanical variable producing the inhomogeneity of recrystallization at a strain rate of 10 sec^{-1} is most likely an inhomogeneous temperature distribution, with the centre being at a higher temperature than the surface. The inhomogeneous temperature distribution results in greater dynamic softening at the centre of the PSC specimen, therefore less stored energy relative to the surface and less likely to recrystallise.

4.3.2 Micro-Hardness Distribution

Micro-hardness measurement of the as deformed specimens can be used to quantitatively obtain a stored energy distribution. Through thickness micro-hardness measurements reveal that the material near the surface of the specimen is harder than material at the centre of the specimen. This is illustrated in Figure 4.28 and 4.29, for specimens deformed at 25, 250 and 325 °C at a strain rate of 10 sec^{-1} to a nominal strain of 1. The material near the surface is harder than the material at the centre which represents a stored energy distribution through the thickness of the PSC specimen, with the harder material being characterised as having more stored energy, therefore likely to recrystallise first during subsequent annealing.

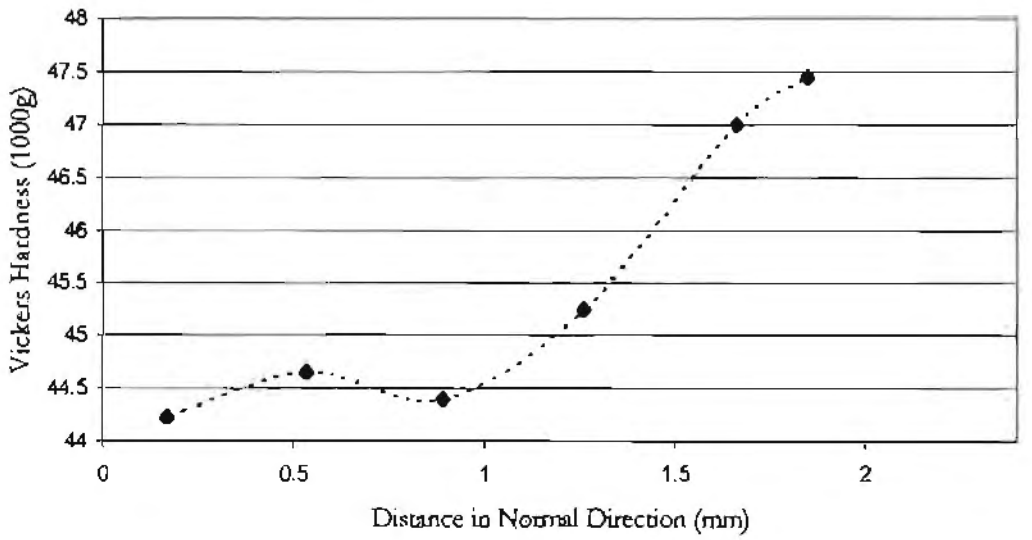

Figure 4.28 VH (1000g) distribution in the ND for PSC specimens deformed at 25 °C at a strain rate of 10 sec^{-1} to a nominal strain of approximately 1, revealing a hardness gradient through the thickness of the as deformed PSC specimen. The 0 mm position is the mid-thickness of the PSC specimen.

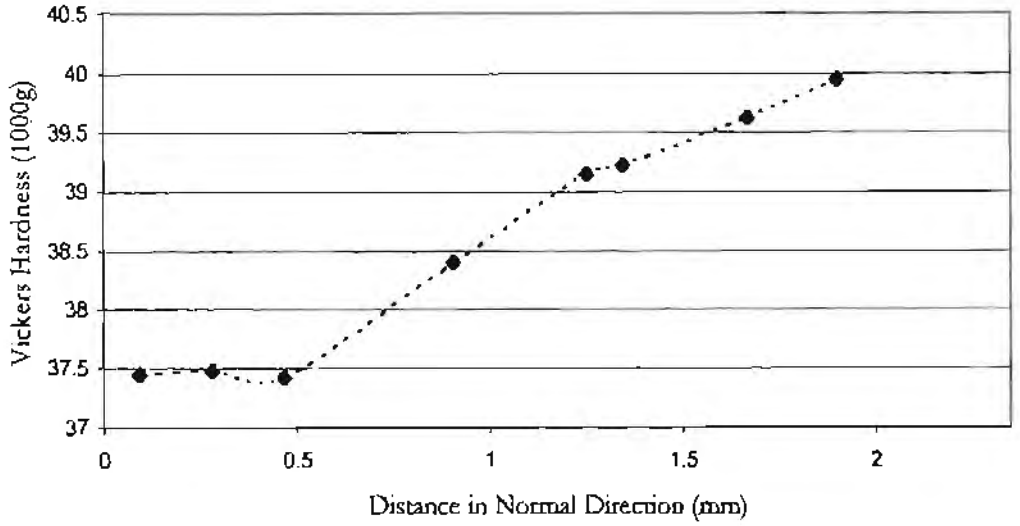

(a)

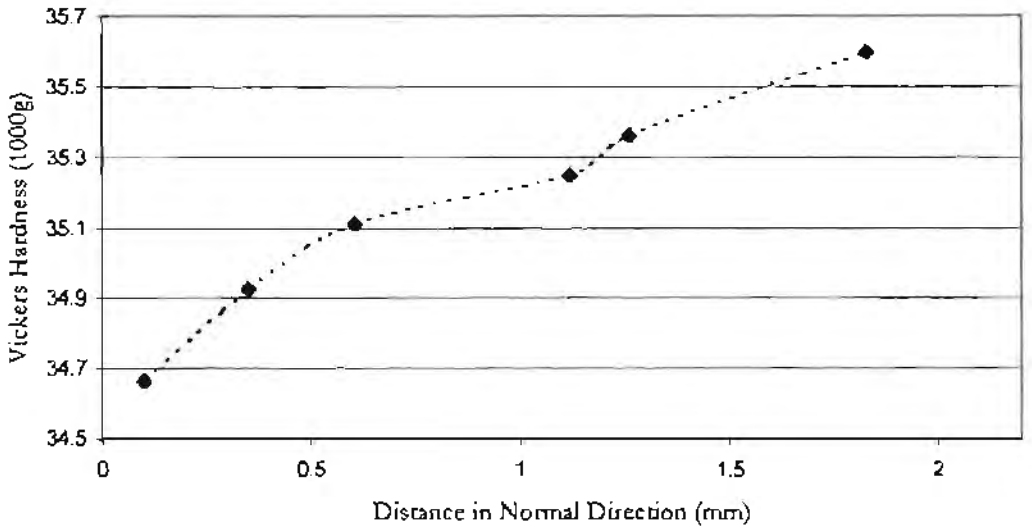

(b)

Figure 4.29 VH (1000g) distribution in the ND for PSC specimens deformed at (a) 250 and (b) 325 °C at a strain rate of 10 sec^{-1} to nominal strains of approximately 1, revealing a higher hardness near the surface of the specimen, which is a direct indicator of the stored energy distribution of the deformed microstructure. The 0 mm position is the mid-thickness of the PSC specimen.

Recovery is a thermally activated restoration process, which is known to occur during deformation in aluminium and is the only dynamic restoration process as there is no evidence to support dynamic recrystallization. Figures 4.28 and 4.29 illustrate the effect of dynamic softening as the test temperature is increased, which indicates dynamic recovery. The microhardness decreases at the centre of the PSC specimens as the deformation temperature is increased. Microhardness distributions were not possible for deformation temperatures greater than 325 °C because of little variation in hardness distribution.

4.3.3 The Effect of Adiabatic Heating on Recrystallization

PSC specimens were deformed at room temperature at a strain rate of 10 sec^{-1} to isolate the effect of adiabatic heating on recrystallization. At room temperature electrical resistance heating is not employed and the possibility of inhomogeneous temperature distribution attributed to electrical resistance heating can be ignored. An inhomogeneity of recrystallization would therefore be attributed to adiabatic heating effects within the specimen.

PSC tests were performed at 25 °C at strain rates of 0.1 and 10 sec^{-1} to investigate the effect of adiabatic heating on recrystallization. A FEM temperature contour for the simulation of the test performed at strain rate of 0.1 sec^{-1} is illustrated in Figure 4.30 (a). Figure 4.30 (a) illustrates a homogeneous temperature distribution within the specimen deformed to a nominal strain of 1. In the FEM simulation the heat generated by plastic work is conducted away from the deforming areas and the specimen remains in an isothermal condition. Recrystallization kinetics would therefore be dependent on the strain and strain rate of deformation. A strain rate of 0.1 sec^{-1} is regarded as a low strain rate relative to industrial hot rolling operations. The variation in strain rate across the RD/ND plane of the PSC specimen does not significantly affect the Zener-Hollomon parameter to cause a variation in recrystallization, with a strain rate of 0.1 and 0.072 at the centre and the surface respectively. Figure 4.30 (b) illustrates the partially recrystallized microstructure of the PSC specimen deformed at a strain rate of 0.1 sec^{-1} annealed at 300 °C for 20 seconds. Recrystallization is observed to be relatively homogeneous with recrystallization initiating in areas of high strain. The area of high strain is illustrated in Figure 4.7 (a), as discussed in Section 4.2.3. The outlined area of Figure 30 (b) is shown in Figure 31 to illustrate the initiation of recrystallization during subsequent annealing. Figure 31 clearly shows fine equiaxed grains in the area of high strain with elongated grains in areas of lower strain.

(a)

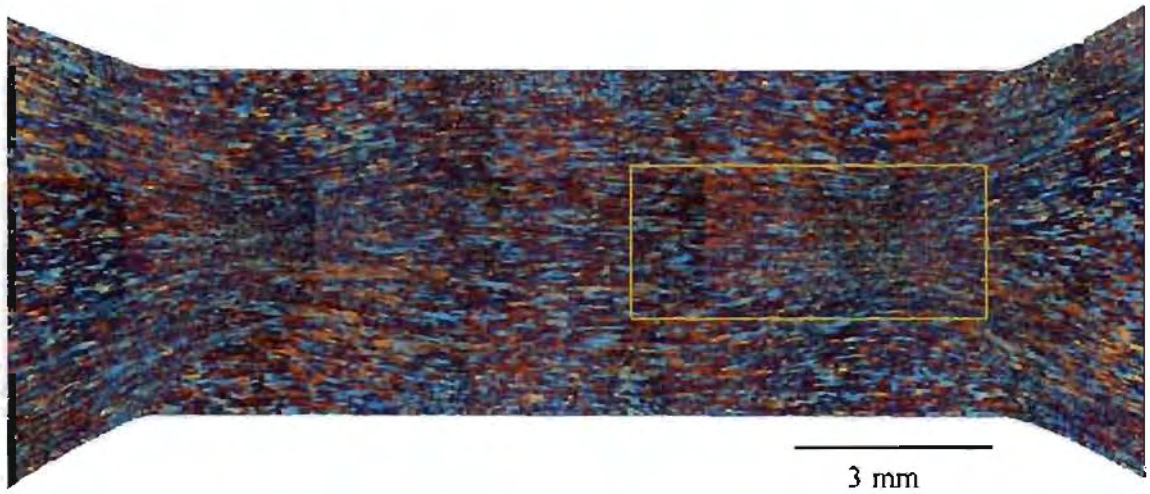

(b)

Figure 4.30 (a) FEM prediction of temperature distribution for PSC specimen deformed at 25 °C at a strain rate of 0.1 sec^{-1} to a nominal strain of 1, showing no significant temperature variation across the RD/ND plane. The legend indicates the temperature in Kelvin. (b) Partially recrystallized PSC specimen deformed at room temperature at a strain rate of 0.1 sec^{-1} to a nominal strain of 1 showing recrystallization initiating in areas of high strain when annealed at 300 °C for 20 seconds.

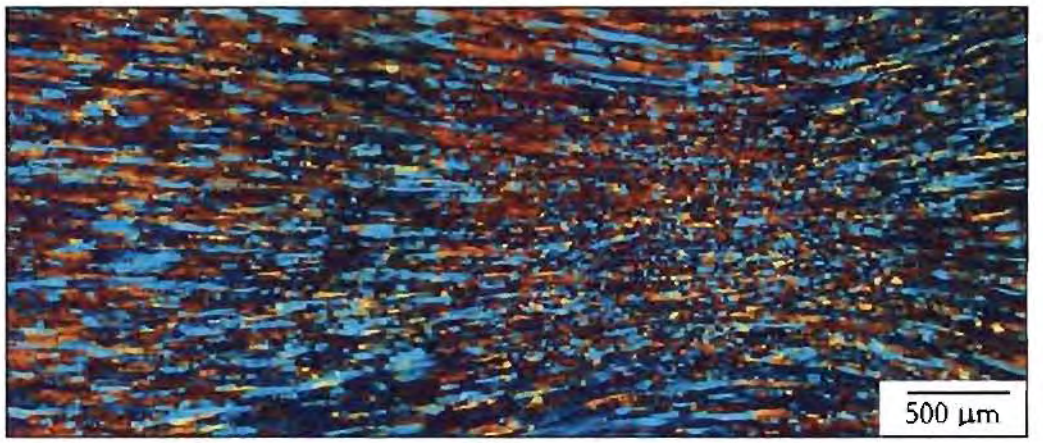

Figure 31 Outlined area of Figure 30, showing recrystallization initiating in area of high strain (right) and elongated grains observed near the centre (left) of the PSC specimen deformed at a strain rate of 0.1 sec^{-1} at room temperature.

Figure 4.31 (a) illustrates the FEM predicted temperature contour for test simulation at 25 °C at a strain rate of 10 sec^{-1} to a nominal strain of 1. In Figure 4.31 (a) adiabatic heating occurs with a localised increase in temperature at the centre of the specimen of 20 °C for the PSC test simulation performed at a strain rate of 10 sec^{-1}. Figure 4.31 (a) shows that the heat generated by plastic work has insufficient time to be conducted away from the deforming regions. Figure 4.31 (b) illustrates inhomogeneous recrystallization across the RD/ND plane of the PSC specimen for a test performed at a strain rate of 10 sec^{-1}. Recrystallization initiates in the material near the surface of the specimen with the material at the centre requiring longer annealing times to fully recrystallise although the strain and strain rate at the centre is greater than that experienced near the surface.

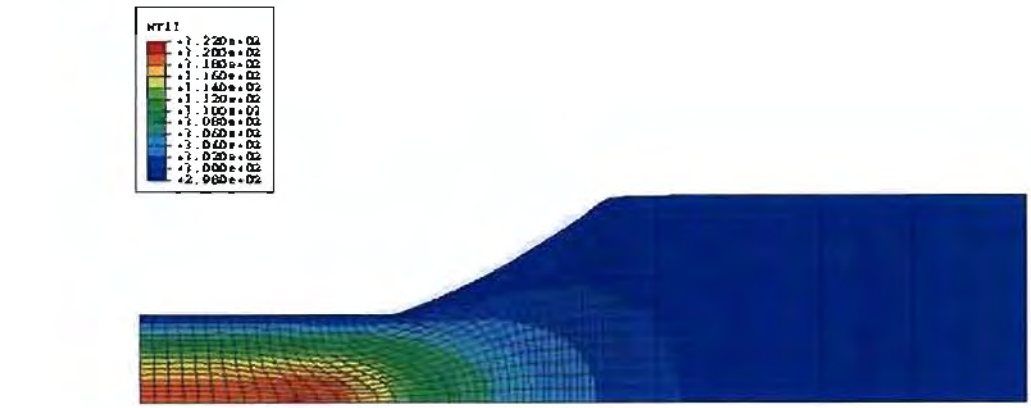

(a)

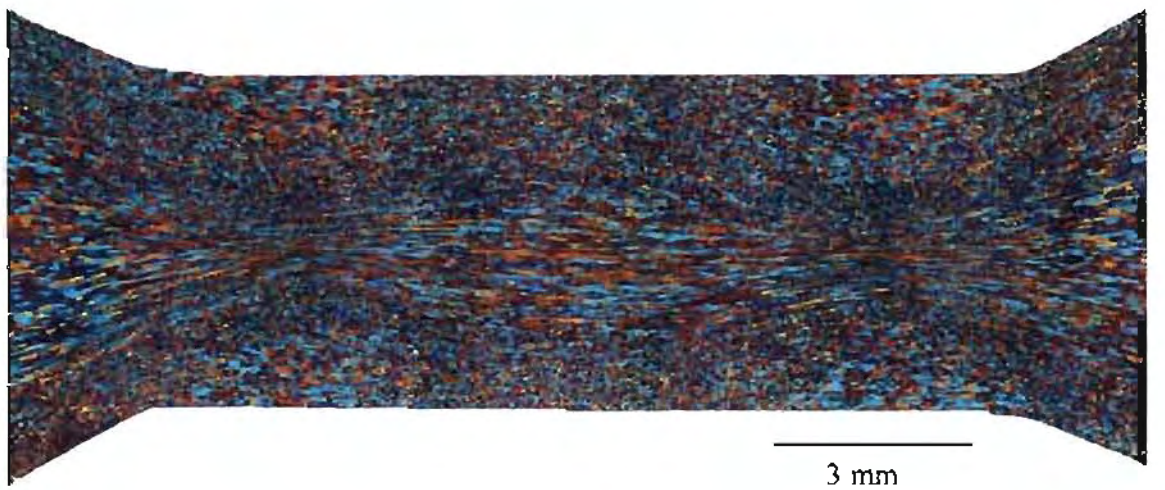

(b)

Figure 4.32 (a) FEM prediction of the temperature distribution across the RD/ND plane of a PSC specimen deformed at 25 °C at a strain rate of 10 sec^{-1} to a nominal strain of 1, showing an increase in temperature of 20 °C at the centre of the PSC specimen as a result of adiabatic heating. The legend indicates the temperature in Kelvin. (b) Partially recrystallized PSC specimen deformed at room temperature at a strain rate of 10 sec^{-1} to a nominal strain of 1, showing inhomogeneous recrystallization when annealed at 300 °C for 20 seconds.

In comparing Figures 4.30 (b) and 4.32 (b) a significant variation in recrystallization is observed for nominal strain rates of 0.1 and 10 sec^{-1} respectively. The inhomogeneity of recrystallization in Figure 4.32 (b) is attributed to dynamic softening of the material as a result of localized adiabatic heating at the centre of the PSC specimen deformed at a strain rate of 10 sec^{-1}. At a strain rate of 10 sec^{-1} the material at the centre of the PSC specimen is at a higher temperature of deformation relative to the material near the surface. Since recovery is a thermally activated restoration process the material at the centre of the PSC specimen experiences greater dynamic recovery, which outweighs the effect of the strain inhomogeneity on recrystallization. The inhomogeneity of recrystallization across the RD/ND plane of the PSC specimen is therefore isolated as a result of adiabatic heating when no heating of the specimen occurs before PSC testing. Adiabatic heating must therefore be considered in determining recrystallization kinetics at elevated temperature testing at strain rates greater than 1 sec^{-1} as it has been shown to significantly affect recrystallization across the RD/ND plane of the PSC specimen at room temperature.

4.3.4 Adiabatic Heating during Elevated Temperature PSC Testing

The investigation by Jahajeeah[38] concluded that the temperature distribution within the PSC specimen was homogeneous before deformation; however, inhomogeneous recrystallization occurs across the RD/ND plane at strain rates of 10 sec^{-1} for deformation temperatures from 250 to 440 °C as illustrated in Figure 4.26 (b) and (c). During elevated temperature testing, the temperature increase at the centre of the PSC specimen is not as large as the temperature increase for PSC specimens deformed at room temperature. This is a result of dynamic softening occurring at elevated temperature testing, resulting in less plastic work converted into heat at strain rates greater than 1 sec^{-1}.

From initial microstructural studies it is believed that the inhomogeneity of recrystallization across the RD/ND plane was significant (see Figure 4.26), and that adiabatic heating may not be the only factor contributing to the inhomogeneity of recrystallization. At elevated temperature PSC testing the inhomogeneity of recrystallization across the RD/ND plane could therefore be attributed to adiabatic heating, heat loss to the anvils or to both effects. It was necessary to investigate the effect of strain rate on recrystallization in order to determine whether the

inhomogeneous recrystallization at elevated temperatures is a result of adiabatic heating and not heat loss to the anvils. If heat loss to the anvils did occur it would result in the material near the surface of the PSC specimen experiencing a lower temperature of deformation with respect to the centre material, irrespective of the strain rate condition. A similar microstructure as illustrated in Figure 4.26 (b) and (c) would evolve during subsequent annealing treatments.

Adiabatic heating leads to a continuous variation in the Zener-Hollomon parameter through the thickness of the PSC specimen. The microstructural evolution during subsequent annealing will therefore not be homogeneous through the thickness of the specimen. In determining microstructural evolution during subsequent annealing and fitting experimental data to analytical recrystallization models an accurate prediction of the temperature of deformation is required.

4.3.5 Simulation of Adiabatic Heating during PSC Testing

Using values of coefficients of friction from Section 4.2.4, the FEM approximation of the temperature rise as a result of adiabatic heating for simulations at 25, 250 and 440 °C and deformed at a strain rate of 10 sec^{-1} to a nominal strain of 1 is shown in Figure 4.33.

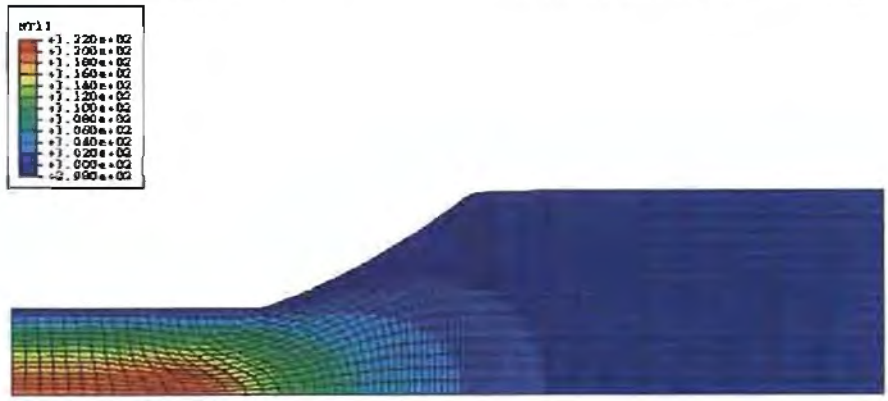

(a)

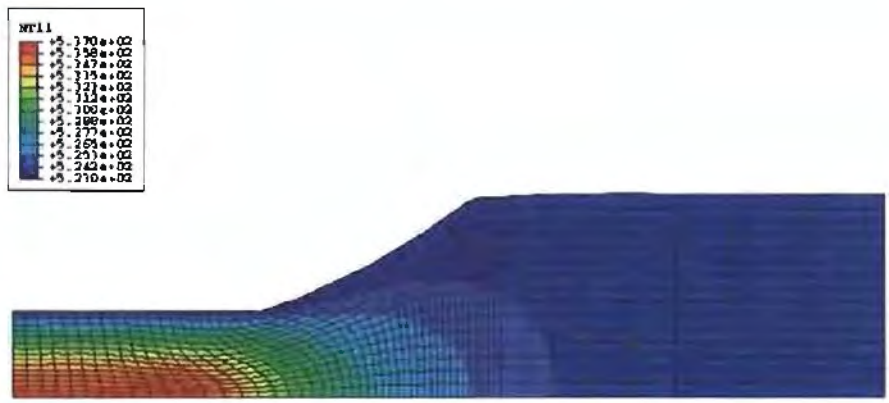

(b)

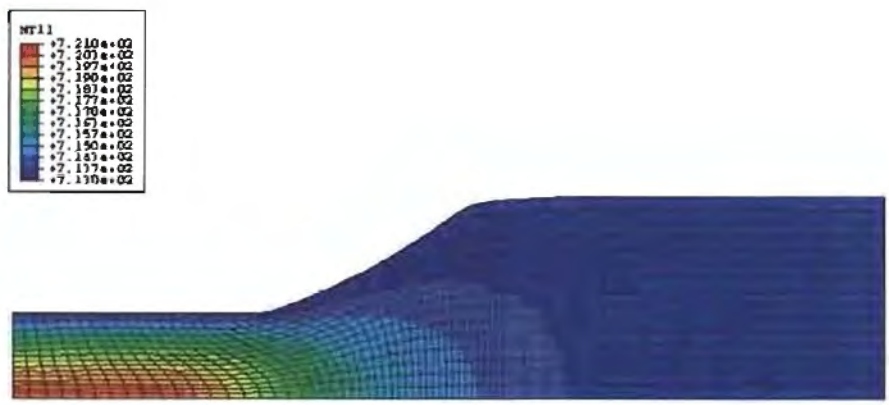

(c)

Figure 4.33 Temperature contour illustrating adiabatic heating effects for PSC test simulations at (a) 25, (b) 250 and (c) 440 °C at a strain rate of 10 sec^{-1} to a nominal strain of 1, showing a temperature rise at the centre of the PSC specimen of 20 (a), 13 (b) and 7 °C (c). The legend indicates the temperature in Kelvin.

The FEM simulations illustrated in Figure 4.33 show that the combination of adiabatic heating and simulated heat loss to the anvils results in a band of localized increase in temperature at the centre of the specimen for the three initial deformation temperatures. The result is a temperature increase from the initial test temperature of approximately 20, 13, and 7 °C for initial test temperatures of 25, 250 and 440 °C respectively. The decrease in temperature rise at the centre of the PSC specimen as the deformation temperature is increased results from less plastic work converted into heat. As the deformation temperature is increased the stress magnitude of the flow curves decreases, namely dynamic softening.

The temperature increase at the centre of the PSC specimen relative to the material at the surface of the specimen cannot be used alone to determine quantitatively where recrystallization would initiate, as recrystallization is also dependent on the strain and strain rate in the deformed volume of material. The Zener-Hollomon parameter is therefore investigated using the results of the FEM simulations for initial test temperatures of 25, 250 and 440 °C deformed at a strain rate of 10 sec^{-1}. FEM predictions of the Zener-Hollomon parameter are plotted from the centre of the specimen along a node path in the ND for initial deformation temperatures of 25, 250 and 440 °C deformed at a strain rate of 10 sec^{-1} to a nominal strain of 1 in Figures 4.34 and 4.35. In this way the temperature variation and strain rate variation are coupled. The average temperature rise used in the calculation of the Zener-Hollomon parameter was obtained by integrating the temperature rise for the FEM simulations.

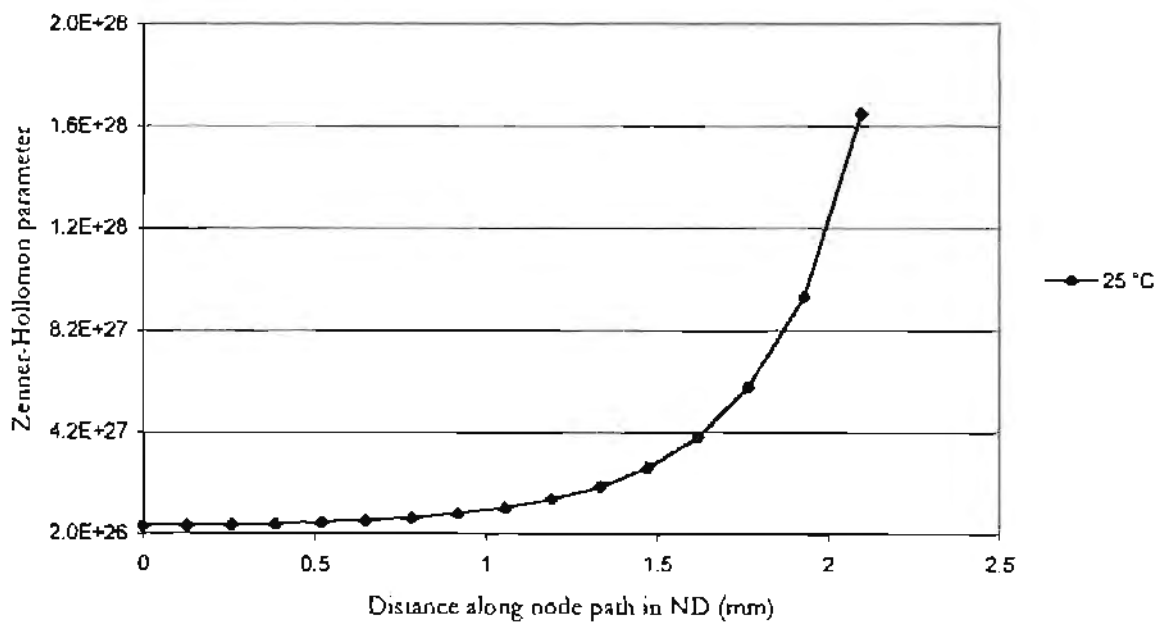

Figure 4.34 Average Zener-Hollomon parameter along node path in the ND for FEM simulation at 25 °C at a strain rate of 10 sec^{-1} to a nominal strain of 1, showing an increase in Zener-Hollomon parameter near the surface of the PSC specimen.

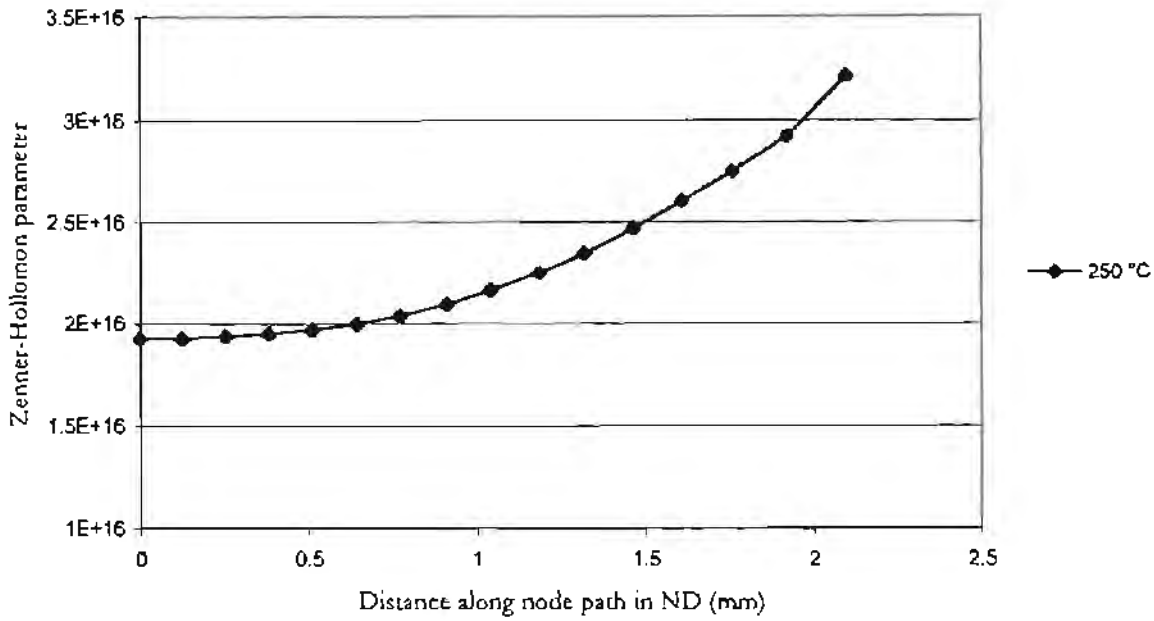

(a)

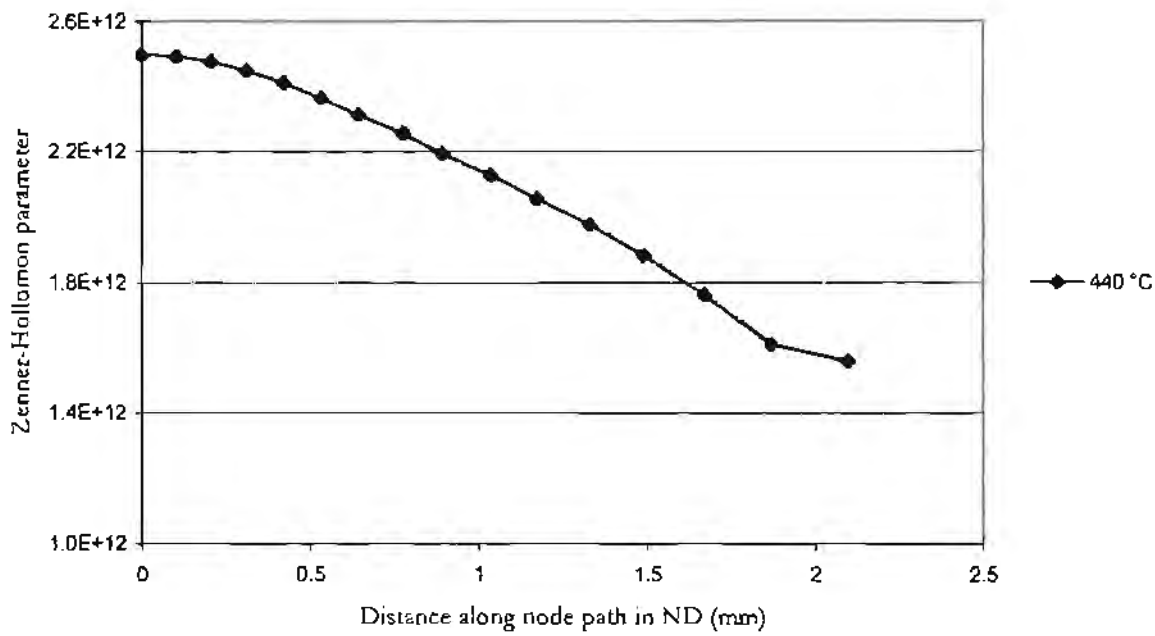

(b)

Figure 4.35 Average Zener-Hollomon parameter along node path in the ND for FEM simulation at (a) 250 and (b) 440 °C deformed at a nominal strain rate of 10 sec^{-1} to a nominal strain of 1. Figure (a) showing an increase in Zener-Hollomon parameter towards the surface of the PSC specimen at a deformation temperature of 250 °C (a) and (b) showing a decrease in Zener-Hollomon parameter towards the surface of the PSC specimen at a deformation temperature of 440 °C.

The Zener-Hollomon parameter is used to qualitatively determine the inhomogeneity of recrystallization experienced at elevated temperature testing. Figures 4.34 and 4.35 clearly show a variation in the Zener-Hollomon parameter through the thickness of the PSC specimen. Figure 4.34 and 4.35 (a) show that the Zener-Hollomon parameter is greatest near the surface of the specimen. Ignoring the inhomogeneity of the strain but considering the strain rate distribution across the RD/ND plane in calculating the Zener-Hollomon parameter, the inhomogeneity of recrystallization discussed in Section 4.3.1, could be attributed to the variation in the Zener-Hollomon parameter through the thickness of the specimen. The Zener-Hollomon parameter is greatest in the volume of material near the surface of the PSC specimen and therefore likely to recrystallise before the material at the centre.

However, Figure 4.35 (b) shows a decrease in the Zener-Hollomon parameter towards the surface of the specimen, which is inconsistent with the partially recrystallized microstructure in Figure 4.26 (b), which shows recrystallization initiating near the surface of the PSC specimen. Furthermore, the FEM predicted strain at the centre is 1.2 and at the surface 0.6, therefore there is increased stored energy at the centre as a result of higher strain. From the FEM prediction in Figure 4.35 (b) recrystallization should initiate at the centre of the PSC specimen and material near the surface should require longer annealing times to fully recrystallise, which has not been shown experimentally.

FEM simulations have shown that the average gradient of the Zener-Hollomon parameter as a function of distance in the ND decreases and eventually becomes negative (Figure 4.35 (b)) as the initial test temperature is increased. The Zener-Hollomon parameter includes strain rate and temperature dependencies. The change in the Zener-Hollomon parameter in the ND as the test temperature is increased is discussed with reference to Figure 4.36, which shows the FEM prediction of temperature variation from (a) initial test temperature and (b) strain rate distribution along node path in the ND assuming homogeneous temperature distribution prior to testing for FEM simulation at 25, 250 and 440 °C. Figure 4.36 (a) shows a decrease in temperature variation from the centre to the surface of the PSC specimen as the initial test temperature is increased. As the temperature of deformation is increased the magnitude of the flow curves decreases, therefore less heat evolves due to plastic work.

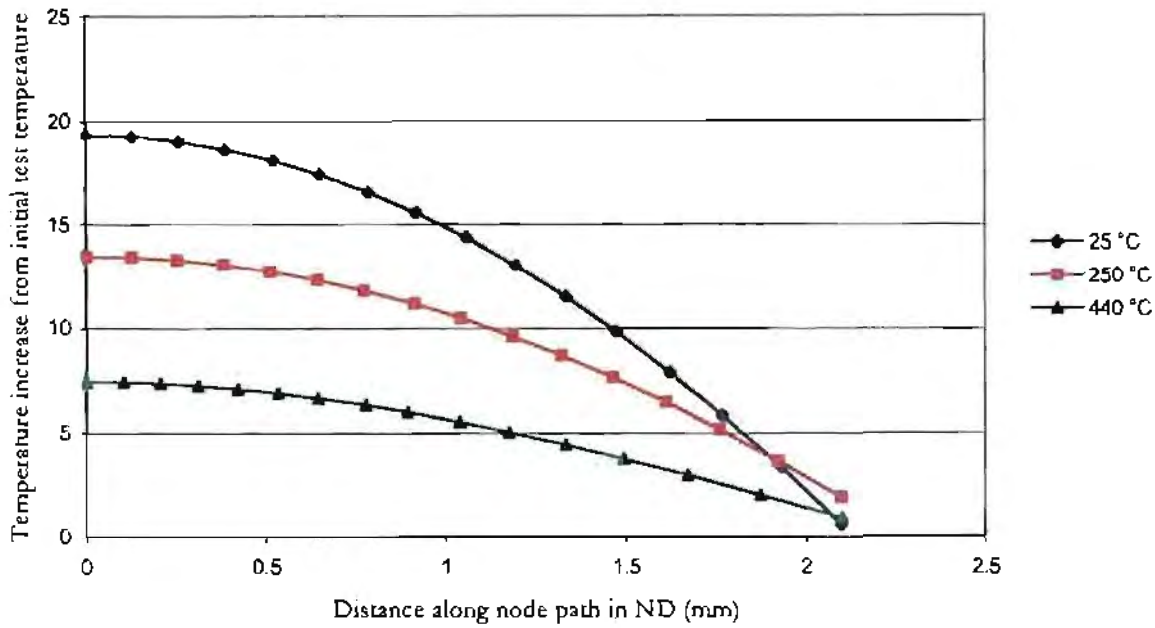

(a)

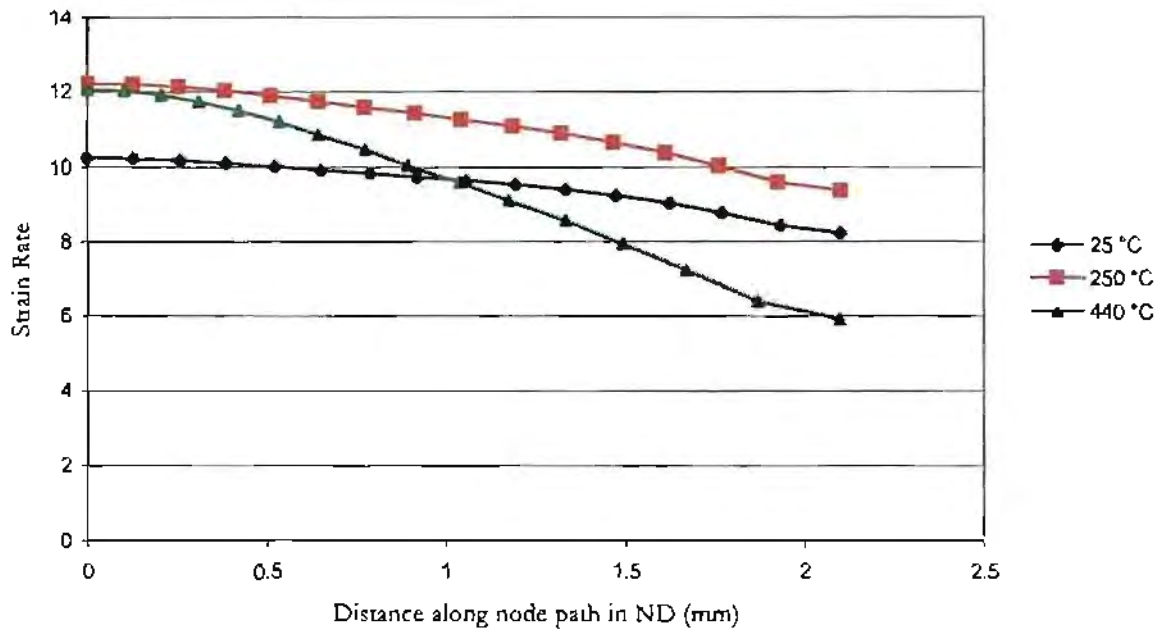

(b)

Figure 4.36 FEM prediction of (a) temperature and (b) strain rate distribution along node path in the ND assuming homogeneous temperature distribution prior to testing. (b) showing a change in the strain rate distribution as lubrication breakdown occurs at elevated temperature PSC testing.

At elevated temperatures lubrication breakdown occurs resulting in a change in the strain distribution across the RD/ND plane of the PSC specimen. The variation in strain therefore increases the strain rate variation between material at the centre and material near the surface. This is shown in Figure 4.36 (b) for the deformation temperature of 440 °C, where the strain rate is approximately double that at the centre of the PSC specimen relative to the material near the surface. It is also noted from Figure 4.36 (b) that the strain rate at the centre of the PSC specimen for deformation at 250 and 440 °C is approximately 12 sec^{-1} for a simulated nominal strain rate of 10 sec^{-1}.

At deformation temperatures above approximately 325 °C a transition in the Zener-Hollomon parameter in the ND occurs, with the Zener-Hollomon parameter becoming greater at the centre than at the surface. At temperatures below 325 °C the Zener-Hollomon parameter at the surface is greater than at the centre because the localized adiabatic heating effect outweighs the effect of strain rate. At temperatures above 325 °C adiabatic heating becomes less significant in changing the Zener-Hollomon parameter because of little variation in temperature from the centre to the surface of the PSC specimen. The strain rate dependency of the Zener-Hollomon parameter becomes dominant with increasing friction changing the strain rate distribution within the PSC specimen.

4.3.6 The Ability to Predict Microstructural Evolution with the FEM Model

In Section 4.3.3 partially recrystallized microstructures are shown for specimens deformed at room temperature at strain rates of 0.1 (Figure 4.30 (b)) and 10 sec^{-1} (Figure 4.32 (b)), where the effects of heat loss to the anvil and environment are ignored. The inhomogeneity of the recrystallized structure in the RD/ND plane of the specimen deformed at a strain rate of 10 sec^{-1} is due to adiabatic heating. This results in a variation in the Zener-Hollomon from the centre of the PSC specimen to the surface for deformation at 25 °C at a strain rate of 10 sec^{-1} of approximately two orders of magnitude, as shown in Figure 4.34. This is considered sufficient to cause an inhomogeneous distribution of stored energy in the deformed microstructure, with the stored energy being greater at the surface of the specimen than at the centre. With the strain being greater at the centre than at the surface, the overall effect of a variation in the Zener-Hollomon parameter and strain is such that the stored energy is greatest in the volume of material near the surface. Recrystallization would therefore initiate in the

volume of material near the surface of the PSC specimen, which is shown experimentally. The FEM prediction of the Zener-Hollomon parameter at 25 °C is therefore valid in providing an explanation for the inhomogeneity of recrystallization.

For the PSC specimen deformed at 250 °C the increase in the Zener-Hollomon parameter from the centre of the PSC specimen to the surface is less than double. The variation in the Zener-Hollomon parameter from the centre to the surface of the PSC specimen in Figure 4.35 (a) is considered negligible in changing the recrystallization kinetics. The strain distribution through the thickness of the PSC specimen is approximately 1 at the centre and 0.72 at the surface. In the description of the mechanical properties for AA1200 at 250 °C the material is still work hardening at a strain of 0.72, therefore the stored energy of the deformed microstructure can still be increased. With little variation in Zener-Hollomon parameter the stored energy of the deformed microstructure would be greater at the centre of the PSC specimen and therefore likely to recrystallise at the centre with longer annealing times for the surface material to fully recrystallise.

For the PSC specimen deformed at 440 °C at a strain rate of 10 sec^{-1} a similar recrystallization inhomogeneity is observed as that of the 25 and 250 °C tests. The FEM prediction of the Zener-Hollomon parameter for the simulation at 440 °C, Figure 4.35 (b), shows that recrystallization should initiate at the centre of the PSC specimen. FEM and microstructural evidence, Figure 4.26 (c), therefore contradict one another in terms of where recrystallization initiates and should initiate assuming homogeneous temperature distribution before deformation.

In view of the strain validation and consequent strain rate, by visioplastic analysis, the disagreement between the observed recrystallization pattern and that suggested by the FEM simulation based on stored energy arguments is most likely due to an inhomogeneous temperature distribution. Although temperature homogeneity has been reported[38], it is believed that there is sufficient microstructural evidence to suggest that the material near the contact surface is at a lower temperature of deformation than the centre of the specimen. The FEM model can therefore not reliably approximate the thermal variables during elevated temperature PSC testing. The inaccurate FEM prediction of thermal variables is attributed to inhomogeneity of temperature distribution

before and during deformation. The inhomogeneity of temperature distribution is attributed to the specimen heating method, that of electrical resistance heating. Further investigation is beyond the scope of the present study and therefore not investigated; however, recommendations are made for future investigation.

It is noted that the heterogeneous recrystallization was not significant for PSC tests performed at strain rates of 0.1 sec^{-1}. This is attributed to a more homogeneous temperature distribution within the deformation zone of the specimen. For the direct resistance heating method, as cross head movement of the anvil occurs the current applied is removed. As cross head movement occurs heat from the specimen is lost to the environment and to the anvils, which however results in a more homogeneous temperature distribution as the specimen temperature drops. This occurs because the high thermal conductivity of aluminium allows the specimen temperature to drop with a relatively homogeneous temperature distribution, whereas the specimen heating method results in a significant inhomogeneity of temperature distribution.

For metallurgical purposes the centre of the sectioned PSC specimen is investigated as the microstructural properties and mechanical variables of deformation are symmetric about the RD and ND centre planes. Since temperature distribution across the RD/ND plane is not homogeneous, determination of the temperature at the centre of the PSC specimen in the deformation zone is required. The true deformation temperature should therefore be measured by placing the thermocouple at the centre of the PSC specimen in the deformation zone. This would allow a more accurate measurement of the true deformation temperature at the centre RD/ND plane of the PSC specimen.

4.3.7 Effect of Inhomogeneous Temperature Distribution on Strain Distribution

The inhomogeneity of temperature distribution would result in material at the centre of the PSC specimen experiencing a higher temperature of deformation relative to the material near the surface of the specimen. Material flow behaviour is dependent on the temperature of deformation with the magnitude of the flow curve decreasing as the temperature of deformation is increased. This is a result of dynamic recovery causing dynamic softening as the temperature of deformation is increased. Within the PSC specimen the material near the surface effectively requires a greater stress for deformation than the material at the centre when an inhomogeneous temperature

distribution occurs. The material at the centre of the PSC specimen will therefore deform preferentially if the temperature distribution is significant in lowering the magnitude of the flow curve at the centre relative to the surface. The inhomogeneity of temperature distribution would therefore affect the strain distribution across the RD/ND plane of the PSC specimen.

From the present study the inhomogeneity of temperature distribution through the thickness of the PSC specimen is believed to increase with increasing deformation temperature. This is attributed to greater temperature differential between the anvils and the PSC specimen as the test temperature is increased. The increase in inhomogeneity is a result of the increased heat loss to the environment at elevated temperatures and equilibrium of temperature distribution between the anvils and the specimen is less likely to occur.

The exact variation in temperature distribution through the thickness of the PSC specimen when electrical resistance heating is employed specimen has not been investigated. However, if a significant temperature variation through the thickness of the PSC specimen occurs, the strain distribution will change for a specific coefficient of friction. Lubrication breakdown which was characterised and discussed in Section 4.2.4, may therefore be a combination of lubrication breakdown and a change in strain distribution attributed to an inhomogeneous temperature distribution through the thickness of the PSC specimen. If this does occur the characterization of the friction condition at elevated temperatures is not valid in describing the coefficient of friction. However, the characterization of coefficient of friction gives a good approximation of lubrication breakdown and strain inhomogeneity attributed to variation in temperature distribution through the thickness of the PSC. The characterization of the coefficient of friction can therefore still be employed to approximate the strain distribution within the PSC specimen using the FEM.

4.4 Program Strain

From the results of the present investigation it has been found that the mechanical variables during PSC testing at the University of Cape Town, can be predicted using the FEM within a certain strain and strain rate range. A more accurate approximation of the mechanical variables is obtained compared to nominal values. A program which determines the mechanical variables for a specific PSC thermo-mechanical process has been developed, and the source code is included in Appendix B.

Program Strain v.1 uses FEM predictions of strain to obtain a more accurate approximation of the strain and strain rate at the centre of the PSC specimen in the RD/ND plane, for any applied nominal strain. In calculating the strain and strain rate the program uses trendline polynomial functions, which have been fitted to FEM predictions for varying coefficients of friction. If the nominal strain of deformation is known, the FEM approximations are used to obtain a FEM predicted strain at the centre of the PSC specimen. The input temperature determines the coefficient of friction using the equations derived in Section 4.2.4.4. The coefficient of friction is then used to calculate the strain and strain rate at the centre of the deformed PSC specimen.

The input variables are:

$\dot{\varepsilon}$	Strain rate (sec^{-1})
ho	Initial specimen height (mm)
hf	Final specimen height (mm)
T	Temperature of deformation (°C)

Program Strain v.1 can then be used by the researcher to obtain a more accurate prediction of the strain and strain rate at a specified deformation temperature at the centre of the deformed PSC specimen in the RD/ND plane for AA1200. In order to adapt Program Strain v.1 for other aluminium alloys a FEM study would be required to be undertaken incorporating the respective flow curve data.

CHAPTER FIVE - SUMMARY

The objectives of the research thesis were to determine the mechanical and thermal variables in an aluminium specimen during PSC testing over a range of thermo-mechanical test variables. Nominal values of strain and strain rate do not approximate the mechanical variables of deformation within the aluminium specimen during PSC testing and the temperature distribution is not homogeneous across the RD/ND plane of the PSC specimen. The mechanical and thermal variables during PSC testing were therefore investigated in order to more accurately predict the true thermo-mechanical parameters during PSC testing, which could then be incorporated into analytical microstructural models.

5.1 Determination of Mechanical Variables during PSC Testing

The mechanical variables, namely strain and strain rate, were investigated using visioplastic experiments, the FEM and a strain-hardness correlation. The visioplastic study was used to verify and validate the FEM predictions.

5.1.2 Visioplasticity

Visioplastic experiments were able to provide the true state of deformation within the PSC specimen for the range of thermo-mechanical test variables investigated. Deformed visioplastic specimens showed a distinct transition in the strain distribution across the RD/ND plane of the PSC specimen. A transition in strain distribution was found to occur above 300 °C for a nominal strain rate of 10 sec^{-1}. The transition in strain distribution is attributed to the graphite lubricant breaking down at elevated temperatures. The increase in strain inhomogeneity at elevated temperatures may also be a result of a temperature inhomogeneity within the PSC specimen when electrical resistance heating is employed.

Visioplastic experiments also revealed that the lubrication condition appears to breakdown in one test but not in another at elevated temperature testing. The change in friction condition is significant in changing the strain and strain rate distribution across the RD/ND plane of the PSC specimen. A range of coefficients of friction is therefore used in predicting a strain and strain rate range that the PSC specimen is likely to have received.

5.1.2 The FEM

The FEM allowed for the determination of the friction condition between the anvil and the specimen by comparison of visioplastic results and simulated coefficients of friction. The FEM is able to approximate the true mechanical deformation variables within the PSC specimen over the range of thermo-mechanical test variables investigated. The FEM therefore provides a more accurate approximation to the true deformation variables to be incorporated in analytical microstructural models.

The FEM has also shown that the strain and strain rate distribution is sensitive to small variations in the coefficient of friction. This is attributed to the low work hardening rate used in the description of the flow curve data used in the FEM model, which is appropriate for commercial purity aluminium.

5.1.3 Strain-Hardness Correlation

The strain-hardness correlation was unsuccessful in determining the mechanical variables within the PSC specimen because of the low work hardening of aluminium resulting in little variation in hardness measurements for incremental variations in strain.

5.2 Determination of Thermal Variable during PSC Testing

The temperature distribution was investigated using the FEM. Microhardness measurements were used to investigate the possible influence of variations in temperature distribution across the RD/ND plane of the PSC specimen on the inhomogeneity of recrystallization.

5.2.1 The FEM

The FEM was used to determine the temperature distribution across the RD/ND plane at nominal strain rates of 10 sec^{-1} assuming homogeneous temperature distribution before testing. At a strain rate of 10 sec^{-1} adiabatic heating occurs with the centre of the PSC specimen being heated above the temperature of the material near the surface due to the strain inhomogeneity. The FEM results are used to determine the Zener-Hollomon parameter variation through the thickness of the PSC specimen. The simulated Zener-Hollomon parameter is greater near the surface of the PSC specimen than at the centre for temperatures below 325 °C. Above 325 °C the simulated Zener-Hollomon is greater in the material at the centre of the PSC specimen than in the material near the surface.

Assuming homogeneous temperature distribution before testing the Zener-Hollomon parameter variation represents a stored energy distribution through the thickness of the PSC specimen. Ignoring the inhomogeneity of strain, but considering the strain rate distribution in calculation of the Zener-Hollomon parameter, at temperatures below 325 °C the FEM predicts that recrystallization should initiate in the material near the surface of the PSC specimen and above 325 °C the FEM predicts that recrystallization should initiate at the centre of the PSC specimen. This is a result of a change in strain rate distribution as lubrication breakdown occurs and at elevated temperatures less plastic work is converted into heat as a result of dynamic recovery reducing the flow curve stress magnitude.

5.2.2 Microhardness Measurement

Microhardness measurements were used to qualitatively determine stored energy distributions through the thickness of PSC specimens deformed at elevated temperatures at a strain rate of 10 sec^{-1}. The microhardness measurements showed that the microhardness at the surface of the PSC specimen was greater than that at the centre of the PSC specimen. This represents a stored energy distribution within the PSC specimen with recrystallization likely to initiate near the surface and the material at the centre requiring longer annealing times to fully recrystallise. This consistently occurs at deformation temperatures above 200 °C and is consistent with microstructural evidence for partially recrystallized specimens deformed at initial deformation temperatures above 200 °C at a strain rate of 10 sec^{-1}.

5.2.3 Microstructural Investigation

Partially recrystallized microstructures across the RD/ND plane of PSC specimens were produced to investigate the stored energy distribution though the thickness of the PSC specimen. Partially recrystallized microstructures show recrystallization initiating in the volume of material near the surface of the PSC specimen, with the centre requiring longer annealing times to fully recrystallise, for specimen deformed at a strain rate of 10 sec^{-1} and when electrical resistance heating is employed. The inhomogeneity represents a stored energy distribution through the thickness of the PSC specimen, which is consistent with microhardness measurements. The inhomogeneity of stored energy is, however, inconsistent with FEM predictions and is attributed to inhomogeneous temperature distribution through the thickness of the PSC specimen before and during testing.

CHAPTER SIX - CONCLUSIONS

Based on the findings of this research thesis the following conclusions are drawn:

1. A FEM model simulating PSC testing of AA1200 at the University of Cape Town has been successfully verified and validated by visioplastic experiments. The FEM model can accurately approximate the mechanical variables during PSC testing.

2. Metallographic investigation of deformed PSC specimens is undertaken at the centre of sectioned PSC specimens to ensure symmetry of thermo-mechanical variables. The strain distribution within the deformation zone of a PSC test specimen is not homogeneous, and consequently the strain rate distribution is not homogeneous. The strain and strain rate at the centre of the sectioned PSC specimen cannot be accurately approximated by nominal values of strain and strain rate. The FEM model gives a more accurate approximation of the mechanical variables at the centre of the PSC specimen when compared with nominal values.

3. The strain rate at the centre of the PSC specimen is linearly related to the nominal strain, for temperatures between 25 and 440 °C but the slope of the relationship varies in magnitude as the friction condition changes the strain distribution at hot working temperatures. The strain rate at the centre of the PSC specimen is determined by the material flow at the centre. At temperatures above 300 °C lubrication breakdown occurs resulting in increased material flow at the centre, therefore a higher strain rate.

4. Lubrication progressively breaks down leading to increased friction above 300 °C. The variation in friction condition above 300 °C results in a variation in strain and strain rate distribution within the PSC specimen.

5. Lubrication breakdown has been characterised to determine the coefficient of friction for temperatures between 25 °C and 440 °C, for strain rates between 0.1 and 10 sec^{-1}. Assumed lubrication breakdown may, however, be a

combination of lubrication breakdown and a variation in temperature distribution through the thickness of the PSC specimen causing a strain inhomogeneity.

6. Reliable determination of the strain and strain rate distribution is not possible due to variations in coefficient of friction for constant deformation temperature. A range of strain and strain rate is more applicable.

7. A true plane strain condition does not exist. The transverse strain is approximately 0.1 of the nominal strain along the centre of the PSC specimen in the TD. Subsequently a three-dimensional FEM model is required to approximate deformation during PSC testing.

8. The material receiving approximate plane strain deformation during PSC testing is the central (w-b) part of the PSC specimen.

9. The assumption of slip line field theory being independent of temperature and strain rate is valid for temperatures above 180 °C assuming constant coefficient of friction.

10. Inhomogeneous recrystallization in the RD/ND plane occurs for PSC specimens deformed at temperatures above 200 °C and is attributed to inhomogeneous temperature distribution before and during deformation.

11. The temperature distribution is not homogeneous within the deformation zone of the PSC specimen before and during deformation when electrical resistance heating is employed. Consequently the FEM model used in the analysis cannot approximate the thermal variables during PSC testing.

CHAPTER SEVEN - RECOMMENDATIONS

Based on conclusions the following recommendations are made:

1. Jahajeeah[38] implemented a coupled thermal-electrical analysis, and concluded that the temperature distribution within the PSC specimen was homogeneous before deformation at elevated temperatures. The temperature distribution has since been found not to be homogeneous from microstructural evidence and is attributed to the specimen heating method and heat loss to the anvils. It is therefore recommended that PSC tests be performed on a PSC rig that does not use electrical resistance heating but uses a furnace containing the anvils and specimen. This would allow the temperature of the anvil and the specimen to be homogeneous before and during testing. Microstructural investigation could be used to directly compare the deformed microstructures for similar tests performed at the University of Cape Town.

   If significant variation in microstructural evolution during subsequent annealing treatments occurs between specimens deformed using electrical resistance heating and a furnace type, it is recommended that either the temperature distribution for electrical resistance heating be further investigated or a suitable solution be found to ensure that the temperature distribution is homogeneous. This could possibly mean the conversion of the present PSC rig to a furnace type rig.

2. The theoretical temperature distribution for electrical resistance heating combined with reliable and accurate experimental results should be investigated to determine the inhomogeneity of temperature distribution within the PSC specimen. This would allow investigation into the effect of temperature inhomogeneity on the strain and strain rate distribution within the PSC specimen.

3. When performing PSC tests, the thermocouple should be situated at the geometric centre of the PSC specimen within the deformation zone to ensure that the test temperature is the test temperature of the material to be analysed. This would result in a thermocouple being destroyed during each test, but using the K-type wire thermocouple little costs would be incurred and the thermocouples take little time to make.

4. For metallographic investigation the material receiving approximate PSC is the central (w-b) part of the PSC specimen. It is therefore recommended that w/2 of the PSC specimen be discarded from each end due to breakdown in the approximate plane strain condition.

5. It is recommended that when using electrical resistance heating a 'dummy' specimen be deformed at or above the test temperature to be used before testing. This would heat the anvils and therefore produce less of a temperature inhomogeneity during subsequent elevated temperature PSC testing.

6. When PSC testing of aluminium alloys other than AA1200 it would be necessary to simulate the thermo-mechanical process using the FEM, by employing constitutive equations that describe the mechanical properties of the alloy being investigated. This is required since the work hardening behaviour of other aluminium alloys may be significant in changing the strain and strain rate distribution within the PSC specimen described in the present study.

References

[1] S.F. Malan and A.E. Paterson, **Introduction to Aluminium**, Aluminium Federation of South Africa, Pietermaritzburg, 1993

[2] H.E. Vatne, T. Furu, R. Orsund and E. Nes, **Modelling Recrystallization After Hot Rolling of Aluminium**, *Acta Metallurgica*, Vol. 44, No. 11, 1996, pp. 4463 - 4473

[3] J.C. Blade, **Recrystallization in Hot Rolling of Dilute Aluminium Alloys**, *Metal Science*, March – April, 1979, pp. 206 -210

[4] F.J. Humphreys, **Modelling Microstructural Evolution During Annealing**, *Material Science and Engineering*, Vol. 8, 2000, pp 893 - 910

[5] T. Siwecki, **Modelling of Microstructure Evolution during Recrystallization Controlled Rolling**, *ISIJ International*, Vol. 32, No. 3, 1992, pp. 258 - 376

[6] N. Ravichandran, Y.V.R.K Prasad, **Dynamic Recrystallization during Hot Deformation of Aluminium: A Study Using Processing Maps**, *Metallurgical Transactions* A, Vol. 22A, October 1991, pp. 2339-2348

[7] W. Blum, H.J. McQueen, **Dynamics of Recovery and Recrystallization**, *Materials Science Forum*, Vols. 217 – 222, 1996, pp. 31 - 42

[8] F.J. Humphreys and M. Hatherly, **Recrystallization and Related Annealing Phenomena**, Elsevier Science LTD., 1995

[9] E.S. Puchi, M.H. Staia, C. Villalobos, **On the Mechanical Behaviour of Commercial-Purity Aluminium Deformed Under Axisymmetric Compression Conditions**, *International Journal of Plasticity*, Vol. 13, No. 8 – 9, 1997, pp. 723 - 742

[10] A. Duckham, **The Formation of Copper Type Shear Bands in Al-1Mg and Their Effect on Recrystallization Behaviour**, PhD Thesis, University of Cape Town, August 1998

[11] D. Duly, G.J. Baxter, H.R. Shercliff, J.A. Whiteman, C.M. Sellars and M.F. Ashby, **Microstructure and Local Crystalographic Evolution in an Al-1wt% Mg Alloy Deformed at Intermediate Temperature and High Strain-Rate**, *Acta Metalurgica*, Vol. 44, No. 7, 1996, pp. 2947 - 2962

[12] M.A. Wells, D.J. Lloyd, I.V. Samarasekera, J.K. Brimacombe and E.B. Hawbolt, **Modelling the Microstructural Changes during Hot Tandem Rolling of AA5XXX Aluminium Alloys: Part III. Overall Model Development and Validation**, *Metallurgical and Materials Transactions B*, Vol. 29B, June 1998, pp. 709 -719

[13] M.A. Wells, D.J. Lloyd, I.V. Samarasekera, J.K. Brimacombe and E.B. Hawbolt, **Modelling Microstructural Changes during Hot Tandem Rolling of AA5XXX Aluminium Alloys: Part I. Microstructural Evolution,** *Metallurgical and Materials Transactions B*, Vol. 29B, June 1998, pp. 611-620

[14] N. Raghunathan, M.A. Zaidi, T.Sheppard, **Recrystallization Kinetics of Al-Mg Alloys AA5056 and AA5083 After Hot Deformation,** *Material Science and Technology*, Vol. 2, September 1986, pp. 938-945

[15] A. Duckham and R.D. Knutsen, **Assymetric Flow During Plane Strain Compression Testing of Aluminium Alloys,** *Materials Science and Engineering A256*, 1998, pp. 220 - 226

[16] S.P. Timothy, H.L. Yiu, J. M. Fine and R.A. Ricks, **Simulation of Single Pass of Rolling Deformation of Aluminium Alloy by Plane Strain Compression,** *Materials Science and Technology*, Vol. 7, March 1991, pp. 255 -261

[17] B. Kowalski, C.M. Sellars and M. Pietrzyk, **Development of a Computer Code for the Interpretation of Results of Hot Plane Strain Compression Tests,** *ISIJ International*, Vol. 40, No. 12, 2000, pp. 1230 - 1236

[18] E. Orowan, **The Calculation of Roll Pressure in Hot and Cold Flat Rolling,** *Proceedures of the Institute of Mechanical Engineers*, Vol. 150, 1943, pp. 140

[19] R. Hill, E.H. Lee and S.J. Tupper, **A Method of Numerical Analysis of Plastic Flow in Plane Strain and its Application to the Compression of a Ductile Material Between Rough Plates,** *The American Society of Mechanical Engineers Transactions, Journal of Applied Mechanics*, Vol. 18, 1951, pp.46 - 52

[20] A.P. Green, **A Theoretical Investigation of the Compression of a Ductile Material Between Smooth Flat Dies,** *Philosophical Magazine*, Vol. 42, No. 331, August 1951, pp. 900 - 918

[21] R. Colas and C.M. Sellars, **Strain Distribution and Temperature Increase During Plane Strain Compression Testing,** *Journal of Testing and Evaluation*, JTEVA, Vol. 15, No. 6, November 1987, pp. 342-349

[22] H. Ford, **Researches into the Deformation of Metals by Cold Rolling,** *Procedures of the Institute of Mechanical Engineers*, Vol. 159, No.39, 1948, pp. 115 - 143

[23] J.M. Alexander, **The Effect of Coulomb Friction in the Plane Strain Compression of a Plastic-Rigid Material,** *Journal of the Mechanics and Physics of Solids*, Vol. 3, 1955, pp. 233 - 245

[24] H. Shi, A.J. Mclaren, C.M. Sellars, R.Shahani and R. Bolingbroke, **Hot Plane Strian Compression Testing of Aluminium Alloys**, *Journal of Testing and Evaluation*, Vol. 25, No. 1, January 1997, pp. 61 - 73

[25] J.C. Gelin, O. Ghouati and R. Shahani, **Modelling the Plane Strain Compression Test to Obtain Constitutive Equations of Aluminium Alloys**, *International Journal of Mechanical Science*, Vol. 36, No. 9, 1994, pp. 773-796

[26] R. Lian and A.S. Khan, **A Critical Review of Experimental Results and Constitutive Models for BCC and FCC Metals Over a Wide Range of Strain Rates and Temperatures**, *International Journal of Plasticity*, Vol. 15, 1999, pp. 963-980

[27] R.W. Evans, P.J. Scharing, **Axisymmetric Compression Test and Hot Working Properties of Alloys**, *Materials Science and Technology*, Vol. 17, 2000, pp 995 - 1004

[28] R.D. Cook, D.S. Malkus, M.E. Plesha, **Concept and Applications of Finite Element Analysis**, Third Edition, John Wiley and Sons Inc., Canada, 1989

[29] D.S. Burnett, **Finite Element Analysis – From Concepts to Applications**, Addison-Wesley Publishing Company, New Jersey, 1987

[30] V. Balden, Introduction to Finite Element Analysis - MEC563Z course notes, Centre for Research in Computational and Applied Mechanics (CERECAM), University of Cape Town, 2000

[31] O.C. Zienkewicz and R.L.Taylor, **The Finite Element Method – Volume 2 Solid Mechanics**, Fifth Edition, Butterworth-Heinemann, Oxford, 2000

[32] H. Shi, A.J. McLaren, C. M. Sellars, R. Shahani, R. Bolingbroke, **Constitutive Equations for High Temperature Flow Stress of Aluminium Alloys**, *Materials Science and Technology*, Vol. 13, march 1997, pp 210 - 216

[33] U.F. Kocks, **Laws for Work-Hardening and Low-Temperature Creep**, *Journal of Engineering Materials and Technology*, January 1976, pp. 76 - 85

[34] J. P. Sah, A. J. McLaren, and C. M. Sellars, *Journal Aust. Institute of Metalurgy*, 1969, 14, pp 292-297

[35] C.M. Sellars and W.J. Tegart, **Hot Workability**, *International Metallurgy Review*, Vol. 17, pp. 1-24

[36] Beynon and C.M. Sellars, **Strain Distribution Patterns During Plane Strain Compression**, *Journal of Testing and Evaluation*, Vol. 13, No. 1, Jan 1985, pp 28-38

[37] A. A. Tseng, S. R. Wang, A. C. W. Lau, **Local Variations of Strain and Strain Rate in the Roll Bite Region During Rolling of Steels**, *Journal of Engineering Materials and Technology*, Vol. 120, January 1998, pp 86-96

[38] N. Jahajeeah, **Design Optimisation of Plane-Strain Compression Dies**, Final Year Mechanical Engineering Thesis, University of Cape Town, June 1996

[39] ABAQUS 6.2.1., Hibbitt, Karlsson and Sorensen, United States, 2000

[40] J.P. Holman, **Heat Transfer**, 8th International Edition, McGraw-Hill, United States of America, 1997

[41] E.G Thomsen, C.T Yang and S Kobayashi, **Mechanics of Plastic Deformation in Metal Processing**, Macmillan, New York, 1965

APPENDIX A – PARAMETRIC STUDY

An optimal mesh in terms of computational time and acceptable convergence was obtained by performing a parametric study. Mesh sensitivity was investigated in the three co-ordinate axes directions. To obtain an optimal number of nodes in each co-ordinate axis direction, the number of nodes in the specific co-ordinate direction was varied keeping the number of nodes in the other two co-ordinate directions constant. The meshes used to obtain an optimal mesh are given in Table A, for the (a) RD, (b) ND and (c) TD.

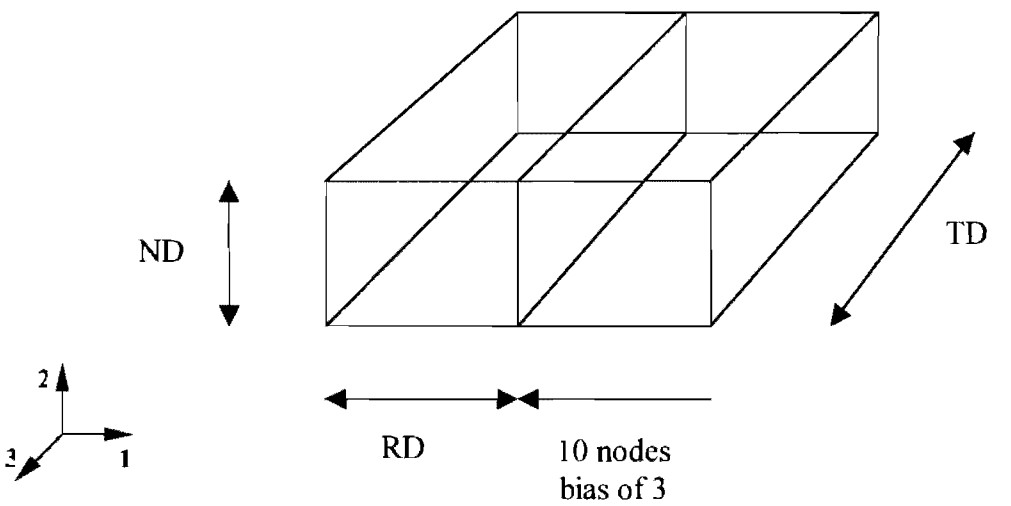

Figure A Eighth PSC specimen showing RD, ND and TD.

Other Axes	Axis being Investigated		
	RD	ND	TD
RD	N/A	40	15
ND	20	N/A	10
TD	4	4	N/A

Table A Number of nodes to be used in other directions for parametric study.

Specimens were deformed to a nominal strain of 0.5 and 1 and the PEEQ plotted along the node path in the specific direction to find an optimal mesh.

Rolling Direction

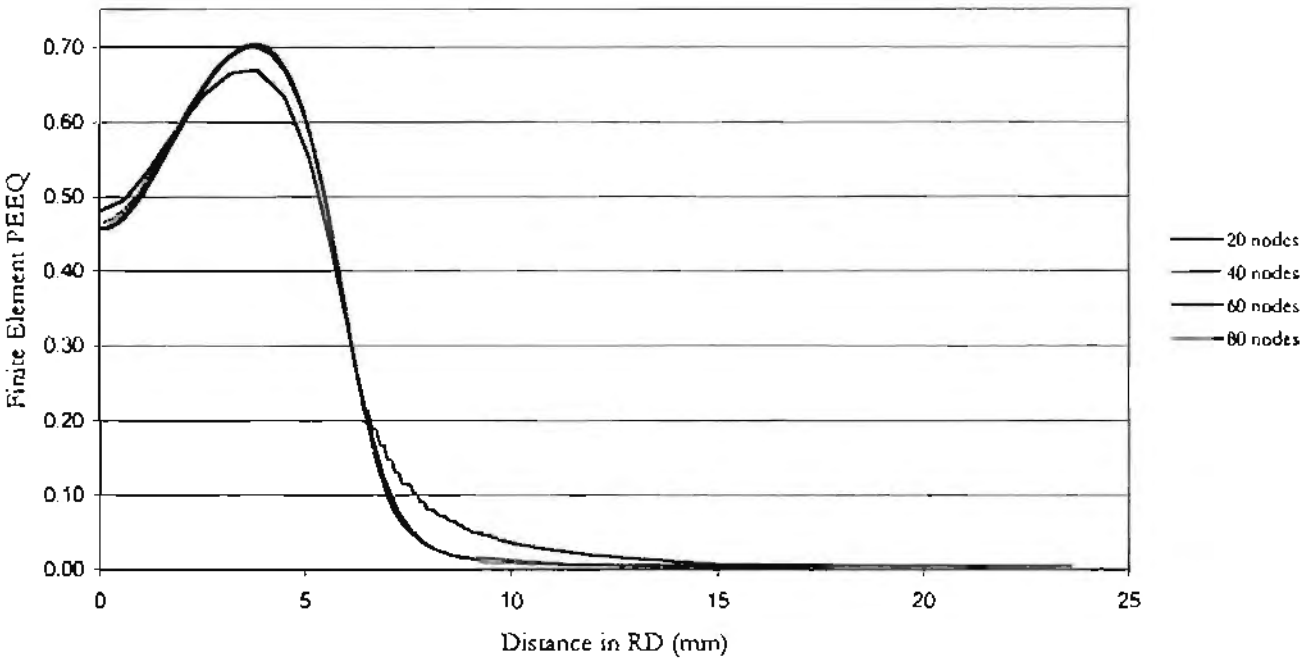

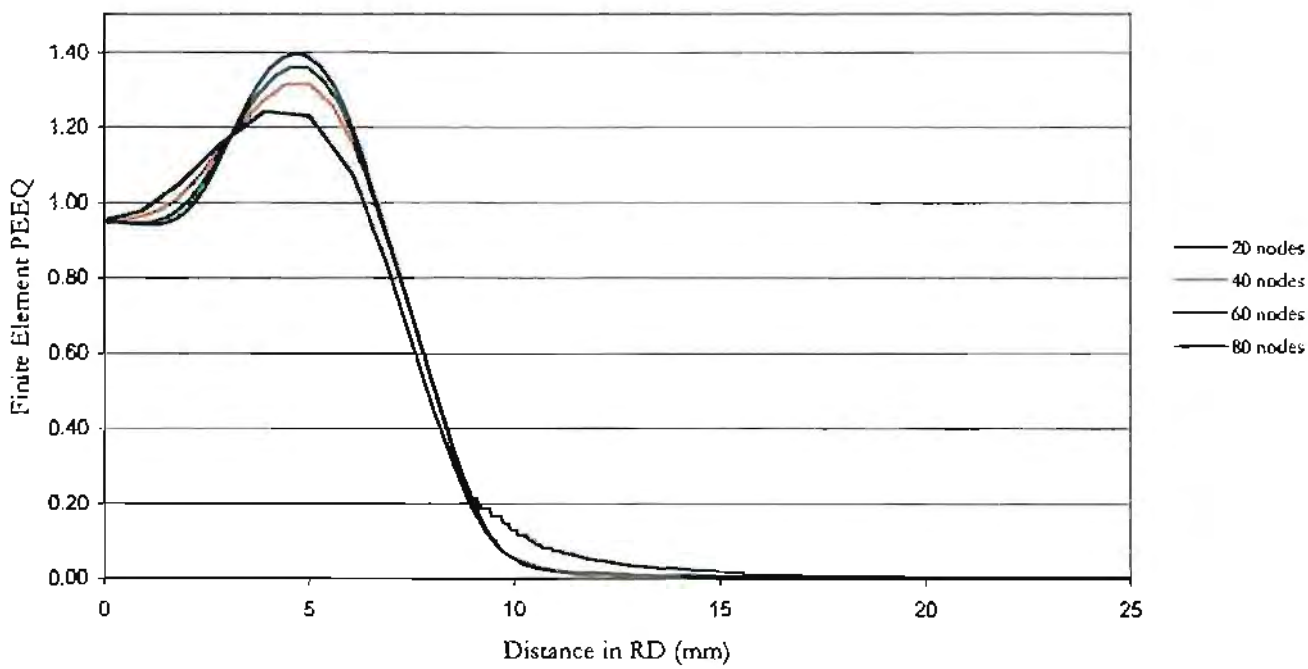

Normal Direction

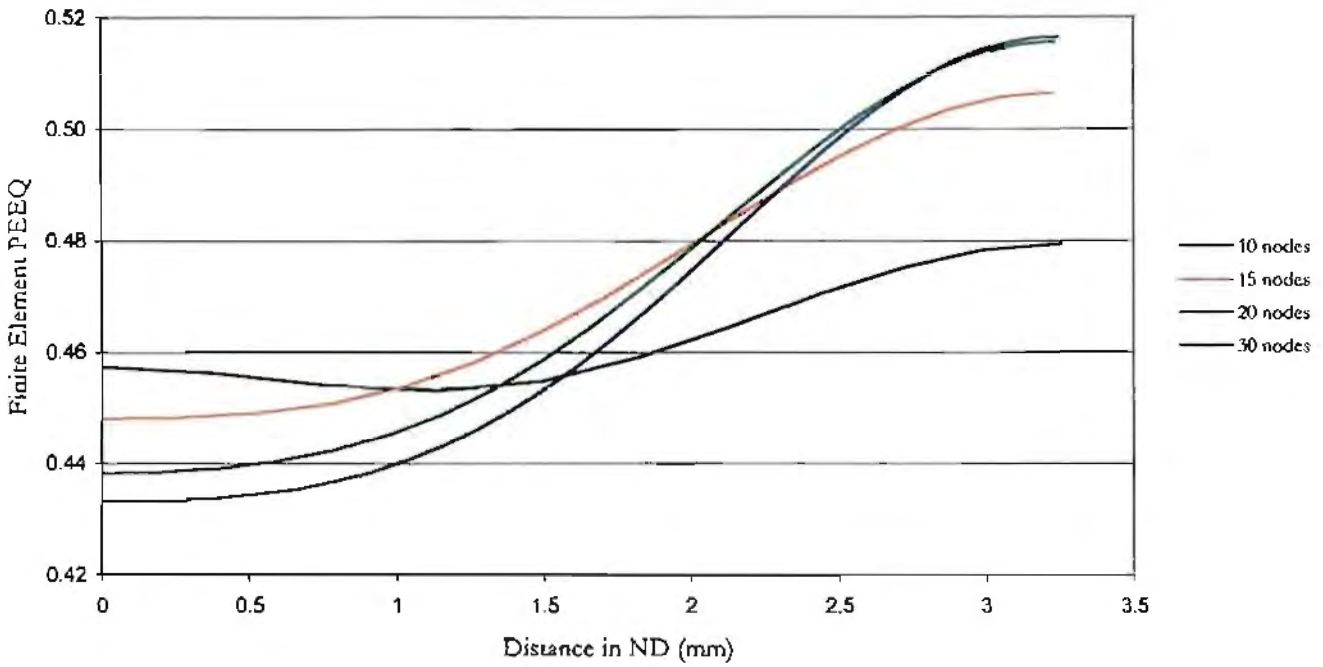

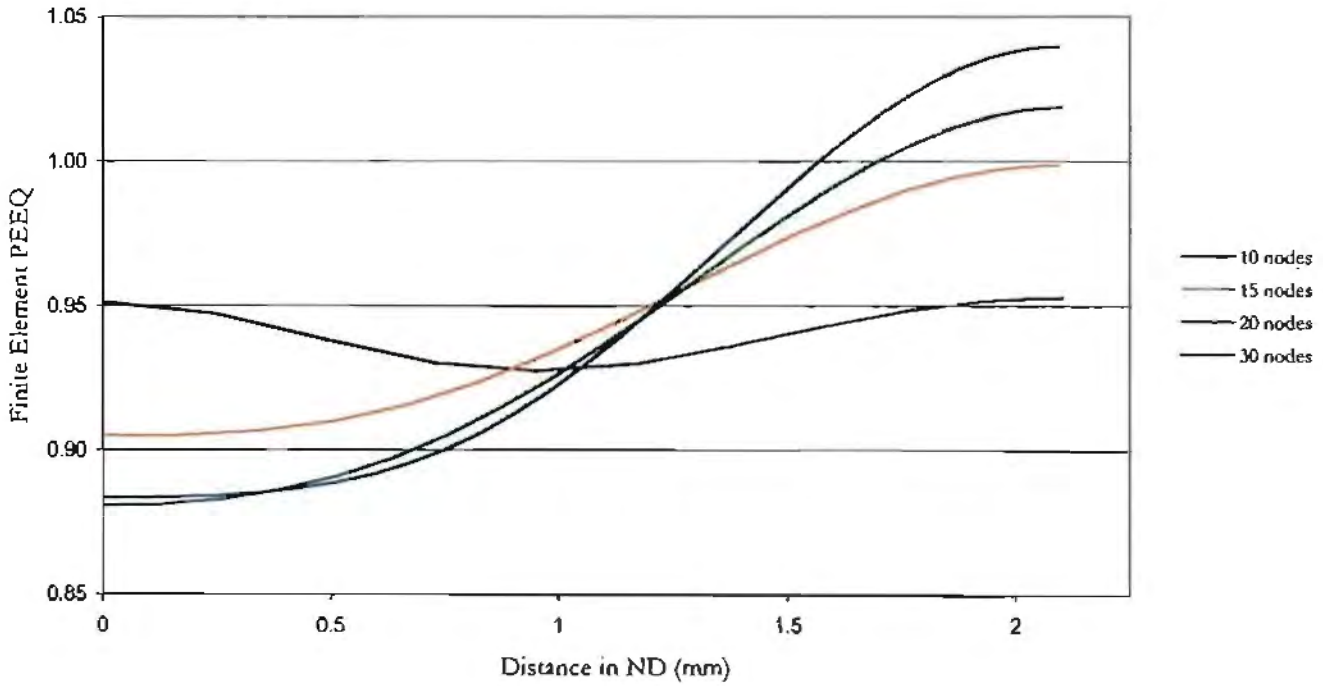

Transverse Direction

A bias of 2.5 was applied in the TD.

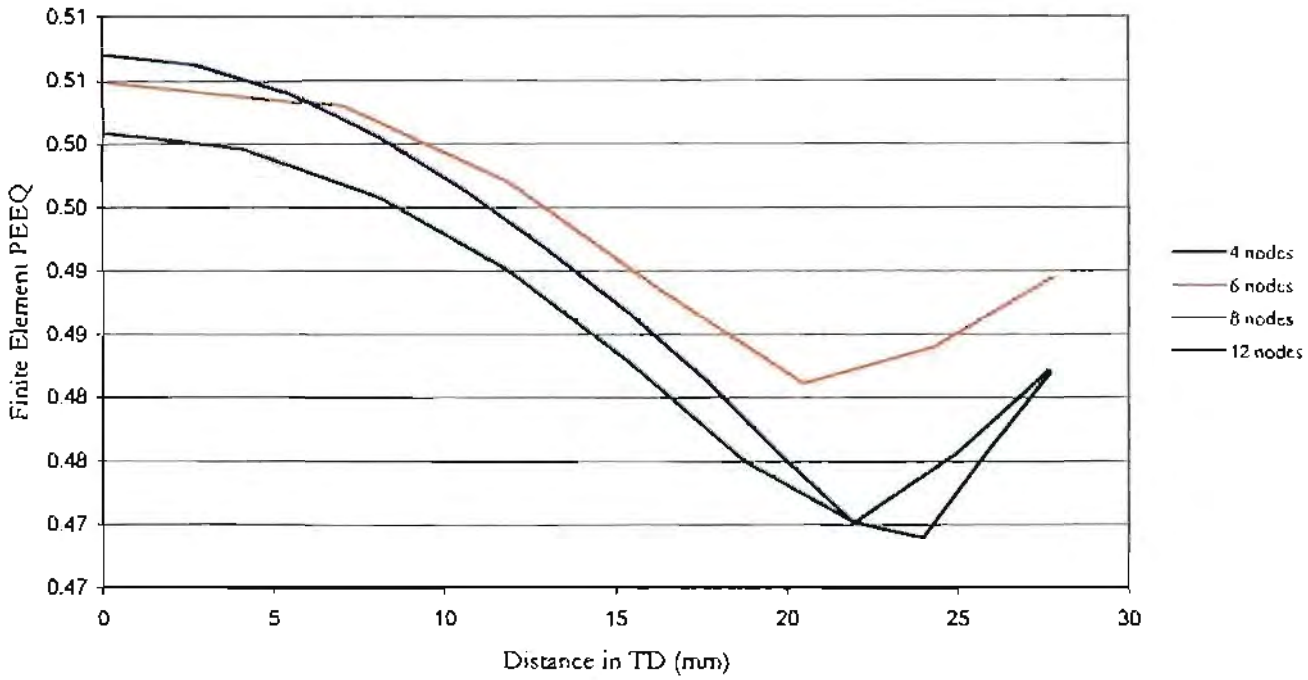

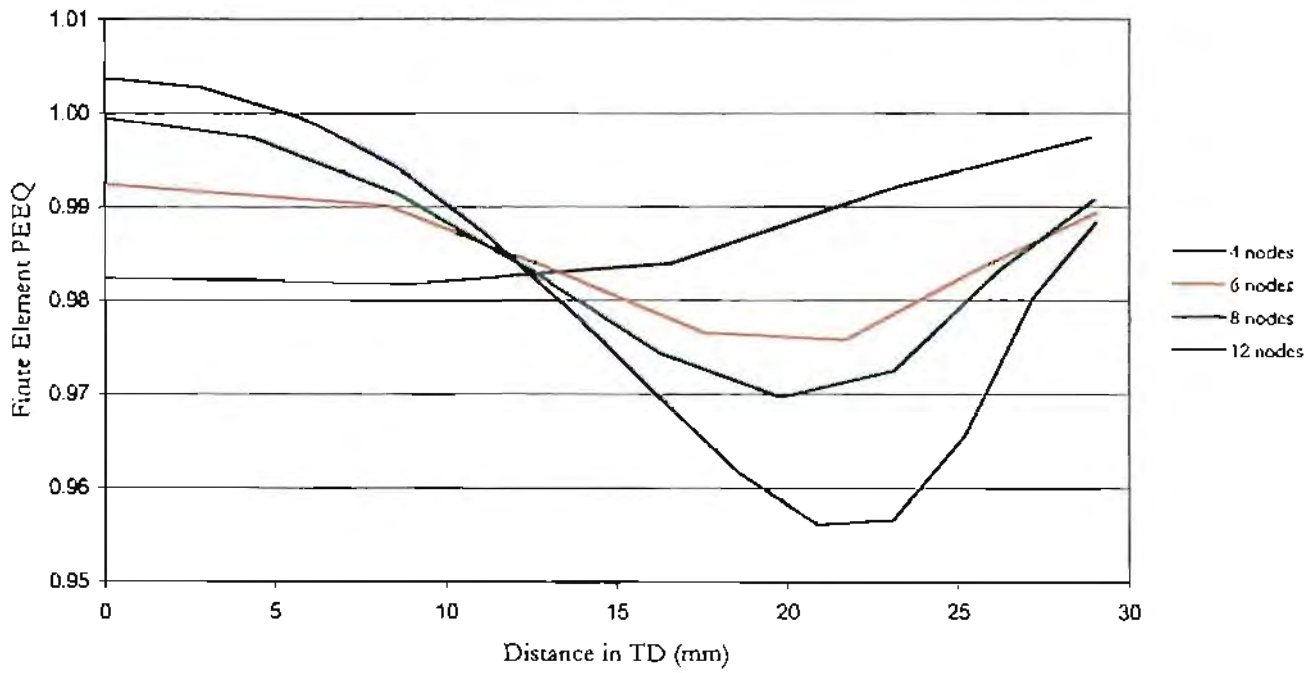

APPENDIX B

SOURCE CODE FOR PROGRAM STRAIN v.1

```
!-------------------------------------------------------------------------
!file: Strain v.1
!-------------------------------------------------------------------------
MODULE subs
CONTAINS
!-------------------------------------------------------------------------
!subroutine:    intro
!
!purpose:       displays program information
!
!argument description
!
!intro_qu       answer to question
!
!programmer:    J.M. Buchanan
!language:      Fortran 90
!date:          12 November 2001
!-------------------------------------------------------------------------
SUBROUTINE intro
IMPLICIT NONE
CHARACTER(len=10)::intro_qu,qu

!program information

WRITE(*,*)' '
WRITE(*,*)'                                PROGRAM '
WRITE(*,*)'                               STRAIN v.1 '
WRITE(*,*)' '
WRITE(*,*)' This Program Calculates the Strain and Strain Rate at the Centre o
f'
WRITE(*,*)'                            a PSC Specimen '
WRITE(*,*)' '
WRITE(*,*)'                       Design and development '
WRITE(*,*)'                                by'
WRITE(*,*)'                            J. Buchanan '
WRITE(*,*)' '
WRITE(*,*)' '
WRITE(*,*)' '
WRITE(*,*)' '
WRITE(*,*)'The required program inputs are:'
WRITE(*,*)' '
WRITE(*,*)'(1) Initial specimen height (mm) '
WRITE(*,*)'(2) Final specimen height (mm)'
WRITE(*,*)'(3) Temperature of deformation (oC) '
WRITE(*,*)'(4) The nominal strain rate (sec-1) '
WRITE(*,*)' '
WRITE(*,*)' '

!question - would user like to continue

qu='redo'
DO WHILE(qu=='redo')

  WRITE(*,*)' Would you like to continue? (y/n)'
  READ(*,*)intro_qu

    IF(intro_qu=='y') THEN
    qu='done'

    ELSE IF(intro_qu=='n') THEN
      qu='done'
          WRITE(*,*)' '
      WRITE(*,*)'Program Strain is terminated'
          STOP
```

```
          ELSE
        WRITE(*,*)' '
          WRITE(*,*)'A vaild answer was not given'
          WRITE(*,*)' '

        END IF
END DO
END SUBROUTINE intro
!-------------------------------------------------------------------------
!subroutine:     inputs
!
!purpose:        user enters PSC test variables
!
!argument description
!
!ho      (out)   initial height of PSC specimen
!hf      (out)   final height of PSC specimen
!t       (out)   temperature of deformation
!rate    (out)   strain rate of test
!
!programmer:     J.M. Buchanan
!language:       Fortran 90
!date:           12 November 2001
!-------------------------------------------------------------------------
SUBROUTINE inputs(ho,hf,t,rate)
IMPLICIT NONE

REAL, INTENT(out)::ho,hf,T,rate
CHARACTER(len=10)::temp,s_rate,h_initial

!user enters initial specimen height

h_initial='bad'
DO WHILE(h_initial=='bad')

  WRITE(*,*)' '
  WRITE(*,*)'(1)  Enter initial height (mm)'
  READ(*,*)ho

    IF (ho>=10.5) THEN
        WRITE(*,*)' '
    WRITE(*,*)'The initial height is not valid'

      ELSE
      h_initial='good'

    END IF

END DO

!user enters final specimen height

WRITE(*,*)' '
WRITE(*,*)'(2)  Enter final height (mm)'
READ(*,*)hf

!user enters the test temperature

temp='bad'
DO WHILE(temp=='bad')

  WRITE(*,*)' '
  WRITE(*,*)'(3)  Enter test temperature (oC)'
```

```
  READ(*,*)t

    IF (t<=450.and.t>=180) THEN
      temp='good'

      ELSE
          WRITE(*,*)' '
      WRITE(*,*)'The test temperature is not valid'

    END IF

END DO

!user enters the strain rate used in the PSC test

s_rate='bad'
DO WHILE(s_rate=='bad')

  WRITE(*,*)' '
  WRITE(*,*)'(4)  Enter nominal strain rate (sec-1)'
  READ(*,*)rate

    IF (rate>=0.1.and.rate<=10) THEN
    s_rate='good'

      ELSE
      WRITE(*,*)'The strain rate is not valid'

    END IF

END DO

END SUBROUTINE inputs
!-----------------------------------------------------------------------
!subroutine:    friction
!
!purpose:       calculates the coefficients of friction
!
!argument description
!
!t      (in)    temperature of deformation
!mean   (out)   mean friction prediction
!up     (out)   upper friction prediction
!low    (out)   lower friction predicting
!
!programmer:    J.M. Buchanan
!language:      Fortran 90
!date:          12 November 2001
!-----------------------------------------------------------------------
SUBROUTINE friction(t,mean,up,low)
IMPLICIT NONE

REAL, INTENT(in)::t
REAL, INTENT(out)::mean,up,low
REAL::error

error=0.15

  IF (t<250.and.t>=180) THEN  !if the temperature is between 250 and 180
                              !the coefficient of frictionis calculated

  mean=(0.01/150)*t+0.0435
  up=mean
  low=mean
```

```
          ELSE IF (t>=250) THEN  !if the temperature is greater than 250
                                 !the coefficient of friction is calculated

               mean=(2.86/1000000)*t*t-(1.33/1000)*t +0.2137
               up=mean+(mean*error)
               low=mean-(mean*error)

                           ELSE

   END IF

END SUBROUTINE friction
!-------------------------------------------------------------------------
!subroutine:     strains
!
!purpose:       calculates strain and strain rate values
!
!argument description
!
!rate            (in)    strain rate of test
!mean            (in)    mean coefficient of friction
!up              (inout) upper coefficient of friction
!low             (inout) lower coefficient of friction
!nom_s           (in)    nominal strain
!s_mean          (out)   mean strain value
!s_up            (out)   upper strain value
!s_low           (out)   lower strain value
!s_rate_m        (out)   mean strain rate
!s_rate_u        (out)   upper strain rate
!s_rate_l        (out)   lower strain rate
!
!programmer:    J.M. Buchanan
!language:      Fortran 90
!date:          12 November 2001
!-------------------------------------------------------------------------
SUBROUTINE strains(rate,mean,up,low,nom_s,s_mean,s_up,s_low,s_rate_m, &
s_rate_u,s_rate_l)

IMPLICIT NONE

REAL, INTENT(in)::mean,rate,nom_s
REAL, INTENT(out)::s_mean,s_up,s_low,s_rate_m,s_rate_u,s_rate_l
REAL, INTENT(inout)::low,up

REAL::friction,s_h,s_l,mu_w,strain,x

INTEGER::mu

x=nom_s
mu=1
DO WHILE (mu<=3)   !do while loop for each friction value

  IF (mu==1) THEN
  friction=mean

  ELSE IF (mu==2) THEN
       friction=up

       ELSE IF (mu==3) THEN
            friction=low

  END IF
```

```
s_h=0
s_l=0

!the model has been developed for coefficients of friction between 0.05 and 0.
225
!if the coefficient is less than 0.05, 0.05 will be used

  IF (friction<=0.05) THEN

  WRITE(*,*)'The lower frition value is 0.05'
  low=0.05
  friction=0.05

!if the coefficient is greater than 0.225, 0.225 will be used

  ELSE IF (friction>=0.225) THEN
       up=0.225
       friction=0.225
       WRITE(*,*)'The upper frition value is 0.225'

       ELSE

  END IF

IF ((friction>=0.05).and.(friction<0.075)) THEN

mu_w=(friction-0.05)/0.025  !coefficient of friction weighting

!0.05 fem prediction
s_h=(0.33103*(x**5) - 1.50612*(x**4) &
+ 2.50768*(x**3) - 1.80981*(x**2) + 1.51245*x - 0.00608)

!0.075 fem prediction
s_l=(-0.0163*(x**5) - 0.2939*(x**4) &
+ 0.9501*(x**3)- 0.9527*(x**2) + 1.3896*x - 0.0019)

ELSE IF ((friction>=0.075).and.(friction<0.1)) THEN

mu_w=(friction-0.075)/0.025  !coefficient of friction weighting

!0.075 fem prediction
s_h=(-0.0163*(x**5) - 0.2939*(x**4) &
+ 0.9501*(x**3)- 0.9527*(x**2) + 1.3896*x - 0.0019)

!0.1 fem prediction
s_l=(0.17383)*(x**5) - (0.85929)*(x**4) &
 + (1.55171)*(x**3) - (1.25715)*(x**2) + 1.52630*x - 0.00288

ELSE IF ((friction>=0.1).and.(friction<0.125)) THEN

mu_w=(friction-0.1)/0.025  !coefficient of friction weighting

!0.1 fem prediction
s_h=(0.17383)*(x**5) - (0.85929)*(x**4) &
 + (1.55171)*(x**3) - (1.25715)*(x**2) + 1.52630*x - 0.00288

!0.125 fem prediction
s_l=(0.15807)*(x**5) - (0.80422)*(x**4) &
 + (1.46951)*(x**3) - (1.19708)*(x**2) + 1.56346*x - 0.00288

ELSE IF ((friction>=0.125).and.(friction<0.15)) THEN

mu_w=(friction-0.125)/0.025  !coefficient of friction weighting
```

```
!0.125 fem prediction
s_h=(0.15807)*(x**5) - (0.80422)*(x**4) &
 + (1.46951)*(x**3) - (1.19708)*(x**2) + 1.56346*x - 0.00288

!0.15 fem prediction
s_l=(0.16752)*(x**5) - (0.81957)*(x**4) &
+ (1.43941)*(x**3) - (1.15594)*(x**2) + 1.62100*x - 0.00256

ELSE IF ((friction>=0.15).and.(friction<0.175)) THEN

mu_w=(friction-0.15)/0.025  !coefficient of friction weighting

!0.15 fem prediction
s_h=(0.16752)*(x**5) - (0.81957)*(x**4) &
+ (1.43941)*(x**3) - (1.15594)*(x**2) + 1.62100*x - 0.00256

!0.175 fem prediction
s_l=(0.11688)*(x**3) - (0.34993)*(x**2) + 1.53148*x + 0.00636

ELSE IF ((friction>=0.175).and.(friction<0.2)) THEN

mu_w=(friction-0.175)/0.025  !coefficient of friction weighting

!0.175 fem prediction
s_h=(0.11688)*(x**3) - (0.34993)*(x**2) + 1.53148*x + 0.00636

!0.2 fem prediction
s_l=(0.17454)*(x**5) - (0.87204)*(x**4) &
+ (1.48625)*(x**3) - (1.14357)*(x**2) + 1.74496*x - 0.00226

ELSE IF ((friction>=0.2).and.(friction<=0.225)) THEN

mu_w=(friction-0.2)/0.025  !coefficient of friction weighting

!0.2 fem prediction
s_h=(0.17454)*(x**5) - (0.87204)*(x**4) &
+ (1.48625)*(x**3) - (1.14357)*(x**2) + 1.74496*x - 0.00226

!0.225 fem prediction
s_l=(0.06197)*(x**5) - (0.29929)*(x**4) &
+ (0.64872)*(x**3) - (0.89172)*(x**2) + 1.95707*x - 0.00074

END IF

strain=(1-mu_w)*s_h+mu_w*s_l

  SELECT CASE(mu)

    CASE(1)
    s_mean=strain

    CASE(2)
    s_up=strain

    CASE(3)
    s_low=strain

  END SELECT

mu=mu+1

END DO

!calculate strain rates
```

```
s_rate_m=(3.5303*(mean**2)+1.5171*mean+0.9461)*rate
s_rate_u=(3.5303*(up**2)+1.5171*up+0.9461)*rate
s_rate_l=(3.5303*(low**2)+1.5171*low+0.9461)*rate

END SUBROUTINE strains
!-----------------------------------------------------------------------
!subroutine:    openfile
!
!purpose:       opens file with user filename
!
!argument description
!
!filename       user file name for results to be writen to
!
!programmer:    J.M. Buchanan
!language:      Fortran 90
!date:          12 November 2001
!-----------------------------------------------------------------------
SUBROUTINE openfile(filename)
IMPLICIT NONE

CHARACTER(len=20),INTENT(out)::filename
CHARACTER(len=20)::file_q
INTEGER::out,ios


file_q='do'
DO WHILE (file_q=='do')

WRITE(*,*)' Enter a file name for the results '
READ(*,*)filename

filename=TRIM(filename)//'.dat'  !data file

out=1
ios=0

!check whether file already exists

OPEN(UNIT=out,FILE=filename,STATUS='old',IOSTAT=ios)

  IF (ios/=0)THEN
  file_q='done'

  ELSE
  WRITE(*,*)'The file already exists'
  WRITE(*,*)' '

  END IF

END DO

END SUBROUTINE openfile
!-----------------------------------------------------------------------
!subroutine:    savedata
!
!purpose:       writes results to file
!
!argument description
!
!filename       (in)    file name
!ho             (in)    initial height
!hf             (in)    final height
```

```
!t              (in)    temperature of deformation
!rate           (in)    strain rate
!mean           (in)    mean coefficient of friction
!up             (in)    upper coefficient of friction
!low            (in)    lower coefficient of friction
!nom_s          (in)    nominal strain
!s_mean         (in)    mean strain
!s_up           (in)    upper strain
!s_low          (in)    lower strain
!s_rate_m       (in)    mean strain rate
!s_rate_u       (in)    upper strain rate
!s_rate_l       (in)    lower strain rate
!
!programmer:    J.M. Buchanan
!language:      Fortran 90
!date:          12 November 2001
!-----------------------------------------------------------------------
SUBROUTINE savedata(filename,ho,hf,t,rate,mean,up,low,&
nom_s,s_mean,s_up,s_low,s_rate_m,s_rate_u,s_rate_l)
IMPLICIT NONE

CHARACTER(len=20), INTENT(in)::filename
REAL,INTENT(in)::ho,hf,t,rate,mean,up,low,nom_s,s_mean,s_up,s_low, &
s_rate_m,s_rate_u,s_rate_l

INTEGER::out,ios2

out=2
ios2=0

OPEN(UNIT=out,FILE=filename,IOSTAT=ios2)
REWIND out

!writes results to file

WRITE(out,*)'                PROGRAM INPUTS '
WRITE(out,*)'               ---------------- '
WRITE(out,*)' '
WRITE(out,*)'Initial Height : ',ho
WRITE(out,*)'Final Height   : ',hf
WRITE(out,*)'Temperature    : ',t
WRITE(out,*)'Strain Rate    : ',rate
WRITE(out,*)' '
WRITE(out,*)'Nominal Strain : ',nom_s
WRITE(out,*)' '
WRITE(out,*)'          Coefficients of Friction '
WRITE(out,*)'         -------------------------'
WRITE(out,*)' '
WRITE(out,*)'Mean Value     : ',mean
WRITE(out,*)'Upper Estimate : ',up
WRITE(out,*)'Lower Estimate : ',low
WRITE(out,*)' '
WRITE(out,*)'     Predicted Strain by Program Strain '
WRITE(out,*)'    ------------------------------------ '
WRITE(out,*)' '
WRITE(out,*)'Mean Strain  : ', s_mean
WRITE(out,*)'Upper Strain : ', s_up
WRITE(out,*)'Lower Strain : ', s_low
WRITE(out,*)' '
WRITE(out,*)'   Predicted Strain Rate by Program Strain '
WRITE(out,*)'  ---------------------------------------- '
WRITE(out,*)' '
WRITE(out,*)'Mean Strain Rate   : ',s_rate_m
WRITE(out,*)'Upper Strain Rate  : ',s_rate_u
```

```
WRITE(out,*)'Lower Strain Rate  : ',s_rate_l
WRITE(out,*)' '


END SUBROUTINE savedata
!-------------------------------------------------------------------------
END MODULE subs
!-------------------------------------------------------------------------
!program:       strain v.1
!
!purpose:       calculates the the strain and strain rate
!               range for a specific PSC test
!
!argument description
!
!prog_qu        program status
!again          program question status
!filename       user file name
!ho             initial specimen height
!hf             final specimen height
!t              test temperature
!rate           test strain rate
!mean           mean prediction of coefficient of friction
!up             upper prediction of coefficient of friction
!low            low prediction of coefficient of friction
!s_mean         mean strain prediction
!s_up           upper strain prediction
!s_low          low strain prediction
!nom_s          nominal strain of test
!s_rate_m       mean strain rate prediction
!s_rate_u       upper strain rate prediction
!s_rate_l       low strain rate prediction
!
!programmer:    J.M. Buchanan
!language:      Fortran 90
!date:          12 November 2001
!-------------------------------------------------------------------------
PROGRAM strain
USE subs
IMPLICIT NONE

CHARACTER(len=5)::prog_qu,again
CHARACTER(len=20)::filename
REAL::ho,hf,t,rate,mean,up,low,s_mean,s_up,s_low,nom_s,s_rate_m, &
s_rate_u,s_rate_l

prog_qu='y'
DO WHILE (prog_qu=='y')   !do loop for program

CALL intro                !call subroutine intro

CALL inputs(ho,hf,t,rate) !call subroutine inputs

nom_s=-1.155*log(hf/ho)   !nominal strain

CALL friction(t,mean,up,low) !call subroutine friction

CALL strains(rate,mean,up,low,nom_s,s_mean,s_up,s_low,s_rate_m, &
s_rate_u,s_rate_l)           !call subroutine strains

CALL openfile(filename)   !call subroutine openfile

CALL savedata(filename,ho,hf,t,rate,mean,up,low,nom_s,s_mean,s_up,s_low, &
s_rate_m,s_rate_u,s_rate_l)  !call subroutine savedata
```

```
again='no'
  DO WHILE(again=='no')

    WRITE(*,*)' Would you like to use Program Strain again (y/n)'
    READ(*,*)prog_qu

      IF(prog_qu=='y') THEN
      again='yes'
      WRITE(*,*)' '

        ELSE IF(prog_qu=='n') THEN
             again='yes'

             WRITE(*,*)'Thank you for using Program STRAIN v.1'
                 STOP

                 ELSE
                 WRITE(*,*)'A vaild answer was not given'
                 WRITE(*,*)' '

          END IF
  END DO

END DO

END PROGRAM strain
!-------------------------------------------------------------------------
```